Contents

1.1 Introduction

Lead has been used in soldering materials for electronic applications for very many years. Lead, with its low melting point and soft, malleable nature, when combined with tin at the eutectic composition gives an alloy which flows easily in the liquid state and solidifies over a very small range of temperature. It lies at the heart of the electronics industry. Present-day society is totally dependent on this industry; through domestic appliances, telecommunications, transport, and so on. Electronic devices now pervade every aspect of life, and with an increasing reliance on mobile devices, such as telephony and computing, the number of components manufactured, and probably more importantly, discarded, is increasing dramatically. For example, for the period 1992-1997, there was a three-fold increase in the number of printed circuit boards manufactured in Europe, the value of which was in the region of $9.7bn. This is a huge industry that is growing, year on year.

The problem with lead, however, is one of health and the environment. Lead can accumulate in the body, leading to many adverse health effects, such as disorders of the nervous and reproductive systems and delays in neurological and physical development. Most developed countries have now banned the use of lead in petrol. The worry over lead in electronic components stems mainly from discarded electronic equipment, much of which ends up in land-fills, with the fear, then, of the contamination of ground water. The decision to remove lead from electronic equipment has been taken by many countries, and in Europe, new legislation was brought into force in July 2006 banning the use of lead in electrical and electronic equipment – the RoHS directives. The search for a replacement solder material has been underway for some time and a number of formulations have already been in use before 2006, notably in Japan. However, it is now an accepted fact that there is no ideal 'drop-in' replacement for the traditional lead-tin solder. One particular formulation, Sn3.8Ag0.7Cu, has a melting point of around 220 °C, which is about 30 °C higher than that of traditional lead-tin solder. This has a number of implications, not least the increase in energy costs associated with using this material. There are also compatibility issues relating to components and their termination finishes, all of which can have an affect on the reliability of an electronic device.

It is clear that knowledge of the phase equilibria involved in the solder-component termination alloy system is crucial in the design of new soldering materials. Traditional methods of experimentation involving trial and error methods for the choice of appropriate compositions are both costly in terms of time and money and are clearly no longer applicable owing to the increasing complexity of materials involved. Over the past 30 years or so, the construction of thermodynamic databases for the calculation of complex phase equilibria has become more important **[07Sch]**. Along with appropriate

software **[02Cal]**, it is possible to predict the stable phase equilibria in multicomponent alloy systems as a function of temperature, pressure and composition. This has obvious implications with respect to saving time, not only by reducing the number of experiments that need to be performed to fully understand the chemistry of an alloy system, but also by being able to predict likely scenarios whilst kinetic constraints may mask the true nature of the equilibrium.

In 2002, European COST Action 531 was initiated in order to study the basic science of lead-free solder alloys and to provide a basis for deciding which alloy to chose for each application. A major aspect of the whole COST Action was the construction of a self-consistent thermodynamic database for the calculation of phase equilibria in lead-free solder alloys and their interaction both with substrates, and with lead (an important consideration is how lead-free solder alloys will perform during the repair of older electronic equipment that may have been assembled using traditional lead-tin solder). The database can also be used to study intermetallic formation – critical to the strength of a soldered joint, and also solidification paths and for the modelling of surface tension.

1.2. The calculation of phase equilibria

A semi-empirical approach, referred to as the CALPHAD method **[98Sau, 07Luk]** is used for the modelling of thermodynamic properties and for the calculation of phase diagrams in complex systems. Its main feature is the combination of experimental observation and theoretical modelling and it is significantly dependent on the amount and quality of experimental data available. The approach is based on the sequential modelling of multicomponent systems, starting from the simplest – the modelling of the Gibbs energy functions for the pure component elements, followed by the modelling of more complex phases such as binary and ternary solutions and intermetallic phases. The Gibbs energy functions of phases are stored in the form of polynomial coefficients. The thermodynamic properties of a binary system can be calculated using the Gibbs energy expressions comprising contributions for both elements in each of the phases existing in the system. Further parameters are introduced to describe the mutual interaction between the elements in each phase. It is possible to model such a system with high precision if reliable experimental data are available that describe both the thermodynamic properties of the phases (*e.g.* specific heat, enthalpies of formation or mixing, activities – thermodynamic data) and the phase equilibria (*e.g.* invariant temperatures, compositions and amounts of phases – phase data). By combining robust thermodynamic descriptions of binary and ternary alloy systems, it is possible to predict phase equilibria in higher order systems. The deviation of the real behaviour of the system from the prediction can be minimized by adding new parameters, but they must not influence the

modelled thermodynamic properties and calculated phase diagrams of the lower order systems.

The basic mathematical method used for the calculation of phase equilibria is a constrained minimisation of Gibbs energy for a given temperature, pressure and overall composition. This approach is common to all currently available software packages for the modelling of thermodynamic properties and phase diagrams of multicomponent systems.

1.3. Models

The molar Gibbs energy of a phase ϕ can be considered as the sum of a number of different contributions:

$$G_m^\phi = G_{ref}^\phi + G_{id}^\phi + G_E^\phi + G_{mag}^\phi + G_P^\phi + \ldots \quad (1)$$

where G_{ref}^ϕ is the molar Gibbs energy of the weighted sum of the system constituents *i* (elements, species, compounds etc.) of the phase ϕ relative to the chosen reference state (typically the Stable Element Reference state - SER),

$$G_{ref}^\phi = \sum_{i=1}^{n} x_i \cdot {}^{\mathrm{O}}G_i^\phi \quad (2)$$

and its temperature dependence is given by

$$G(T) = \mathrm{a} + \mathrm{b}T + \mathrm{c}T\ln(T) + \sum_i \mathrm{d_i}T^{\mathrm{n}} \quad (3)$$

where a-d_i are adjustable coefficients.

In the case where the constituent in question is a stoichiometric compound, its contribution to the G_{ref}^ϕ is usually expressed by the Gibbs energy of formation relative to the chosen reference state.

$$G_{ref}^\phi = \sum_{i=1}^{n} x_i \cdot {}^{\mathrm{O}}G_i^\phi + G_f \quad (4)$$

There is also a contribution to the Gibbs energy from ideal random mixing of the constituents on the crystal lattice, denoted G_{id}^ϕ,

$$G_{id}^\phi = \mathrm{R}T\sum_{i=1}^{n} x_i \cdot \ln(x_i), x=1,\ldots, \mathrm{n} \quad (5)$$

for an n-constituent system.

G_E^ϕ is the excess Gibbs energy, which describes the influence of non-ideal mixing behaviour on the thermodynamic properties of a solution phase and

is given by the Muggianu extension of the Redlich-Kister formalism **[75Mug, 48Red]**

$$G_E^{\phi} = \sum_{\substack{i,j=1 \\ i \neq j}}^{n} x_i x_j \sum_{z=0}^{m} {}^{z}L(x_i - x_j)^z + \sum_{\substack{i,j,k=1 \\ i \neq j \neq k}}^{n} x_i x_j x_k L_{ijk} \quad z = 0, \ldots, \mathrm{m} \qquad (6)$$

where the temperature dependent interaction parameters, describing the mutual interaction between constituents *i* and *j*, are denoted as ${}^{z}L$. The liquid phase and solid solution phases are modelled in this way, but more complex phases, such as intermetallic compounds, are usually modelled using the compound energy formalism **[86And]**, where the crystal structure can be considered as comprising a number of sublattices *l*, which may exhibit preferential occupancy by one or more constituents. For such a phase, G_{ref}^{ϕ} is now given by

$$G_{ref}^{\phi} = \sum y_i^s \cdot y_j^t \cdots y_k^u {}^{\mathrm{O}}G_{(i:j:\cdots:k)}, \; i,j,k = 1, \ldots, \mathrm{n}, \; s,t,u = 1, \ldots, \mathrm{l} \qquad (7)$$

where the *y* terms are the site fractions of each constituent on relevant sublattice, *s,t,...u*. The term $G_{(i:j:\cdots:k)}$ represents the Gibbs energy of formation (Eqn. (4)) of 'virtual compounds' or unaries where each sublattice is occupied by just one component. Typically only few of these compounds can exist in the reality, but all relevant end members are needed for the modelling. The way these are obtained will be briefly described later in section 1.4.3.

The ideal mixing term is given by

$$G_{id}^{\phi} = \sum_{p=1}^{l} f_p \cdot \sum_{i=1}^{m} y_i^p \cdot \ln(y_i^p) \qquad (8)$$

where f_p is the stoichiometric coefficient for a given sublattice and the second sum describes the effect of the ideal mixing within the sublattice *p*. The excess contribution is now given by (for a case of two sublattices)

$$G_E^{\phi} = \sum y_i^p \cdot y_j^p \cdot y_k^q L_{(i,j:k)} \text{ where } L_{(i,j:k)} = \sum_z {}^{z}L_{(i,j:k)} \cdot (y_i^p - y_j^q)^z \qquad (9)$$

The parameter $L_{(i,j:k)}$ describes the mutual interaction of constituents *i* and *j* in the first sublattice, when the second sublattice is fully occupied by constituent *k*. This description can be extended in the same way to any number of sublattices.

This model was used extensively for the intermetallic compounds present in the database. The specific model used for each of the phases in the database is given in Appendix including the number of sublattices and their constituents. Some of the sublattices have three or more constituents indicating dissolution

of additional elements as the phase extends into multicomponent systems from a binary system.

Additional terms may be necessary for the proper description of the Gibbs energy from Eqn (1). G^{ϕ}_{mag} in Eqn (1) is the magnetic contribution after **[78Hil]** and G^{ϕ}_{P} is the pressure term. The excess Gibbs energy term G^{ϕ}_{E} and the magnetic contribution G^{ϕ}_{mag}, if the material exhibits magnetic behaviour, are the most important terms for the modelling of the thermodynamic properties of the phase. Other terms may describe contributions e.g. from the interface energy, energy of plastic deformation, etc. The size of these contributions is usually significantly lower in metallic systems than the terms for the excess Gibbs energy and the magnetic contribution and they were not taken into account in the compilation of this database.

In order to maintain the scope of the database and to keep the work involved at a manageable level, it was decided to restrict the modelling of chemical ordering of solution phases to the B2/A2 phases in the Cu-Zn system using the formalism described in **[07Luk]**.

1.4. The creation of consistent thermodynamic databases

Successful modelling of thermodynamic properties and phase equilibria of multicomponent systems rely not only on the existence of theoretically sound and proper models, but also the existence of reliable and consistent thermodynamic databases. The parameters describing the Gibbs energies of the elements of the different phases, their mutual interactions, deviations from ideality, etc., are obtained through the critical assessment of data for such systems. The parameters are then collected in databases, which are usually oriented towards some specific group of materials; a database for lead-free solders is a typical example.

A thermodynamic database, however, cannot be simply a collection of thermodynamic assessments published by various authors for relevant binary and higher order systems. Even if the individual assessments reproduce the thermodynamic properties and phase diagram in each case, and the assessors have followed the generally accepted good practice for such work **[07Sch]**, a database compiled in such a way may contain problems and errors. Several important rules have to be respected when such a database is compiled; some of them are quite obvious, while others are rather more subtle and treacherous. The consistency of the database is the main condition for its successful exploitation; all the Gibbs energy descriptions for all constituents and phases have to be unique, based on the same assumptions, conditions and models.

A reliable thermodynamic database must be consistent with respect to:

- The models used to represent the Gibbs energy of a phase in terms of its in unaries and the interactions between its constituents,
- the models and names used for the description of the same phase existing in different systems, eg. hcp_A3,
- the thermodynamic data used for the Gibbs energies of the same elements or species in related systems published by different authors.

1.4.1. First condition of consistency

The first condition is now usually fulfilled as assessments available in the current literature use standard models for the temperature and concentration dependence of Gibbs energy in the same form as those given above. However, the consistency problem can arise even if the same model is used. It is important to check the order of elements *i* and *j* when various assessments are accepted for addition to the database. An incorrect choice may require the sign of the interaction parameters of the odd order (^1L, ^3L....) to be changed. The use of an alphabetical element order is usually recommended to prevent this problem.

Other Gibbs energy formalisms can be used, however, instead of Redlich-Kister-Muggianu equation, e.g. the T.A.P (**T**hermodynamic **A**dapted **P**ower) polynomial, the Kohler equation or Toop equation (for ternary systems) **[98Sau]**. Therefore, the type of the polynomials used for the expression of excess Gibbs energy has to be checked.

1.4.2. Second condition of consistency

It is much more difficult to fulfil the second condition of consistency, as various authors are free to select the model for the description of a particular phase and to allocate any name to it. The sublattice model – used in the compound energy formalism **[81Sun, 86 And]**, which is widely used for metallic systems, gives the authors complete freedom in selection of the number of sublattices, their ratios, site occupancies, etc., respecting existing experimental information, mainly in relation to the crystallography of the phase. As many systems have often been modelled on a number of occasions by different assessors, it is very important to identify carefully the models used and to avoid careless mixing of data from different sources. Complications with model consistency usually arise when lower order systems assessed by different authors are used for the prediction and further work on a higher order system. Serious problems can appear, *e.g*. when complete solubility occurs between intermediate phases existing in related subsystems that was not envisaged when the subsystems were assessed. Careful adjustment of the models and names of the affected phases has to be carried out, sometimes forcing complete reassessment of one or more of the lower-order systems.

1.4.3. Third condition of consistency

The third problem concerns the consistency of the description of the Gibbs energy for an element (Lattice Stability) or compound in a given crystallographic structure, either stable or metastable, in the different subsystems. It is important to use the same set of thermodynamic parameters for the calculation of Gibbs energies of such unaries for every system included in the database. This is essential for the pure elements, even for Gibbs energy descriptions for crystallographic structures in which the element does not exist in the nature. These may differ significantly not only between different assessors, but also in different versions of the database from the same source **[SGTE1, SGTE4]**. In such cases the thermodynamic properties cannot be measured and therefore the parameters are either estimated (in the past) or modelled during the assessment of a higher order system where such a crystallographic structure exists and the element dissolves into it. Recently, *ab-initio* methods have been used to calculate the energy difference of such hypothetical phases at 0 K with respect to the stable phases. While there are still many discrepancies between the two approaches such a combination of the semi-empirical CALPHAD method and the purely theoretical but time consuming, *ab-initio* calculation is an opportunity to involve the *ab-initio* modelling in applied research, exploiting in this way the advantages of both approaches.

As the lattice stability values are continuously being revised, it is necessary to check the Gibbs energies of pure elements and of simple compounds to avoid the use of assessments using different data for the same element in the same crystallographic structure.

1.5. The scope of the COST 531 thermodynamic database for lead-free solders

A critically assessed thermodynamic database for lead free solders was defined as one of the key outputs from the COST 531 Action. It was decided at an early stage not to include the gas phase in the database as it was recognised that the main application of the database would be for calculations relating to solidification and the formation of intermetallic phases.

A starting point for the database is the accepted standard reference data for the pure elements recommended by SGTE, ver. 4.4 **[SGTE4]**. The COST 531 database was formed initially by the merger of two separate databases developed by members of the project, at NPL and in the Institute of Physics of Materials and Masaryk University, Brno. There were, in addition, other smaller databases available in the public domain **[NIST]**. A considerable degree of overlap existed between the databases in terms of data for some of the key systems. However these systems were often based on different data for the pure elements.

In database development, it is always beneficial to restrict the range of elements it covers so that the database is focused only on the relevant components, optimising consistency and minimising the amount of effort required in compiling and testing the database. There are obvious choices for the elements that should be included in a database for lead-free solders. Cu and Sn (Cu is a substrate material as well) along with Ag have already been identified as component elements for lead-free soldering materials (Sn3.5Ag, Sn0.7Cu, or Sn3.8Ag0.7Cu). Low melting point elements such as In and Bi were added to the list, along with termination materials Ni and Pd. Au, Sb and Zn were considered as important for the lead free soldering and also added to the database. Some elements were not included in the list for toxicity reasons, e.g. Cd, Hg and Tl. Other elements, such as Al, Ge and As were not considered as important alloying elements for solder applications at this time and hence were not included in the database in order to minimise effort. Pb was included in order to model equilibria relating to rework when old electrical components may be repaired using the new lead-free materials. However, it will be necessary to include P as it is an impurity associated with Ni, which is a substrate material. This will be a feature of a later development of the database.

The scope of the database is therefore 11 elements: Ag, Au, Bi, Cu, In, Ni, Pb, Pd, Sb, Sn and Zn.

1.6. Critical assessment of thermodynamic data

To produce a good critical assessment of any binary or ternary system, several basic guidelines should be followed by the assessor. Recently, Schmid-Fetzer *et al*. **[07Sch]** described good practice guidelines for conducting thermodynamic assessment. It is recommended that all experimental data for a given system be used plus *ab initio* calculations for specific compositions, if possible. There is a need for well tested, reliable models based on the crystal structure of the phases. Assessors should pay attention to the availability of various types of experimental data; it is important to have both thermodynamic and phase equilibrium data in the assessment in order to describe the thermodynamic properties and the phase diagram correctly. Using optimisation software allows the assessor to derive a small number of thermodynamic coefficients to represent the whole of the accepted experimental dataset.

To produce thermodynamic descriptions for all possible binary and ternary combinations of elements chosen for the database is a colossal task – for instance, there are a total of 55 binary combinations of elements, all of which are crucial in preparing a reliable database.

As mentioned above, version 4.4 of the SGTE unary database was chosen as the backbone of the database. It is fairly straightforward to change the unary data

in a thermodynamic database, but it can have implications in the binary and ternary assessments already present. Of course, it was necessary to use the SGTE v4.4 unary data with any assessments taken from the literature, and where the unary data were different to make changes to ensure that the phase diagram and thermodynamic properties are reproduced correctly. Some adjustment was necessary for some binary and ternary parameters. This critical reassessment was more important for ternary assessments taken from the literature as it was often the case that binary data that had been used in the assessment work were different from those already held in the database.

Secondly, it was necessary to harmonise the phase names. It was important to make sure that the same phase has the same name in all systems where it appears. This is not only to allow consistency in the phase names themselves, but also to allow for the possibility of mixing in higher order systems. To enable this mixing, it is also important that each phase has the same thermodynamic model for all systems in which it occurs. Where conflicts occur in the modelling of a binary phase a decision has to be made on which model to choose, often based on any ternary information available. For example, in the assessment of the Ag-In system by Moser *et al.* **[01Mos]**, the Ag_2In-phase has been modelled as a stoichiometric phase, although it has a narrow range of homogeneity in the binary phase diagram. In the Cu-In system, a phase with the same crystal structure exists at higher temperatures and was modelled by **[01Liu]** with three sublattices. Although the two binary phases are stable over different temperature ranges, the phase does exist in the ternary Ag-Cu-In system, which requires that the Ag_2In phase is described with three sublattices so that the ternary extension of this phase can be modelled. This phase is now described with one model and one set of parameters, which allows the stability of this phase in both binary and the ternary systems to be calculated.

Similarly, complete solubility was found experimentally between phases in some ternary systems, which had not been considered as identical from a crystallographic point of view when the assessments of relevant binary systems had been made. The high temperature modification of the Cu_6Sn_5 phase and CuIn-η phase are typical examples, where a unique name and model for both phases had to be selected necessitating reassessment of data for the Cu-Sn system.

The other source of assessed parameters came from new work undertaken under the COST Action. After the compilation of the first version of the database and a thorough search of the literature, it became clear where experimental data were sparse and for which systems assessments were missing. This led to the initiation of experimental programmes under the COST Action to fill the gaps in the knowledge.

1.6.1. Testing

A critical aspect of the database development was testing. There were two levels of testing of the database. Firstly, each individual dataset was tested to ensure that the parameters entered into the database faithfully reproduced the phase diagram and thermodynamic properties as given in the source of the data. Typing errors can easily find their way into printed publications so it was important to check calculated diagrams and sections particularly with respect to experimental data where these were available.

The second aspect of testing was that of the database itself. With data being added to the database from different sources, the only real way to check for consistency was through thorough testing. At each stage in the development of the database, it was tested using three different currently available software packages for computational thermodynamics; Thermo-Calc, MTDATA and Pandat. Each version of the database was initially prepared in Thermo-Calc compatible "tdb" format before being converted and modified for use with the other two packages. Having access to different software gave a number of distinct advantages. Firstly, it is desirable that the database is portable, i.e. the data within the database should be compatible with more than one software package and thus software independent. Secondly, each of the software packages has its own strengths and weaknesses. Therefore, it is interesting to compare the results of calculations and noting any differences. The calculations obtained from each of the software packages should be identical, and if not, the modelling should be checked.

1.7. Organisation of the volume

The volume is split into three sections:

1.7.1· Binary systems

o Each binary system covered by the database is described in some detail with information about the phase diagram, the phases covered in the database, the quality of the experimental information and the source of the critically assessed data.

o Diagrams are presented showing the phase diagram and, in some cases, selected plots of thermodynamic properties showing a comparison with experimental data where these have been measured during the project.

o Tables are presented showing the phases present in the system with their common names, important crystallographic information **[Vil]** and calculated invariant reactions.

o Diagrams are presented using T/ C and mole fractions

o MTDATA/ Pandat/ Thermo-Calc have all been used to provide diagrams

1.7.2. Ternary systems

o Each ternary system covered by the database is described in some detail with information about the phase diagram, the phases covered in the database, the quality of the experimental information and the source of the critically assessed data.

o The phase diagram is displayed in various ways. A conventional liquidus projection is given where the triangular axes are the mole fractions of the components and the monovariant lines and isotherms are projected onto this grid. The liquidus projection is also displayed with temperature as the ordinate and the mole fraction of one of the components selected as the abscissa. This projection allows very clear graphic description about the temperatures and character of any particular invariant reaction. A number of isothermal sections are provided to provide more detail of the phase diagram for specific temperatures. Isopleths are also given to show agreement between calculation and any experimental data obtained during the project, or presenting the phase diagrams for significant compositions (e.g. near invariant points) or composition ratios. Similarly selected plots of thermodynamic properties may be given showing a comparison with experimental data where these have been measured during the project.

o Tables are presented showing the ternary phases present in the system with their common names, important crystallographic information **[Vil]** and calculated invariant reactions involving the liquid phase. These invariant reactions are designated according to their nature: E, for decomposition reactions (eutectic reactions of the type Liquid $\rightarrow$ solid 1 + solid 2 + solid 3 and other reactions of the type solid 1 $\rightarrow$ liquid + solid 2 + solid 3), P for formation reactions (peritectic reactions of the type liquid + solid 1 + solid 2 $\rightarrow$ solid 3), U for transformation reactions of the type liquid + solid 1 $\rightarrow$ solid 2 + solid 3 and D for degenerate equilibria which cannot be assigned to any one of the above with any confidence. Within each class the invariant reactions are numbered sequentially, increasing with a decrease in temperature. In each case the product phases are shaded.

1.7.3. Table of Crystallographic Structures

This table contains additional crystallographic information **[Vil]** and the description of the sublattice model, used in the COST 531 thermodynamic database, for all phases appearing in the Atlas.

1.8. Concluding remarks

The database has been implemented for use with MTDATA **[02Dav]**, Thermo-Calc **[02And]** and Pandat **[02Che]**. The calculations reported here relate to version 3.0 of the database.

The database currently holds thermodynamic descriptions for the 53 binary systems associated with 11 elements in scope of the database (all but Ni-Sb and Pd-Sb). Added to these are critically assessed data for 20 ternary systems.

1.9. References

[48Red] Redlich, O., Kister, A.: *Indust. Eng. Chem.,* 1948, **40**, 345-248.
[75Mug] Muggianu, Y.-M., Gambino, M., Bros ,J.-P.: *J. Chim. Phys.,* 1975, **72**, 83-88.
[78Hil] Hillert, M., Jarl, M.: *CALPHAD*, 1978, **2**, 227-238.
[81Sun] Sundman, B., Ågren, J.: *J. Phys. Chem. Solids,* 1981, **42**, 297-301.
[86And] Andersson, J.-O., Fernandez Guillermet, A., Hillert, M., Jansson, B., Sundman, B.: *Acta Metall.*, 1986, **34**, 437-445.
[98Sau] Saunders, N., Miodownik, A.P.: CALPHAD (A Comprehensive Guide), Elsevier, London, 1998.
[01Liu] Liu, X.J., Liu, H.S., Ohnuma, I., Kainuma, R., Ishida, K., Itabashi, S., Kameda, K., Yamaguchi, K.: *J. Electron. Mater*., 2001, **30**, 1093-1103.
[01Mos] Moser, Z., Gasior, W., Pstrus, J., Zakulski, W., Ohnuma, I., Liu, X. J., Inohana, Y., Ishida, K: *J. Electron. Mater*., 2001, **30**, 1120-1128.
[02And] Andersson, J.-O., Helander, T., Höglund, L., Pingfang Shi, Sundman, B.: *CALPHAD*, 2002, **26**, 273-312.
[02Cal] *CALPHAD*, 2002, **26**, 141-312.
[02Che] Chen, S.-L., Daniel, S., Zhang, F., Chang, Y.A., Yan, X.-Y., Xie, F.-Y., Schmid-Fetzer, R., Oates, W.A.: *CALPHAD*, 2002, **26**, 175-188.
[02Dav] Davies,R.H, Dinsdale, A.T, Gisby, J.A., Robinson, J.A.J., Martin, S.M.: *CALPHAD*, 2002, **26**, 229-271.
[07Luk] Lukas, H.L., Fries, S.G., Sundman, B.; *Computational Thermodynamics*, Cambridge University Press, Cambridge, UK 2007.
[07Sch] Schmid-Fetzer, R., Anderson, D., Chevalier, P.Y., Eleno, L., Fabrichnaya, O., Kattner, U.R., Sundman, B., Wang, C., Watson, A., Zabdyr, L., Zinkevich, M.: *CALPHAD*, 2007, **31**, 38-52.

1.10. General References (referred to throughout the whole volume)

[MAS] Massalski, T.B. (ed.): "Binary Alloy Phase Diagrams", 2nd edition, ASM Int., Metals Park, Ohio, USA, 1996.
[NIST] http://www.metallurgy.nist.gov/phase/solder/solder.html.
[SGTE] SGTE (Scientific Group Thermodata Europe), www.sgte.org.
[SGTE1] Dinsdale, A.T.: *CALPHAD,* 1991, **15**, 317-425.
[SGTE4] Dinsdale, A.T.: "SGTE unary database, version 4.4", www.sgte.org.
[VIL] Villars, P.: "Pearson's Handbook, Desk Edition", Materials Park, OH, 1997.

2. Binary systems

Ag-Au System

The Ag-Au system has a simple isomorphous phase diagram showing complete solid solubility over the whole composition range. The data are taken from the assessment of Hassam *et al.* **[88Has]**.

References:

[88Has] Hassam, S., Gambino, M., Gaune-Escard, M., Bros, J. P., Agren, J.: *Metall. Trans.* 1988, **19A**, 409-416.

Table of invariant reactions

T / °C	Phases			Compositions / x_{Au}		
1064.2	LIQUID	FCC_A1		1.000	1.000	
961.8	LIQUID	FCC_A1		0.000	0.000	

Phase information

Phase Name	Common Name	Strukturbericht designation	Pearson Symbol
LIQUID	Liquid		
FCC_A1	(Ag, Au)	*A*1	*cF*4

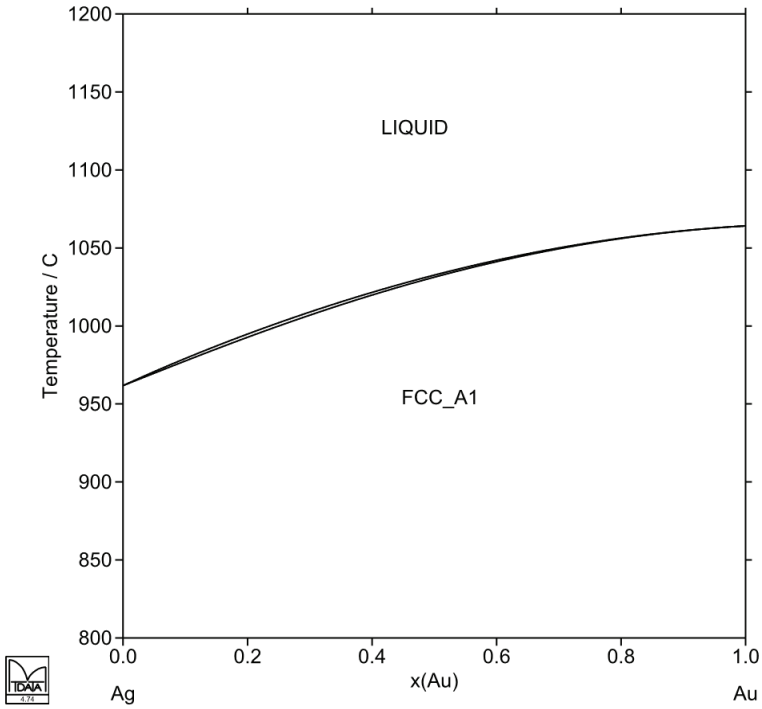

Fig. 1: Phase diagram of the Ag-Au system

Ag-Bi System

This system exhibits a simple eutectic type phase diagram with very limited solubilities in terminal solid solutions at lower temperatures. The theoretical description is from the assessment of Lukas **[98Luk]** based on Zimmermann's original work **[76Zim]**.

References:

[76Zim] Zimmermann, B.: "Rechnerische und experimentelle Optimierung von binären und ternären Systemen aus Ag, Bi, Pb und Tl", thesis, Universität Stuttgart, Germany, 1976.

[98Luk] Lukas, H.-L., Zimmermann, B.: Unpublished work, 1998.

Table of invariant reactions

T / °C	Phases			Compositions / x_{Bi}		
961.8	LIQUID	FCC_A1		0.000	0.000	
271.4	LIQUID	RHOMBO_A7		1.000	1.000	
261.8	FCC_A1	LIQUID	RHOMBO_A7	0.008	0.950	1.000

Phase information

Phase Name	Common Name	Strukturbericht designation	Pearson Symbol
LIQUID	Liquid		
FCC_A1	(Ag)	*A*1	*cF*4
RHOMBO_A7	(Bi)	*A*7	*hR*2

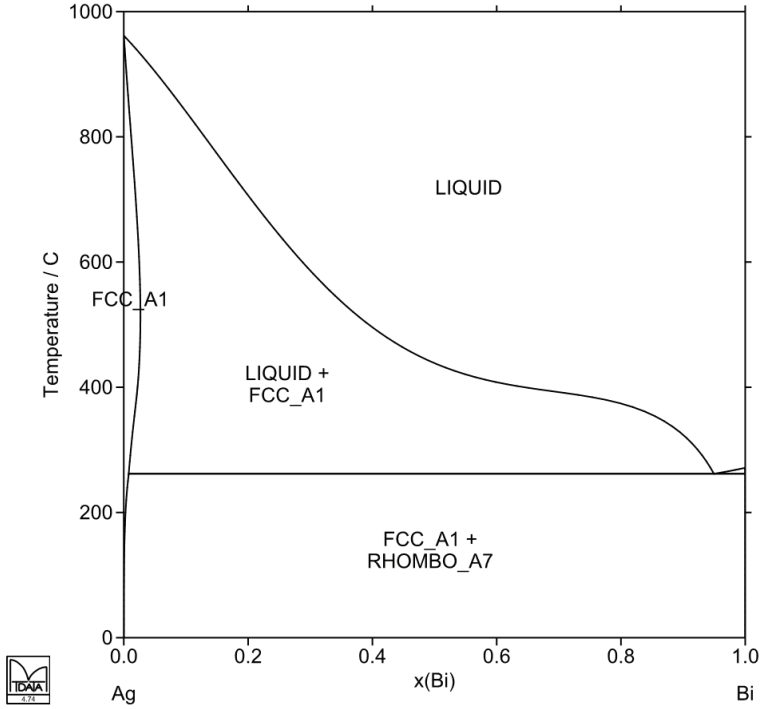

Fig. 2: Phase diagram of the Ag-Bi system

Ag-Cu System

The adopted assessment for the Ag-Cu system is an update from Lukas **[98Luk]** of his earlier published assessment **[77Hay]**.

References:

[77Hay] Hayes, F. H., Lukas, H. L., Effenberg, G., Petzow, G.: *Z. Metallkde*. 1986, **77**, 749-754.

[98Luk] Lukas, H.-L.: Unpublished work, 1998.

Table of invariant reactions

T / °C	Phases			Compositions / x_{Cu}		
1084.6	LIQUID	FCC_A1#2		1.000	1.000	
961.8	LIQUID	FCC_A1#1		0.000	0.000	
779.9	FCC_A1#1	LIQUID	FCC_A1#2	0.131	0.403	0.955

Phase information

Phase Name	Common Name	Strukturbericht designation	Pearson Symbol
LIQUID	Liquid		
FCC_A1	(Ag), (Cu)	*A*1	*cF*4

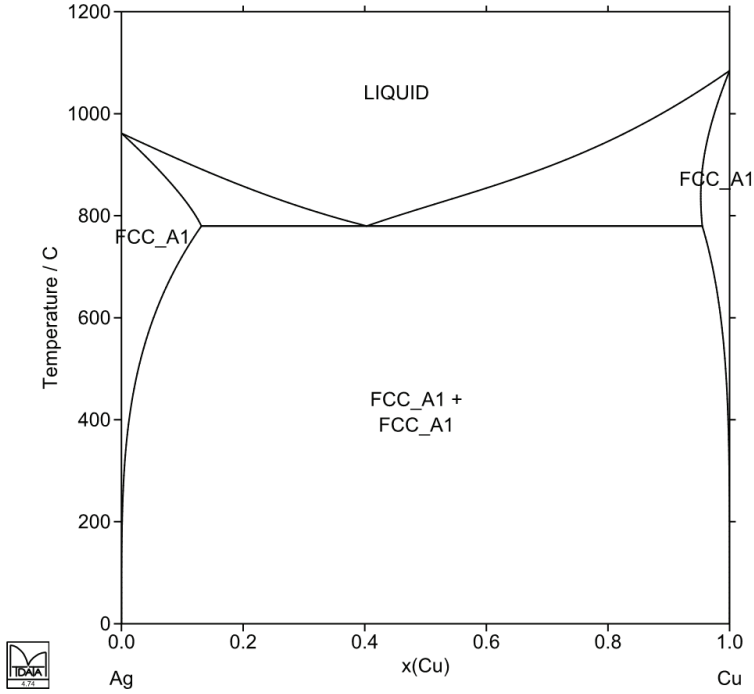

Fig. 3: Phase diagram of the Ag-Cu system

Ag-In System

Assessed data for this system were taken from **[01Mos]**. However, the model used for the γ-phase (Ag_2In) was changed to make it compatible with that utilized for the γ-phase in the Cu-In system (CUIN_GAMMA). This was necessary as complete solubility between the two binary phases exists in the Ag-Cu-In ternary system **[88Woy]**. The original work of **[01Mos]** also ignored the high-temperature β-phase (BCC_A2), which exists over a very limited temperature range. The description of this BCC-phase was added to the assessment in the scope of the COST 531 Action so that the liquidus surface could be modelled correctly. The presence of this phase leads to extra invariant reactions at high-temperatures that correspond to the metatectic decomposition of BCC_A2 to the HCP_A3 phase and the liquid and to the peritectoid reaction FCC_A1 + BCC_A2 —> HCP_A3.

References:

[88Woy] Woychik, C. G., Massalski, T. B.: *Met. Trans. A.*, 1988, **19A**, 13-21.

[01Mos] Moser, Z., Gasior, W., Pstrus, J., Zakulski, W., Ohnuma, I., Liu, X. J., Inohana, Y., Ishida, K: *J. Electron. Mater.*, 2001, **30**, 1120-1128.

Table of invariant reactions

T / °C	Phases			Compositions / x_{In}		
961.8	LIQUID	FCC_A1		0.000	0.000	
688.5	FCC_A1	BCC_A2	LIQUID	0.191	0.245	0.290
666.4	FCC_A1	HCP_A3	BCC_A2	0.198	0.242	0.250
661.9	HCP_A3	BCC_A2	LIQUID	0.254	0.260	0.321
309.3	HCP_A3	CUIN_GAMMA		0.320	0.320	
204.7	CUIN_GAMMA	HCP_A3	LIQUID	0.328	0.359	0.933
167.7	CUIN_GAMMA	AGIN2	LIQUID	0.329	0.667	0.954
156.6	LIQUID	TETRAG_A6		1.000	1.000	
144.8	AGIN2	LIQUID	TETRAG_A6	0.667	0.976	1.000

Phase information

Phase Name	Common Name	Strukturbericht designation	Pearson Symbol
LIQUID	Liquid		
FCC_A1	(Ag)	$A1$	$cF4$
BCC_A2	β	$A2$	$cP2$
HCP_A3	ζ	$A3$	$hP2$
CUIN_GAMMA	γ	$D8_3$	$cP52$
AGIN2	$AgIn_2$	$C16$	$tI12$
TETRAG_A6	(In)	$A6$	$tI2$

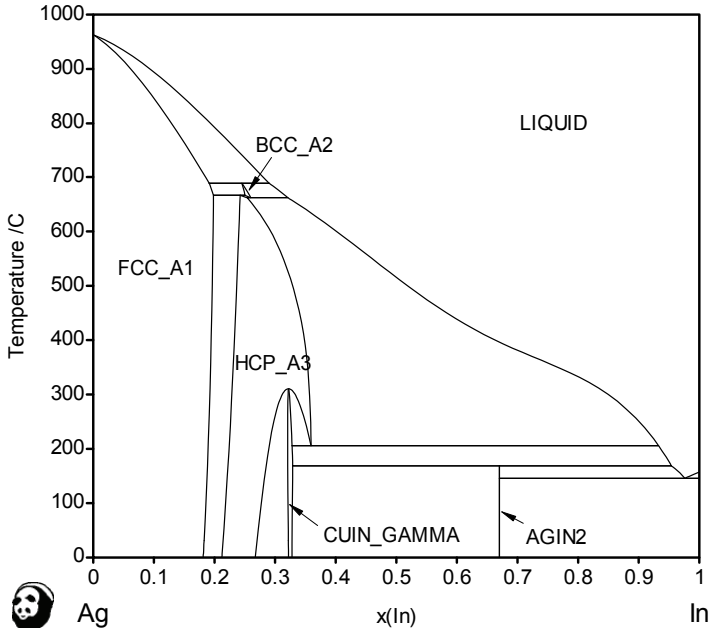

Fig. 4: Phase diagram of the Ag-In system

Ag-Ni System

The data for this system have been critically assessed within the scope of the COST 531 Action based on the experimental data from Tammann and Oelson **[30Tam]**, Stevenson and Wulff **[61Ste],** Borukhin and Khayutin **[74Bor]**, Burylev and Ivanova **[74Bur]**, Popel and Kozhurkov **[74Pop]**, Ladet *et al.* **[76Lad]**, Siewert and Heine **[77Sie]** and Xu *et al.* **[96Xu]**. Experimental work prior to 1987 has been reviewed by Singleton and Nash **[87Sin]**. New experimental data by Schmetterer *et al.* **[07Sch]** have yet to be incorporated.

References:

[30Tam] Tammann, G., Oelson, W.: *Z. Anorg. Chem.*, 1930, **186**, 264-266.

[61Ste] Stevenson, D. A., Wulff, J.: *Trans. Metall. Soc.*, AIME 1961, **221**, 271-275.

[74Bor] Borukhin, L. M., Khayutin, S. G.: *Strukt. Faz. Fazovye Prevrashch. Diagr. Sostoyaniya Met. Sist.*, 1974, 172-174.

[74Bur] Burylev, B. P., Ivanova, V. D.: *Tr. Krasnodar. Politekh. Inst.*, 1974, **63**, 111-113.

[74Pop] Popel, S. I., Kozhurkov, V. N.: *Izv. Akad. Nauk SSSR, Met.*, 1974, **2**, 49-52.

[76Lad] Ladet, J., Beradini, J., Cabane-Brouty, F.: *Scr. Metall.*, 1976, **10**, 195-199.

[77Sie] Siewert, T. A., Heine, R. W.: *Metall. Trans. A*, 1977, **8A**, 515-518.

[87Sin] Singleton, M., Nash, P.: *Bull. Alloy Phase Diagrams*, 1987, **8**, 119-121.

[96Xu] Xu, J., Herr, U., Klassen, T., Averback, R. S.: *J. Appl. Phys.*, 1996, **79** 3935-3945.

[07Sch] Schmetterer, C., Flandorfer, H., Ipser, H.: *Acta Mater*. ,2008, **56,** 155-164.

Table of invariant reactions

T / °C	Phases			Compositions / x_{Ni}		
2447.2	LIQUID	LIQUID#1	LIQUID#2	0.580	0.580	0.580
1455.1	LIQUID#2	FCC_A1#2		1.000	1.000	
1430.3	LIQUID#1	LIQUID#2	FCC_A1#2	0.038	0.970	0.990
961.8	LIQUID#1	FCC_A1#1		0.000	0.000	
961.1	FCC_A1#1	LIQUID#1	FCC_A1#2	0.003	0.003	0.997

Phase information

Phase Name	Common Name	Strukturbericht designation	Pearson Symbol
LIQUID	Liquid		
FCC_A1	(Ag), (Ni)	$A1$	$cF4$

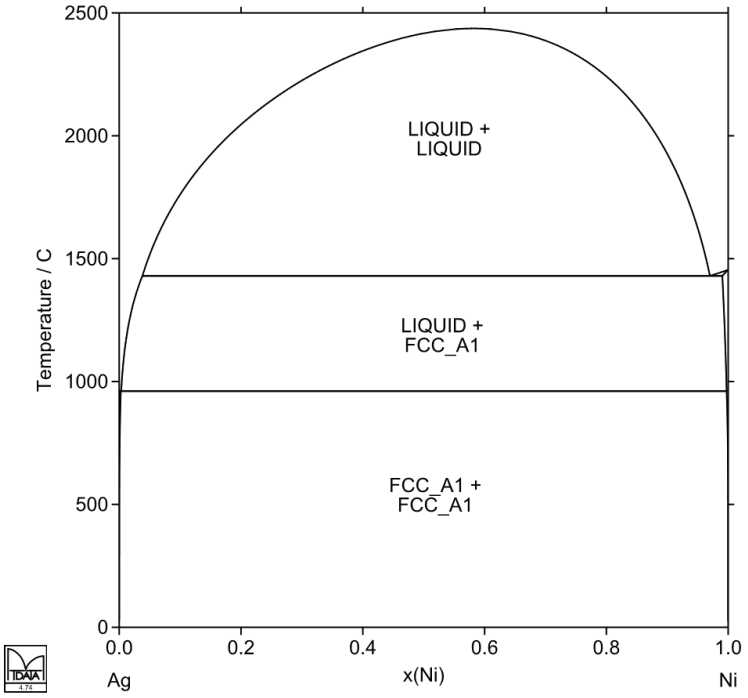

Fig. 5: Phase diagram of the Ag-Ni system

Ag-Pb System

The most recent data for this simple eutectic system come from **[00Luk]**. The system is characterised by a wide region of solid state immiscibility between the two component elements, their mutual solid solubility being very limited. This dataset is based on original work by **[76Zim]**.

References:

[76Zim] Zimmermann, B.: "Rechnerische und experimentelle Optimierung von binären und ternären Systemen aus Ag, Bi, Pb und Tl", thesis, Universität Stuttgart, Germany, 1976.

[00Luk] Lukas, H.-L..: Unpublished work, 2000.

Table of invariant reactions

T / °C	Phases			Compositions / x_{Pb}		
961.8	LIQUID	FCC_A1#1		0.000	0.000	
327.5	LIQUID	FCC_A1#2		1.000	1.000	
302.0	FCC_A1#1	LIQUID	FCC_A1#2	0.006	0.995	0.998

Phase information

Phase Name	Common Name	Strukturbericht designation	Pearson Symbol
LIQUID	Liquid		
FCC_A1	(Ag), (Pb)	*A*1	*cF*4

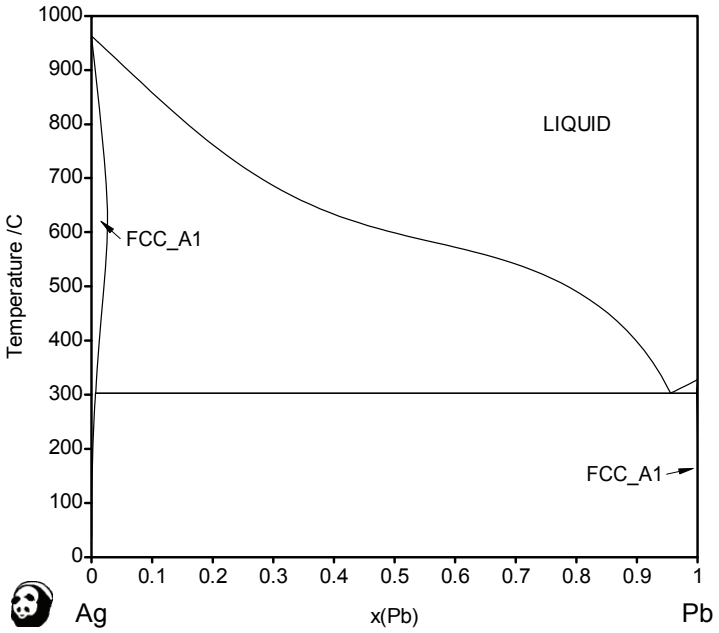

Fig. 6: Phase diagram of the Ag-Pb system

Ag-Pd System

The data for this system are from the assessment of Ghosh *et al.* **[99Gho]**. The data imply a miscibility gap in the FCC_A1 phase at low temperatures. The partial and integral enthalpies of mixing were determined at 1400 °C by Luef *et al.* **[05Lue]** but have yet to be incorporated into the assessment.

References:

[99Gho] Ghosh, G., Kantner, C., Olson, G.-B.: *J. Phase Equilb*., 1999, **20**, 295-308.

[05Lue] Luef, Ch., Paul, A., Flandorfer, H., Kodentsov, A., Ipser, H.: *J. Alloys Compd.*, 2005, **391**, 67-76.

Table of invariant reactions

T / °C	Phases			Compositions / x_{Pd}		
1554.8	LIQUID	FCC_A1#2		1.000	1.000	
961.8	LIQUID	FCC_A1#1		0.000	0.000	
341.1	FCC_A1	FCC_A1#1	FCC_A1#2	0.842	0.842	0.842

Phase information

Phase Name	Common Name	Strukturbericht designation	Pearson Symbol
LIQUID	Liquid		
FCC_A1	(Ag, Pd)	*A*1	*cF*4

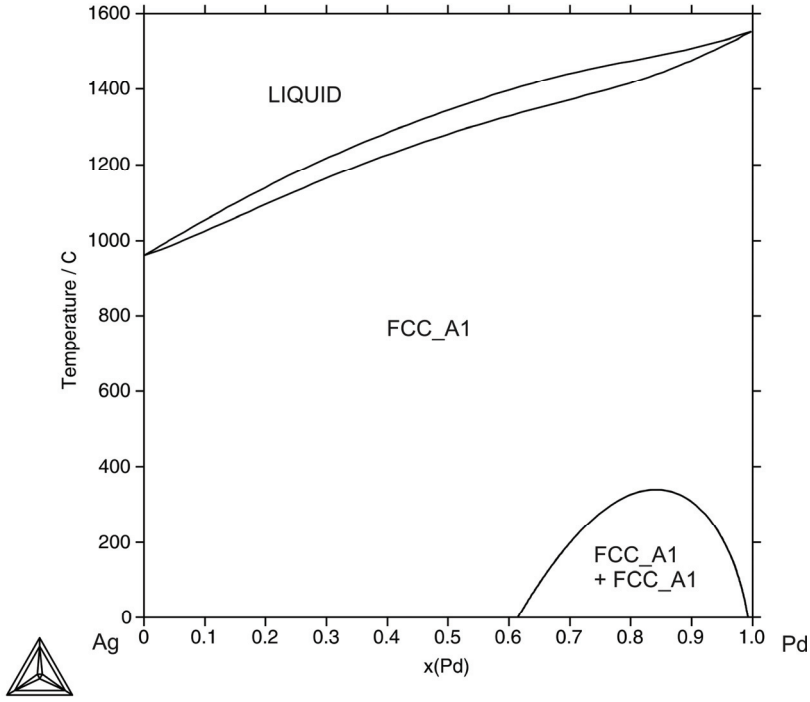

Fig. 7: Phase diagram of the Ag-Pd system

Ag-Sb System

The data for the Ag-Sb system are taken from a recent assessment by Zoro *et al.* **[07Zor]** carried out within the framework of COST 531 and based on their new experimental data. The calculated diagram is broadly similar to that from the earlier assessment of Oh *et al.* **[96Oh]**. The solubility of Ag in solid Sb has been ignored.

References:

[96Oh] Oh, C. S., Shim, J. H., Lee, B. J., Lee, D. N.: *J. Alloys Compd.*, 1996, **238**, 155-166.

[07Zor] Zoro, E., Servant, C., Legendre, B.: *J. Phase Equil. Diff.*: 2007, **28**, 250-257.

Table of invariant reactions

T / °C	Phases			Compositions / x_{Sb}		
961.8	LIQUID	FCC_A1		0.000	0.000	
694.5	FCC_A1	HCP_A3	LIQUID	0.054	0.080	0.161
630.6	LIQUID	RHOMBO_A7		1.000	1.000	
556.3	HCP_A3	AGSB_ORTHO	LIQUID	0.138	0.217	0.265
482.7	AGSB_ORTHO	LIQUID	RHOMBO_A7	0.272	0.423	1.000

Phase information

Phase Name	Common Name	Strukturbericht designation	Pearson Symbol
LIQUID	Liquid		
RHOMBO_A7	(Sb)	$A7$	$hR2$
FCC_A1	(Ag)	$A1$	$cF4$
HCP_A3	ζ	$A3$	$hP2$
AGSB_ORTHO	ε'(LT) ε(HT)	… $D0_a$	$oP4$ $oP8$

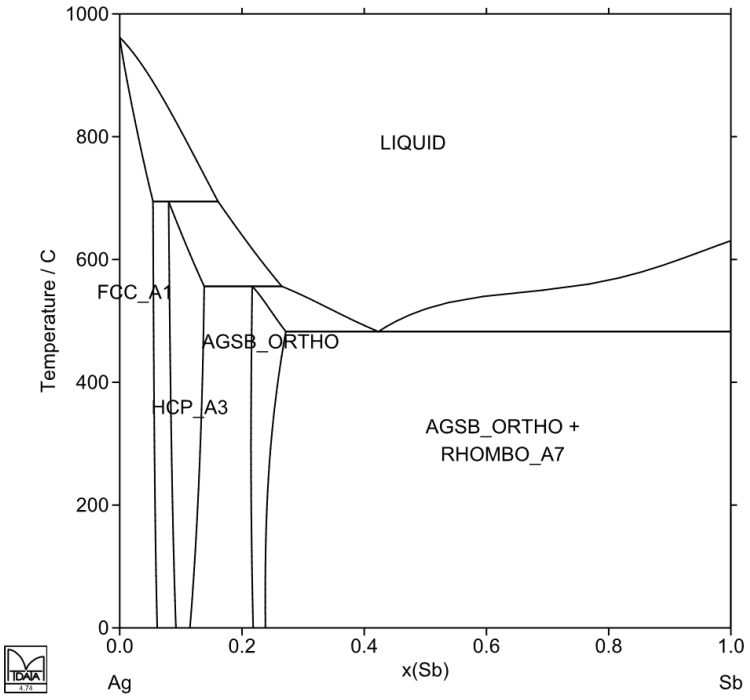

Fig. 8: Phase diagram of the Ag-Sb system

Ag-Sn System

The data for the Ag-Sn system are taken from the assessment of Oh *et al.* **[96Oh]**. The data for the FCC_A1 phase have been remodelled within the scope of the COST 531 project to be compatible with the adopted data for FCC_A1 (Sn) **[SGTE4]**. The Gibbs energy expression of the liquid phase was re-optimised using the raw enthalpy of mixing data from Flandorfer **[05Fla]** in addition to the other experimental data compiled by Chevalier **[05Che]**.

References:

[96Oh] Oh, C.-S., Shim, J.-H., Lee, B.-J., Lee, D. N.: *J. Alloys Compd.*, 1996, **238**, 155-166.

[05Che] Chevalier, P. Y.: Unpublished work, 2005.

[05Fla] Flandorfer, H.: Unpublished work, 2005.

Table of invariant reactions

T / °C	Phases			Compositions / x_{Sn}		
961.8	LIQUID	FCC_A1		0.000	0.000	
719.3	FCC_A1	HCP_A3	LIQUID	0.115	0.131	0.211
481.7	HCP_A3	AGSB_ORTHO	LIQUID	0.239	0.250	0.484
231.9	LIQUID	BCT_A5		1.000	1.000	
219.8	AGSB_ORTHO	LIQUID	BCT_A5	0.250	0.961	1.000
13.1	AGSB_ORTHO	BCT_A5	DIAMOND_A4	0.250	1.000	1.000
13.0	BCT_A5	DIAMOND_A4		1.000	1.000	

Phase information

Phase Name	Common Name	Strukturbericht designation	Pearson Symbol
LIQUID	Liquid		
AGSB_ORTHO	ε	$D0_a$	$oP8$
HCP_A3	ζ	$A3$	$hP2$
DIAMOND_A4	(αSn)	$A4$	$cF8$
BCT_A5	(βSn)	$A5$	$tI4$
FCC_A1	(Ag)	$A1$	$cF4$

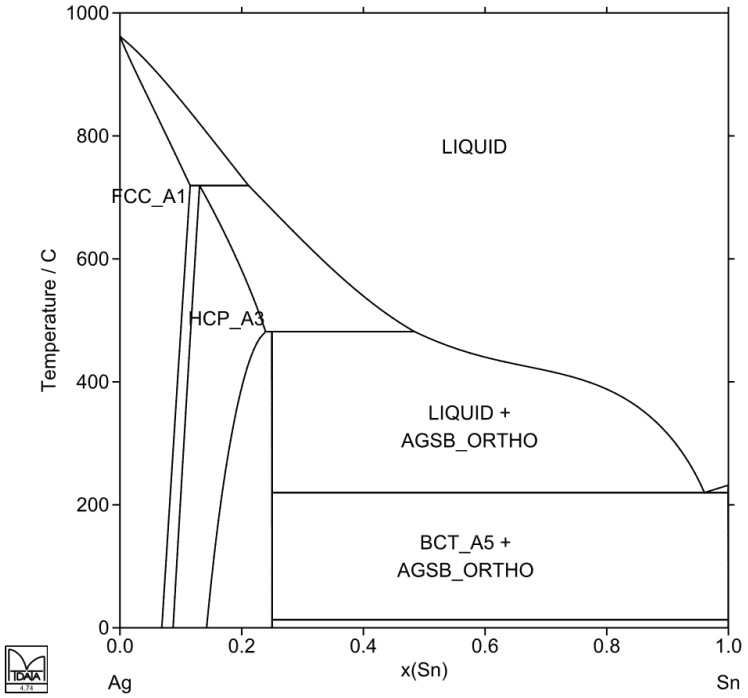

Fig. 9: Phase diagram of the Ag-Sn system

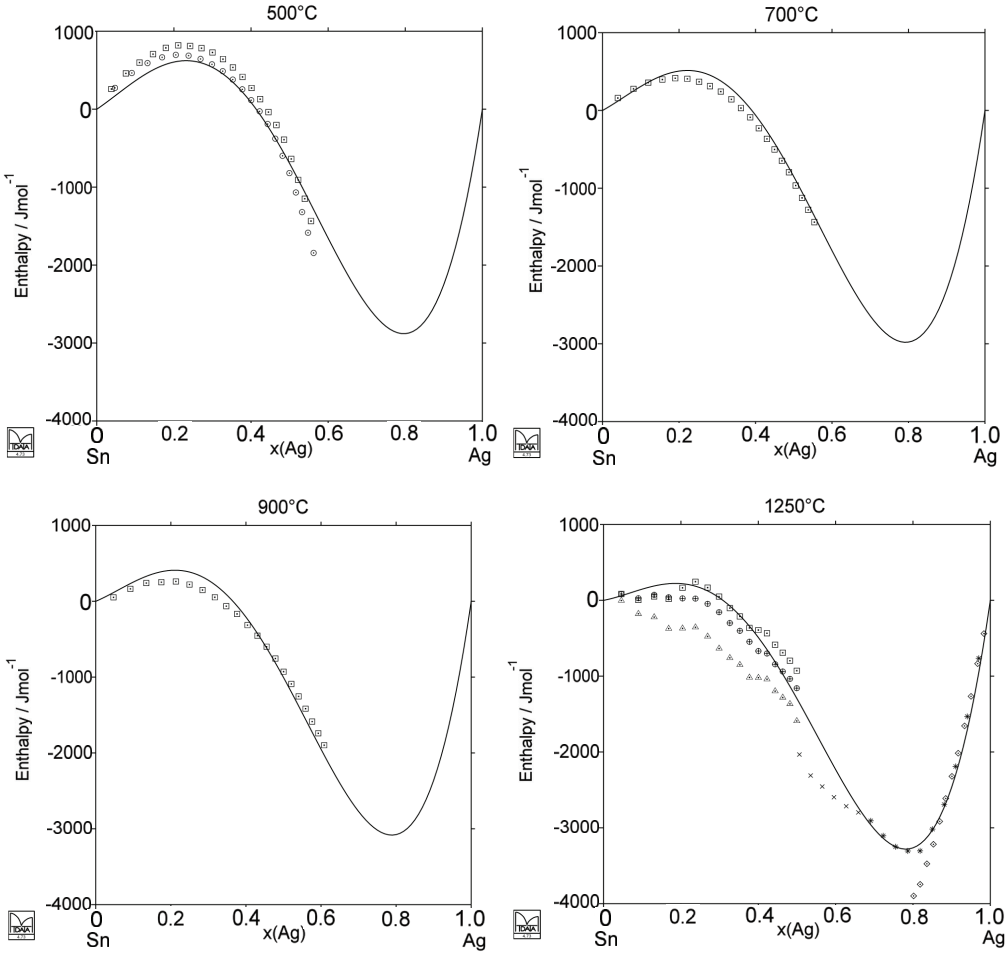

Fig. 10: Calculated enthalpies of mixing of the Ag-Sn system with experimental data of Flandorfer [05Fla] superimposed

Ag-Zn System

The data for this system are from an unpublished assessment by Fries and Witusiewicz **[02Fri]**. This is a more rigorous modelling of the system than documented in their later published data assessment **[06Wit]**.

References:

[02Fri] Fries, S. G., Witusiewicz V. T.: Unpublished work, 2002.

[06Wit] Witusiewicz, V. T., Fries, S. G., Hecht, U., Drevermann, A., Rex, S.: *Int. J. Mater. Res.*, 2006, **97**, 556-568.

Table of invariant reactions

T / °C	Phases			Compositions / x_{Zn}		
961.8	LIQUID	FCC_A1		0.000	0.000	
709.6	FCC_A1	BCC_A2	LIQUID	0.324	0.371	0.373
660.0	BCC_A2	AGZN_BRASS	LIQUID	0.583	0.612	0.624
630.2	AGZN_BRASS	HCP_A3	LIQUID	0.635	0.689	0.708
430.5	HCP_A3	HCP_ZN	LIQUID	0.865	0.963	0.978
419.5	LIQUID	HCP_ZN		1.000	1.000	
270.0	BCC_A2	AGZN_ZETA	AGZN_BRASS	0.487	0.492	0.606
261.8	FCC_A1	BCC_A2	AGZN_ZETA	0.404	0.450	0.458

Phase information

Phase Name	Common Name	Strukturbericht designation	Pearson Symbol
LIQUID	Liquid		
HCP_ZN	(Zn)	*A*3 *mod*	*hP*2
FCC_A1	(Ag)	*A*1	*cF*4
HCP_A3	ε	*A*3	*hP*2
BCC_A2	β	*A*2	*cI*2
AGZN_ZETA	ζ	B_b	*hP*9
AGZN_BRASS	γ	$D8_2$	*cI*52

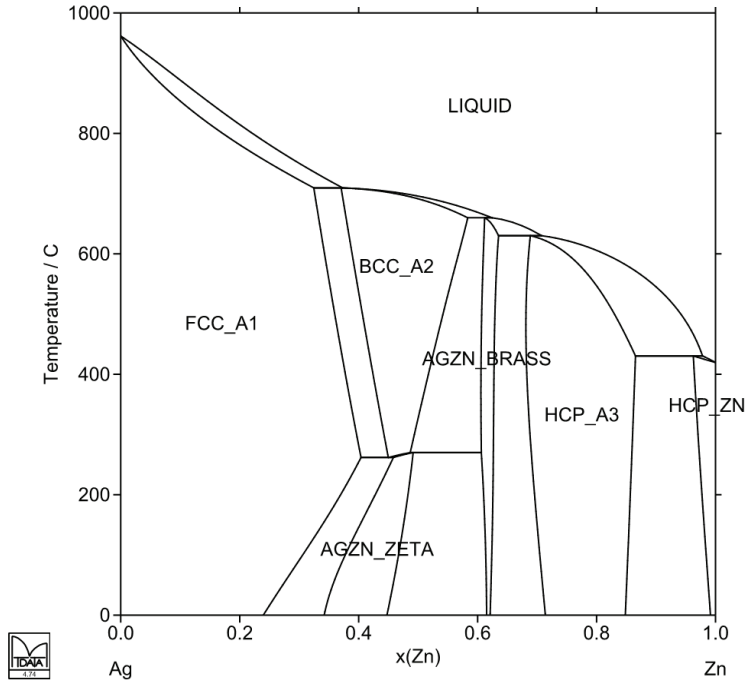

Fig. 11: Phase diagram of the Ag-Zn system

Au-Bi System

The data for this system are taken from a recent assessment by Servant *et al.* **[06Ser]** carried out within the framework of COST 531 using new experimental data **[05Zor]**. The major difference between this assessment and that of Chevalier **[88Che]** is the revised solubility of Bi in Au (FCC_A1) and the temperature of the invariant reaction, AU2BI_C15 → FCC_A1 + RHOMBO_A7. The new theoretical description is in better agreement with the experimental data.

References:

[88Che] Chevalier, P. Y.: *Thermochimica Acta*, 1988, **130**, 15-24.

[05Zor] Zoro, E., Boa, D., Servant, C., Legendre, B.: *J. Alloys. Compd.*, 2005, **398**, 106-112.

[06Ser] Servant, C., Zoro, E., Legendre, B.: *CALPHAD*, 2006, **30**, 443-448.

Table of invariant reactions

T / °C	Phases			Compositions / x_{Bi}		
1064.2	LIQUID	FCC_A1		0.000	0.000	
377.5	FCC_A1[(a)]	AU2BI_C15	LIQUID	0.000	0.333	0.667
271.4	LIQUID	RHOMBO_A7		1.000	1.000	
240.9	AU2BI_C15	LIQUID	RHOMBO_A7[(b)]	0.333	0.854	1.000
110.0	FCC_A1[(a)]	AU2BI_C15	RHOMBO_A7[(b)]	0.000	0.333	1.000

[(a)] The FCC_A1 composition is almost pure Au.
[(b)] The RHOMBO_A7 composition is almost pure Bi.

Phase information

Phase Name	Common Name	Strukturbericht designation	Pearson Symbol
LIQUID	Liquid		
RHOMBO_A7	(Bi)	$A7$	$hR2$
AU2BI_C15	Au_2Bi	$C15$	$cF24$
FCC_A1	(Au)	$A1$	$cF4$

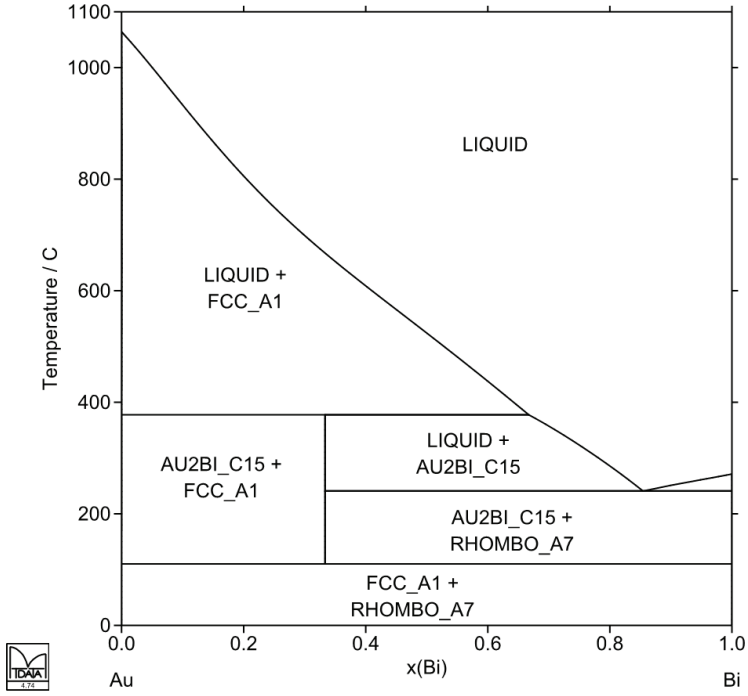

Fig. 12: Phase diagram of the Au-Bi system

Au-Cu System

Data for the Au-Cu system are taken from the critical assessment of Sundman *et al.* **[98Sun]**. The authors presented two datasets in their publication, the first taking into account and modelling the low temperature chemical ordering phases derived from a FCC lattice and the second dataset ignoring the chemical ordering. The second dataset has been selected for the COST 531 database, as this feature does not have a significant influence in the systems for lead free solders.

References:

[98Sun] Sundman, B., Fries, S. G., Oates, W. A.: *CALPHAD*, 1998, **22**, 335-354.

Table of invariant reactions

T / °C	Phases			Compositions / x_{Cu}		
1084.6	LIQUID	FCC_A1		1.000	1.000	
1064.2	LIQUID	FCC_A1		0.000	0.000	
911.1	LIQUID	FCC_A1		0.446	0.446	

Phase information

Phase Name	Common Name	Strukturbericht designation	Pearson Symbol
LIQUID	Liquid		
FCC_A1	(Au, Cu)	*A*1	*cF*4

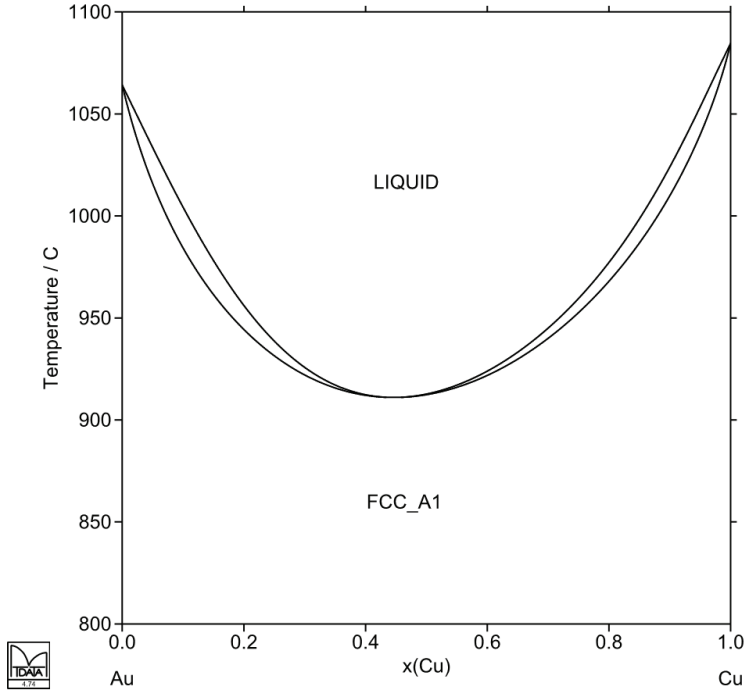

Fig. 13: Phase diagram of the Au-Cu system

Au-In System

There are a number of assessments of this system in the scientific literature, the major differences between them being associated with the homogeneity range of the DHCP phase in the Au-rich side of the system and its decomposition with decreasing temperature. The data accepted for this work was taken from **[03Liu]** in order to be compatible with experimental data available for the Au-In-Sn ternary system. The phase diagram is highly complex with many intermetallic compounds. Owing to this complexity, it was not possible to label all phases in **Fig. 14**; the unlabelled phase at x(In) ~ 0.2 is AUIN_BETA. The AU3IN (ε) phase was modelled as a single stoichiometric phase, whereas two variants have been reported experimentally; ε and the low temperature variant ε'. An ordering reaction between the two phases takes place at approximately 339.5 °C **[MAS]**.

References:

[03Liu] Liu, H. S., Cui, Y., Ishida, K., Jin, Z. P.: *CALPHAD*, 2003, **27**, 27-37.

Table of invariant reactions

T / °C	Phases			Compositions / x_{In}		
1064.2	LIQUID	FCC_A1		0.000	0.000	
647.2	FCC_A1	DHCP	LIQUID	0.139	0.145	0.225
640.5	DHCP	HCP_A3	LIQUID	0.148	0.159	0.228
494.7	AUIN	LIQUID	AUIN2	0.500	0.545	0.667
538.5	LIQUID	AUIN2		0.667	0.667	
505.7	LIQUID	AUIN		0.500	0.500	
486.8	HCP_A3	AU3IN	LIQUID	0.209	0.250	0.290
482.6	AU3IN	AUIN_GAMMA	LIQUID	0.250	0.290	0.293
460.6	LIQUID	AUIN_PSI		0.381	0.381	
455.7	AUIN_PSI	LIQUID	AUIN	0.393	0.408	0.500
452.3	AUIN_GAMMA	LIQUID	AUIN_PSI	0.305	0.344	0.363
376.5	AUIN3	AU7IN3	AUIN_GAMMA	0.250	0.300	0.301
364.5	AU7IN3	AUIN_GAMMA	AUIN_PSI	0.300	0.306	0.370
337.3	HCP_A3	AUIN_BETA	AU3IN	0.188	0.215	0.250
295.0	AUIN_BETA	AUIN_BETAP	AU3IN	0.215	0.222	0.250
274.9	HCP_A3	AUIN_BETA	AUIN_BETAP	0.178	0.215	0.222
224.1	AU7IN3	AUIN_PSI	AUIN	0.300	0.390	0.500
156.6	LIQUID	TETRAG_A6		1.000	1.000	
156.2	AUIN2	LIQUID	TETRAG_A6	0.667	0.999	1.000

Phase information

Phase Name	Common Name	Strukturbericht designation	Pearson Symbol
LIQUID	Liquid		
FCC_A1	(Au)	$A1$	$cF4$
DHCP	α_1	$D0_{24}$	$hP16$
HCP_A3	ζ	$A3$	$hP2$
AUIN_BETA	β	···	hP^*
AUIN_BETAP	β_1	···	$hP26$
AU3IN	ε' (LT) ε (HT)	$D0_a$ ···	$oP8$ ···
AU7IN3	γ'	···	$hP60$
AUIN_GAMMA	γ	$D8_3$	$cP52$
AUIN_PSI	ψ	$D5_{19}$	$hP5$
AUIN	AuIn	···	(triclinic)
AUIN2	$AuIn_2$	$C1$	$cF12$
TETRAG_A6	(In)	$A6$	$tI2$

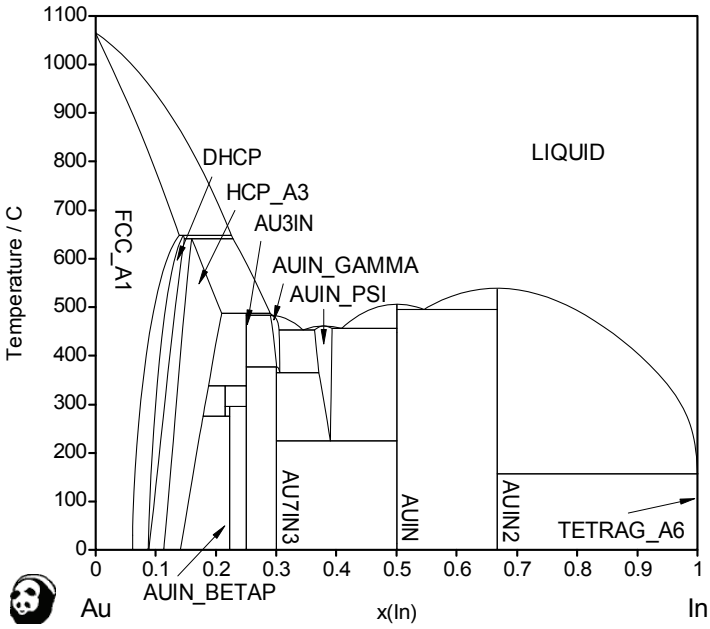

Fig. 14: Phase diagram of the Au-In system

Au-Ni System

Data for the Au-Ni system are taken from a recent assessment by Wang *et al.* **[05Wan]**. This agrees much better with experimental data for the system than earlier assessments **[99Mor]**, **[05Liu]**. Use of the new data did not adversely affect agreement between calculated and experimental properties for the ternary Au-Ni-Sn system which had been based on the assessment of Liu *et al.* **[05Liu]**.

References:

[99Mor] Morioka, S., Hasebe, M.: *J. Phase Equil.*, 1999, **20**, 244-257.

[05Liu] Liu, X. J., Knaka, M., Takaku, Y., Ohnuma, I., Kainuma, R., Ishida, K.: *J. Electron. Mater.*, 2005, **34**, 670-679.

[05Wan] Wang, J., Lu, X.-G., Sundman, B., Su, X.: *CALPHAD*, 2005, **29**, 263-268.

Table of invariant reactions

T / °C	Phases			Compositions / x_{Ni}		
1455.1	LIQUID	FCC_A1#2		1.000	1.000	
1064.2	LIQUID	FCC_A1#1		0.000	0.000	
816.4	FCC_A1	FCC_A1#1	FCC_A1#2	0.730	0.730	0.730

Phase information

Phase Name	Common Name	Strukturbericht designation	Pearson Symbol
LIQUID	Liquid		
FCC_A1	(Au) (Ni)	*A*1	*cF*4

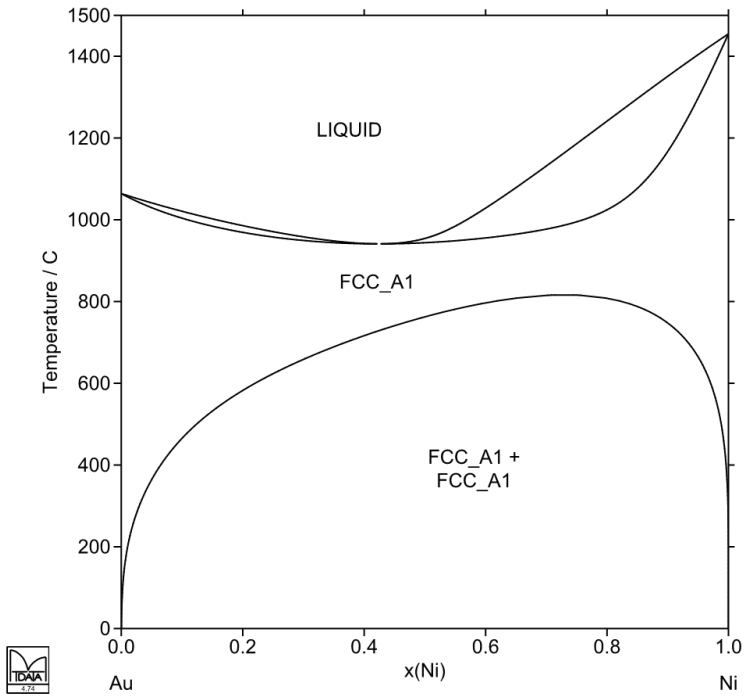

Fig. 15: Phase diagram of the Au-Ni system

Au-Pb System

The dataset for this system was taken from v.4.4 of the SGTE solution database **[SGTE]**, and the source of this data is the thesis of Nabot **[86Nab]**. The system is fairly simple and contains three peritectically forming intermetallic compounds, each one being modelled as a stoichiometric phases. According to **[MAS]**, there is some uncertainty as to the temperature range over which the AUPB3 phase is stable. There are reports that it decomposes below 52 °C.

References:

[86Nab] Nabot, J.-P.: Thesis, LTPCM, Grenoble, France, 1986.

Table of invariant reactions

T / °C	Phases			Compositions / x_{Pb}		
1064.2	LIQUID	FCC_A1#1		0.000	0.000	
430.5	FCC_A1#1	AU2PB_C15	LIQUID	0.022	0.333	0.445
327.5	LIQUID	FCC_A1#2		1.000	1.000	
253.1	AU2PB_C15	AUPB2	LIQUID	0.333	0.667	0.735
221.9	AUPB2	AUPB3	LIQUID	0.667	0.750	0.821
213.9	AUPB3	LIQUID	FCC_A1#2	0.750	0.845	0.994

Phase information

Phase Name	Common Name	Strukturbericht designation	Pearson Symbol
LIQUID	Liquid		
FCC_A1	(Au), (Pb)	*A*1	*cF*4
AU2PB_C15	Au_2Pb	*C*15	*cF*24
AUPB2	$AuPb_2$	*C*16	*tI*12
AUPB3	$AuPb_3$	...	*tI*32

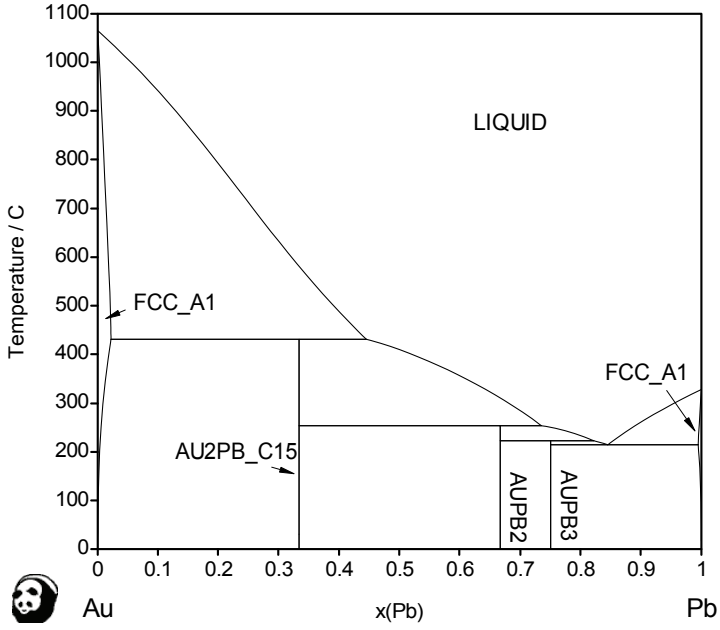

Fig. 16: Phase diagram of the Au-Pb system

Au-Pd System

The Au-Pd system has a simple isomorphous phase diagram showing complete solid solubility over the whole composition range. The thermodynamic data for this system was taken from the v.4.4 of the SGTE solution database **[SGTE]**. Ordering in the solid state has been confirmed at compositions of Au_3Pd, AuPd and $AuPd_3$ **[MAS]**, but it has not been modelled here.

Table of invariant reactions

T / °C	Phases			Compositions / x_{Pd}		
1554.8	LIQUID	FCC_A1#2		1.000	1.000	
1064.2	LIQUID	FCC_A1#1		0.000	0.000	

Phase information

Phase Name	Common Name	Strukturbericht designation	Pearson Symbol
LIQUID	Liquid		
FCC_A1	(Au, Pd)	*A*1	*cF*4

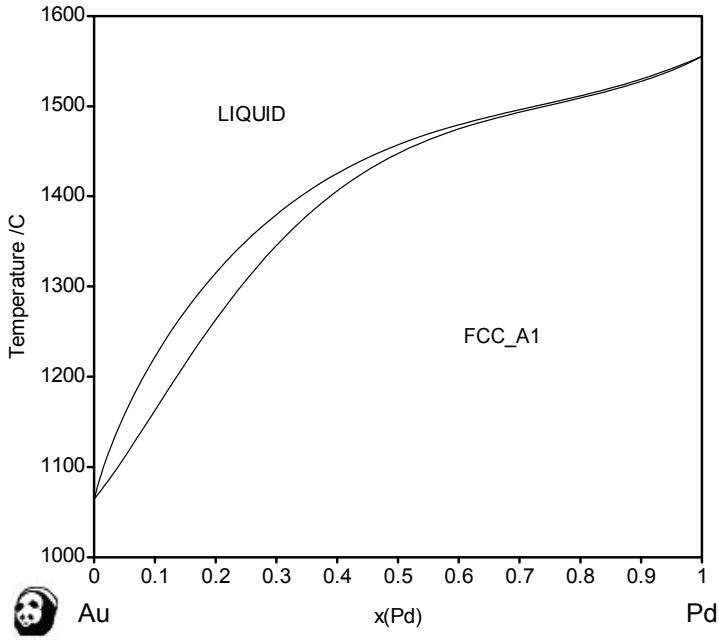

Fig. 17: Phase diagram of the Au-Pd system

Au-Sb System

The data for the Au-Sb system were taken from a recent assessment by Zoro *et al.* **[07Zor]** which incorporated earlier assessed data from Kim *et al.* **[02Kim]**. Zoro *et al.* found that the assessment of Kim *et al.* was in better agreement with experimental measurements of phase equilibria they had carried out than an earlier assessment of Chevalier **[89Che]**.

References:

[89Che] Chevalier, P. Y.: *Thermochimica Acta*, 1989, **155**, 211-225.

[02Kim] Kim, J. H., Jeong, S. W., Lee, H. M.: *J. Electron. Mater.*, 2002, **31**, 557-563.

[07Zor] Zoro, E., Servant, C., Legendre, B.: *J. Phase Equil. Diff.*, 2007, **28**, 250-257.

Table of invariant reactions

T / °C	Phases			Compositions / x_{Sb}		
1064.2	LIQUID	FCC_A1		0.000	0.000	
630.6	LIQUID	RHOMBO_A7		1.000	1.000	
460.0	LIQUID	AUSB2	RHOMBO_A7	0.655	0.667	1.000
359.5	FCC_A1	LIQUID	AUSB2	0.007	0.362	0.667

Phase information

Phase Name	Common Name	Strukturbericht designation	Pearson Symbol
LIQUID	Liquid		
FCC_A1	(Au)	*A*1	*cF*4
AUSB2	$AuSb_2$	*C*2	*cP*12
RHOMBO_A7	(Sb)	*A*7	*hR*2

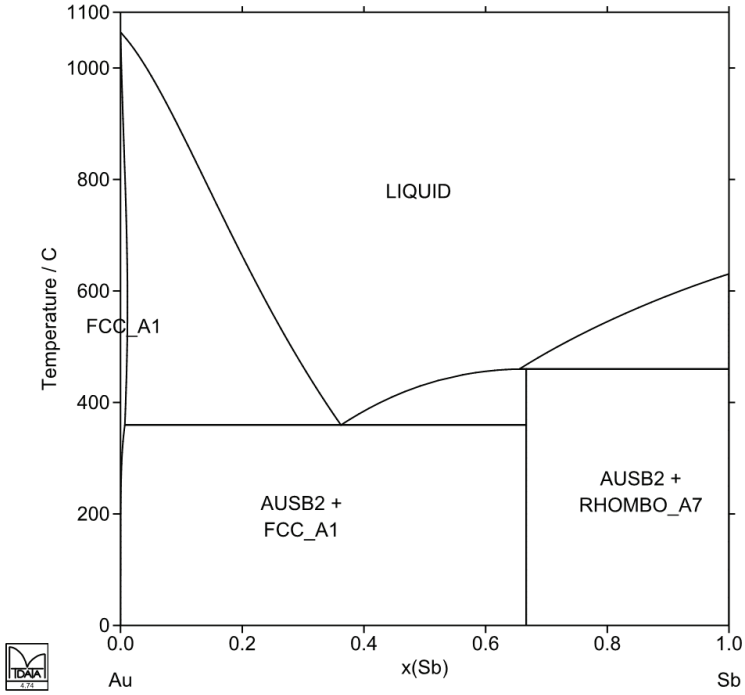

Fig. 18: Phase diagram of the Au-Sb system

Au-Sn System

The critically assessed data for the Au-Sn system from Liu *et al.* **[03Liu1]** were adopted for the COST 531 database because of their compatibility with data selected for the Au-In system **[03Liu2]** and in particular with data for the AUIN_ALPHA phase which is isomorphous with the $Au_{10}Sn$ phase. The data for the Au-Sn system were adjusted to be consistent with adopted unary data for Sn in the HCP_A3 and FCC_A1 phases.

References:

[03Liu1] Liu, H. S., Liu, C. L., Ishida, K., Jin, Z, P.: *J. Electron. Mater*., 2003, **32**, 1290-1296.

[03Liu2] Liu, H. S., Cui, Y., Ishida, K., Jin, Z. P.: *CALPHAD*, 2003, **27**, 27-37.

Table of invariant reactions

T / °C	Phases			Compositions / x_{Sn}		
1064.2	LIQUID	FCC_A1		0.000	0.000	
532.0	FCC_A1	DHCP	LIQUID	0.073	0.090	0.206
522.2	DHCP	HCP_A3	LIQUID	0.092	0.111	0.209
418.8	LIQUID	AU1SN		0.500	0.500	
310.6	AU1SN	AUSN2	LIQUID	0.500	0.667	0.723
277.8	HCP_A3	LIQUID	AU1SN	0.163	0.304	0.500
251.8	AUSN2	AUSN4	LIQUID	0.667	0.800	0.887
231.9	LIQUID	BCT_A5		1.000	1.000	
214.9	AUSN4	LIQUID	BCT_A5	0.800	0.954	1.000
179.3	HCP_A3	AU5SN	AU1SN	0.138	0.160	0.500
49.8	AUSN2	AUSN4	BCT_A5	0.667	0.800	1.000
13.1	AUSN2	BCT_A5	DIAMOND_A4	0.667	1.000	1.000
13.0	BCT_A5	DIAMOND_A4		1.000	1.000	

Phase information

Phase Name	Common Name	Strukturbericht designation	Pearson Symbol
LIQUID	Liquid		
FCC_A1	(Au)	$A1$	$cF4$
DHCP	β/$Au_{10}Sn$	$D0_{24}$	$hP16$
HCP_A3	ζ	$A3$	$hP2$
AU5SN	ζ'/Au_5Sn	...	$hP*$
AU1SN	δ/AuSn	$B8_1$	$hP4$
AUSN2	ε/$AuSn_2$	...	$o**$
AUSN4	η/$AuSn_4$	$D1_c$	$oC20$
BCT_A5	(βSn)	$A5$	$tI4$
DIAMOND_A4	(αSn)	$A4$	$CF8$

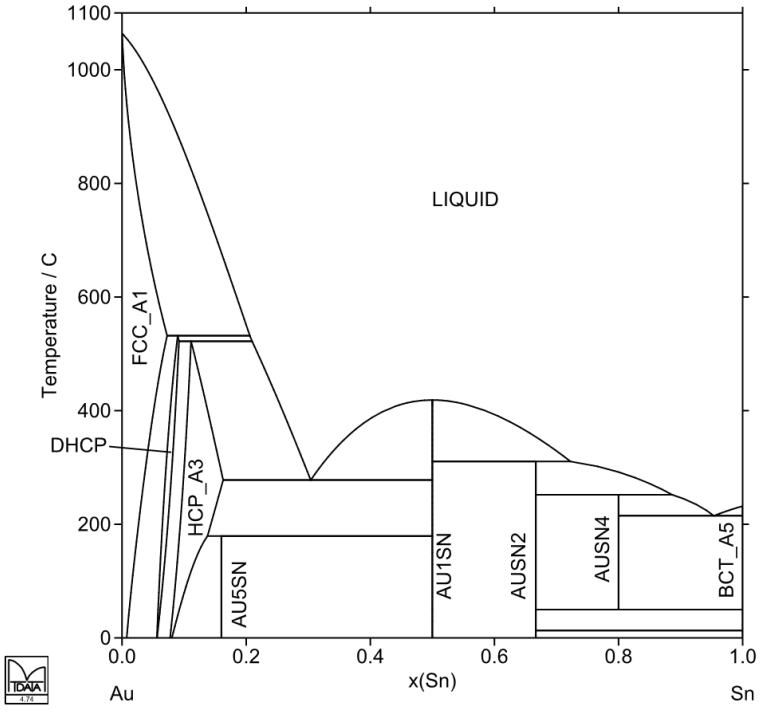

Fig. 19: Phase diagram of the Au-Sn system

Au-Zn System

The Au-Zn phase diagram is exceedingly complex and is characterised by a cascade of peritectic reactions on the zinc side of the diagram. There are 13 intermetallic phases (11 of which have been modelled) including an ordered bcc phase (AUZN_BETA) and a γ-brass phase (AUZN_BRASS). There are reports that the ordered bcc phase undergoes a low temperature transition **[MAS]** but this is not modelled here. The α'_2 phase given in **[MAS]** has also been ignored in the present work. The dataset chosen for this work comes from **[03Liu]** with modifications being made to the data for the AUZN_G3 phase to make it compatible with other hcp phases in the database, and to the data for the AUZN_BETA phase in order to remove a very narrow unrealistic miscibility gap that appears during calculation. Owing to the complexity of the phase diagram, two of the intermetallics have not been labelled in **Fig. 20**. These are AUZN_DELTA at x(Zn)=0.56 and AUZN_E1 at x(Zn)=0.85. The crystallography of many of the intermetallic phases in this system still remains a mystery and hence it has been convenient to model many of them as stoichiometric compounds. Owing to pure Zn having a different c/a ratio from other elements with the hcp structure, it is modelled as a different phase and is labelled HCP_ZN.

References:

[03Liu] Liu, H. S., Ishida, K., Jin, Z. P., Du, Y.: *Intermetallics*, 2003, **11**, 987-994.

Table of invariant reactions

T / °C	Phases			Compositions / x_{Zn}		
1064.2	LIQUID	FCC_A1		0.000	0.000	
734.6	LIQUID	AUZN_BETA		0.490	0.490	
681.7	FCC_A1	LIQUID	AUZN_BETA	0.346	0.361	0.397
680.7	LIQUID	AUZN_BRASS		0.667	0.667	
673.2	AUZN_BETA	LIQUID	AUZN_BRASS	0.572	0.625	0.647
584.7	AUZN_BRASS	AUZN_G3	LIQUID	0.740	0.801	0.819
521.8	AUZN_BRASS	AUZN_G2	AUZN_G3	0.742	0.750	0.800
489.8	AUZN_G3	HCP_A3	LIQUID	0.846	0.880	0.927
442.7	HCP_A3	HCP_ZN	LIQUID	0.903	0.954	0.965
419.5	LIQUID	HCP_ZN		1.000	1.000	
406.9	FCC_A1	AUZN_A1		0.256	0.256	
401.2	AUZN_A1	FCC_A1	AUZN_BETA	0.270	0.283	0.369
305.3	AUZN_A1	AU5ZN3	AUZN_BETA	0.288	0.375	0.399
297.1	FCC_A1	AUZN_A3	AUZN_A1	0.160	0.185	0.220
272.9	AUZN_A1	AUZN_A2		0.250	0.250	
179.8	AUZN_BETA	AUZN_DELTA	AUZN_BRASS	0.547	0.560	0.661
169.9	AUZN_G3	AUZN_E1	HCP_A3	0.841	0.850	0.869
33.9	AUZN_G2	AUZN_G3	AUZN_E1	0.750	0.827	0.850

Phase information

Phase Name	Common Name	Strukturbericht designation	Pearson Symbol
LIQUID	Liquid		
FCC_A1	(Au)	*A*1	*cF*4
AUZN_A1	α_1	…	Tetragonal (antiphase domain)
AUZN_A2	α_2	…	Orthorhombic (antiphase domain)
AUZN_A3	α_3	…	*tP*28
AU5ZN3	Au_5Zn_3	…	Orthorhombic (antiphase domain)
AUZN_BETA	β’	*B*2	*cP*2
AUZN_DELTA	δ	…	…
AUZN_BRASS	γ /γ-brass	$D8_2$	*cI*52
AUZN_G2	γ_2	…	*cP*32
AUZN_G3	γ_3	…	*hP**
HCP_A3	ε	*A*3	*hP*2
AUZN_E1	ε’	…	Orthorhombic (pseudocell)
HCP_ZN	(Zn)	*A*3 *mod*	*hP*2

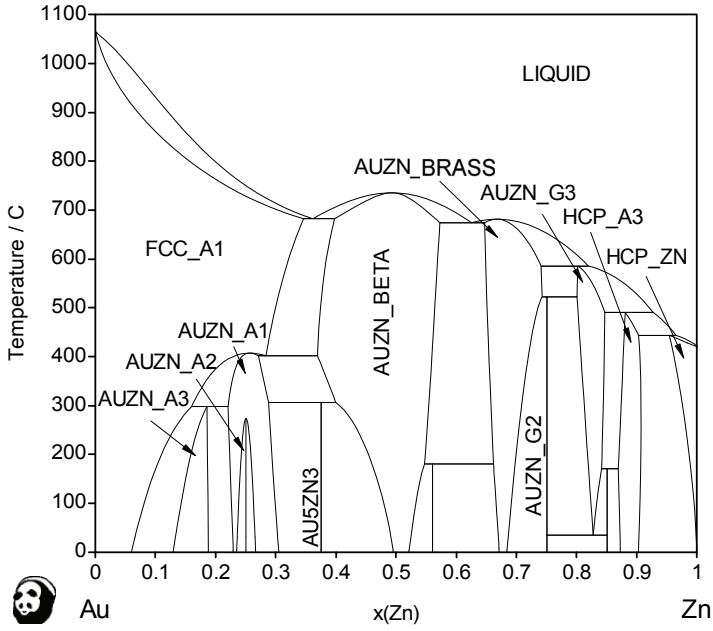

Fig. 20: Phase diagram of the Au-Zn system

Bi-Cu System

The Bi-Cu system is a simple eutectic system showing virtually no mutual solubility of the component elements. The thermodynamic description is taken from **[89Tep]**.

References:

[89Tep] Teppo, O., Niemela, J., Taskinen, P.: Report TKK-V-B50, 1989, Helsinki University of Technology.

Table of invariant reactions

T / °C	Phases			Compositions / x_{Cu}		
1084.6	LIQUID	FCC_A1		1.000	1.000	
271.4	LIQUID	RHOMBO_A7		0.000	0.000	
270.5	RHOMBO_A7	LIQUID	FCC_A1	0.000	0.004	0.999

Phase information

Phase Name	Common Name	Strukturbericht designation	Pearson Symbol
LIQUID	Liquid		
RHOMBO_A7	(Bi)	*A*7	*hR*2
FCC_A1	(Cu)	*A*1	*cF*4

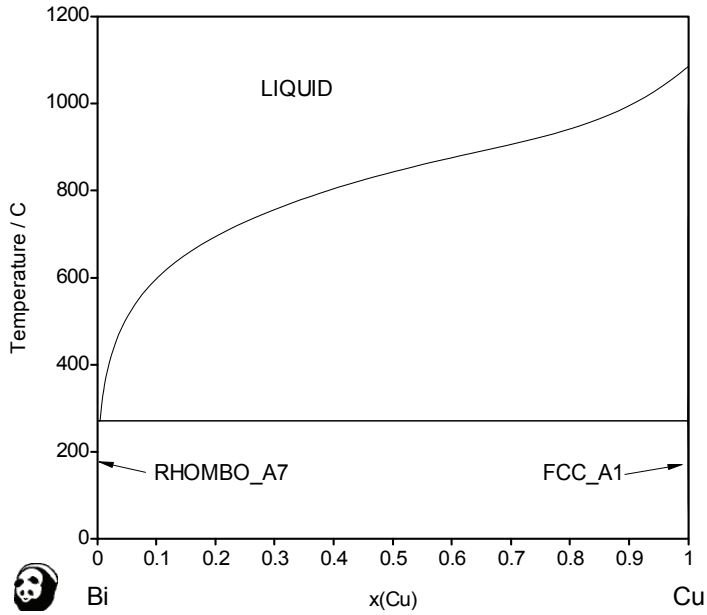

Fig. 21: Phase diagram of the Bi-Cu system.

Bi-In System

The data from Boa and Ansara **[94Boa]** were accepted for most of the phases in the system. A reassessment of the ε-BiIn phase was necessary, as this phase is isomorphic from the crystallographic point of view with the In-Pb phase, named TET-ALPHA1 in the database. New parameters were also derived within the scope of COST 531 Action since different unary data for the pure elements in this phase were used by **[94Boa]** from those selected from the COST 531 database. Very good agreement was reached, both in the terms of the temperatures of the invariant reaction and range of homogeneity of the TET_ALPHA1 phase, using the old and new descriptions.

References:

[94Boa] Boa, D., Ansara. I.: *Thermochim. Acta*, 1998, **314**, 79-86.

Table of invariant reactions

T / °C	Phases			Compositions / x_{In}		
271.4	LIQUID	RHOMBO_A7		0.000	0.000	
156.6	LIQUID	TETRAG_A6		1.000	1.000	
109.8	LIQUID	BIIN		0.500	0.500	
109.2	RHOMBO_A7	LIQUID	BIIN	0.000	0.474	0.500
90.9	LIQUID	TET_ALPHA1	TETRAG_A6	0.829	0.900	0.921
88.7	BIIN	BI3IN5	LIQUID	0.500	0.625	0.650
87.8	LIQUID	BIIN_BRASS		0.667	0.667	
87.8	BI3IN5	LIQUID	BIIN_BRASS	0.625	0.663	0.667
71.6	BIIN_BRASS	LIQUID	TET_ALPHA1	0.667	0.779	0.847
46.6	BIIN_BRASS	TET_ALPHA1	TETRAG_A6	0.667	0.891	0.919

Phase information

Phase Name	Common Name	Strukturbericht designation	Pearson Symbol
LIQUID	Liquid		
RHOMBO_A7	(Bi)	*A*7	*hR*2
BIIN	BiIn	*B*10	*tP*4
BI3IN5	Bi_3In_5	$D8_1$	*tI*32
BIIN_BRASS	$BiIn_2$	$B8_2$	*hP*6
TET_ALPHA1	ε	*A*6 *mod*	*tI*2
TETRAG_A6	(In)	*A*6	*tI*2

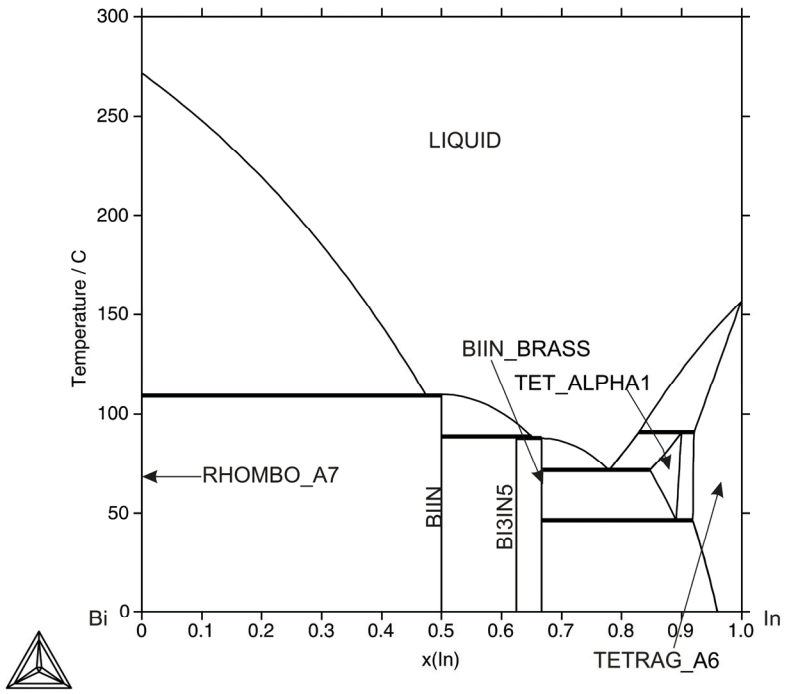

Fig. 22: Phase diagram of the Bi-In system

Bi-Ni System

Data for the Bi-Ni system were assessed by Vassilev *et al.* **[07Vas]** within the scope of the COST 531 Action. This assessment incorporated new experimental data for the activity of Bi in the liquid phase and so required a re-evaluation of an earlier assessment **[05Vas].**

References:

[05Vas] Vassilev, G. P., Liu, X. J., Ishida, K.: *J. Phase Equilib. Diffus.*, 2005, **26**, 161-168.

[07Vas] Vassilev, G. P., Romanowska, J., Wnuk, G.: *Int. J. Mat. Res.*, 2007, **98**, 468-475.

Table of invariant reactions

T / °C	Phases			Compositions / x_{Ni}		
1455.1	LIQUID	FCC_A1		1.000	1.000	
645.8	LIQUID	BINI	FCC_A1	0.238	0.490	0.978
464.8	LIQUID	BI3NI	BINI	0.123	0.250	0.485
271.4	LIQUID	RHOMBO_A7		0.000	0.000	
269.8	RHOMBO_A7	LIQUID	BI3NI	0.000	0.007	0.250

Phase information

Phase Name	Common Name	Strukturbericht designation	Pearson Symbol
LIQUID	Liquid		
RHOMBO_A7	(Bi)	*A*7	*hR*2
FCC_A1	(Ni)	*A*1	*cF*4
BI3NI	$NiBi_3$	...	...
BINI	NiBi	$B8_1$	*hP*4

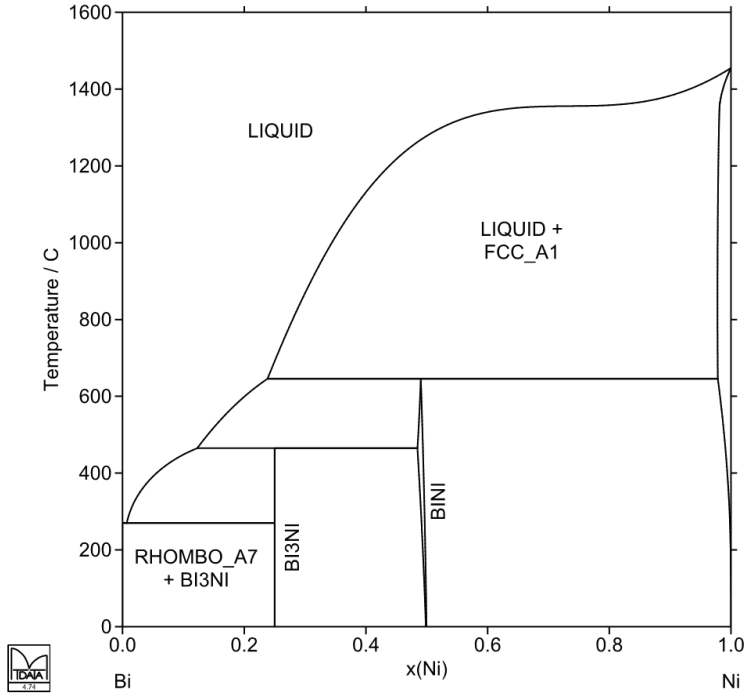

Fig. 23: Phase diagram of the Bi-Ni system

Bi-Pb System

The Bi-Pb system exhibits both a eutectic reaction and the peritectic formation of an intermetallic HCP phase. A considerable amount of Bi may dissolve in crystalline Pb but there is negligible solubility for Pb in crystalline Bi. The thermodynamic description for this system is taken from **[98Boa]** quoting private communication with H.L. Lukas.

References:

[98Boa] Boa D., Ansara, I.: *Thermochim. Acta*, 1998, **314**, 79-86.

Table of invariant reactions

T / °C	Phases			Compositions / x_{Pb}		
327.5	LIQUID	FCC_A1		1.000	1.000	
271.4	LIQUID	RHOMBO_A7		0.000	0.000	
183.6	LIQUID	HCP_A3	FCC_A1	0.625	0.705	0.769
125.0	RHOMBO_A7	LIQUID	HCP_A3	0.001	0.445	0.572

Phase information

Phase Name	Common Name	Strukturbericht designation	Pearson Symbol
LIQUID	Liquid		
RHOMBO_A7	(Bi)	*A*7	*hR*2
HCP_A3	ε	*A*3	*hP*2
FCC_A1	(Pb)	*A*1	*cF*4

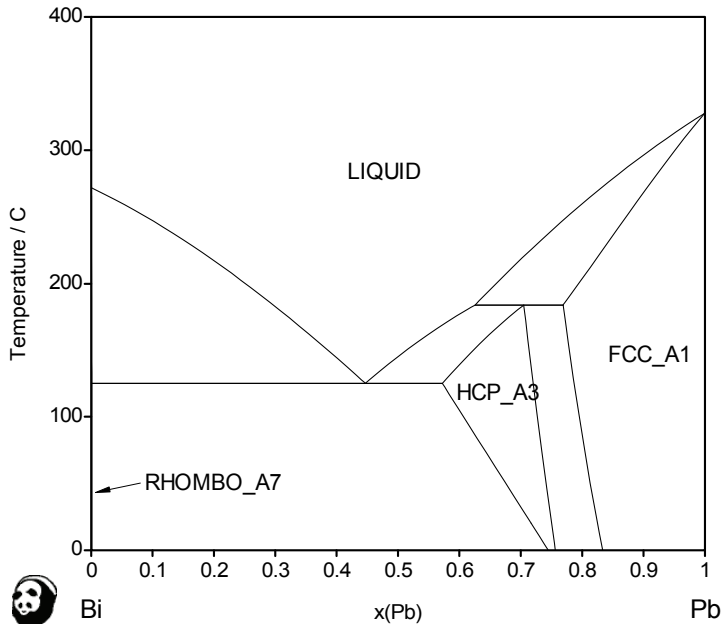

Fig. 24: Phase diagram of the Bi-Pb system

Bi-Pd System

Several versions of the Bi-Pd phase diagram are available in the literature, the main difference between them being associated with the Pd-rich equilibria. Little work has been carried out on this part of the system and so it is relatively unknown. Also, no thermodynamic assessment of this system had been carried out prior to COST 531, which made the Bi-Pd system subject to extensive study during the Action. According to **[MAS]**, there are 6 intermetallic phases in the system, 3 of which have high and low-temperature modifications. The Bi-rich α,β-Bi_2Pd phase (BI2PD) has a narrow homogeneity range, and it is unclear whether it forms congruently or peritectically from the liquid. The remaining phases are present as line compounds apart from the γ-phase (BI3PD5) which exists as a 'triangular' phase field over approximately 6 at% but only from about 400 – 683 °C, although the lower temperature limit for this phase is uncertain.

As part of the study undertaken under COST 531, enthalpies of mixing of liquid alloys were determined by high-temperature solution calorimetry for compositions from 0 – 50 at% Pd at 1028K, and enthalpies of formation of the BI2PD and BIPD intermetallic phases were determined by *ab initio* methods. Selected DTA and SEM studies were carried out on alloys in the Pd-rich region of the diagram in order to ascertain the phase relationships in the unknown part of the system. The experimental data were used in conjunction with phase diagram information taken from the literature to perform a thermodynamic assessment of the system. Some simplifications were made in that the distinction between high and low-temperature modifications of the phases was ignored, as were the Bi_2Pd_5 and $Bi_{12}Pd_{31}$ phases owing to uncertainties in their stability. Reference to these two phases is found only in the work of **[79Sar]**. However, these phases were not found in the present experimental study, and hence they were not included in the optimisation. The experimental details, results and the modelling are presented in **[06Vre]**.

Fig. 25 shows the calculated phase diagram, which retains the 'degenerate' nature of the melting of BI2PD. As a result of the experimental study, the melting of BIPD3 is now shown as congruent rather than incongruent as presented in **[MAS]**. The γ-phase (BI3PD5) has now a much larger temperature stability range.

References:

[79Sar] Sarah, N., Schubert, K.: *J. Less-Common Met*., 1979, **63**, P75-P82.

[06Vre] Vřešťál, J., Pinkas, J., Watson, A., Scott, A., Houserová, J., Kroupa, A.: *CALPHAD*, 2006, **30**, 14-17.

Table of invariant reactions

T / °C	Phases			Compositions / x_{Pd}		
1554.8	LIQUID	FCC_A1		1.000	1.000	
931.5	LIQUID	BIPD3		0.750	0.750	
930.0	BIPD3	LIQUID	FCC_A1	0.750	0.761	0.819
684.9	LIQUID	BI3PD5	BIPD3	0.604	0.665	0.750
622.8	LIQUID	BIPD		0.500	0.500	
610.9	BIPD	LIQUID	BI3PD5	0.500	0.548	0.629
512.8	LIQUID	BI2PD		0.334	0.334	
512.6	BI2PD	LIQUID	BIPD	0.334	0.341	0.500
285.4	BIPD	BI3PD5	BIPD3	0.500	0.666	0.750
271.4	LIQUID	RHOMBO_A7		0.000	0.000	
244.4	RHOMBO_A7	LIQUID	BI2PD	0.000	0.075	0.334

Phase information

Phase Name	Common Name	Strukturbericht designation	Pearson Symbol
LIQUID	Liquid		
RHOMBO_A7	(Bi)	$A7$	$hR2$
BI2PD	βBi_2Pd αBi_2Pd	$C11_b$ …	$tI6$ …
BIPD	$\beta BiPd$ $\alpha BiPd$	… …	$oC32$ $mP32$
BI3PD5	γ	…	$hP16$
BIPD3	$\beta BiPd_3$ $\alpha BiPd_3$	… …	… $oP16$
FCC_A1	(Pd)	$A1$	$cF4$

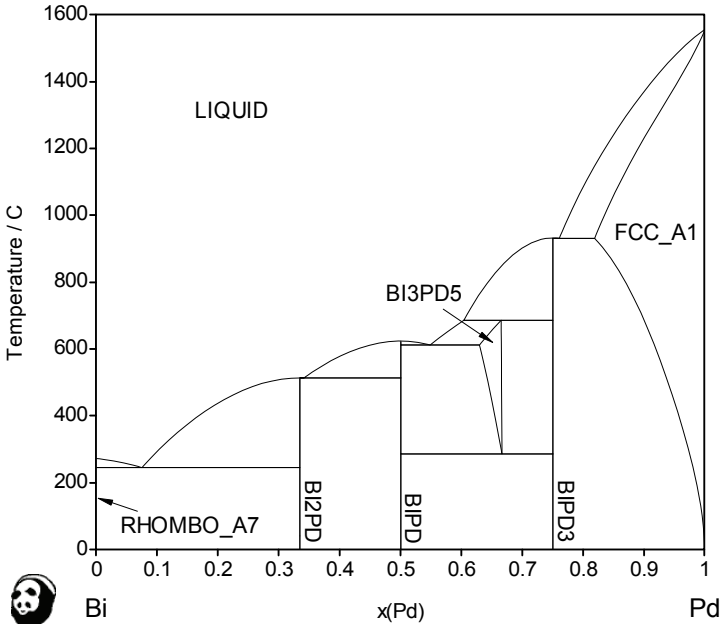

Fig. 25: Phase diagram of the Bi-Pd system

Bi-Sb System

DATA for this system were assessed by Ohtani and Ishida **[94Oht]**. The data were checked for consistency in the scope of the COST 531 Action and no discrepancies were found. This system exhibits the wide mushy zone between the LIQUID and RHOMBO_A7 phase and also a RHOMBO_A7 miscibility gap at lower temperatures.

References:

[94Oht] Ohtani, H., Ishida, K.: *J. Electron. Mater.*, 1994, **23**, 747-755.

Table of invariant reactions

T / °C	Phases			Compositions / x_{Sb}		
630.6	LIQUID	RHOMBO_A7		1.000	1.000	
271.4	LIQUID	RHOMBO_A7		0.000	0.000	
169.8	RHOMBO_A7	RHOMBO_A7#1	RHOMBO_A7#2	0.482	0.482	0.482

Phase information

Phase Name	Common Name	Strukturbericht designation	Pearson Symbol
LIQUID	Liquid		
RHOMBO_A7	(Bi, Sb)	*A*7	*hR*2

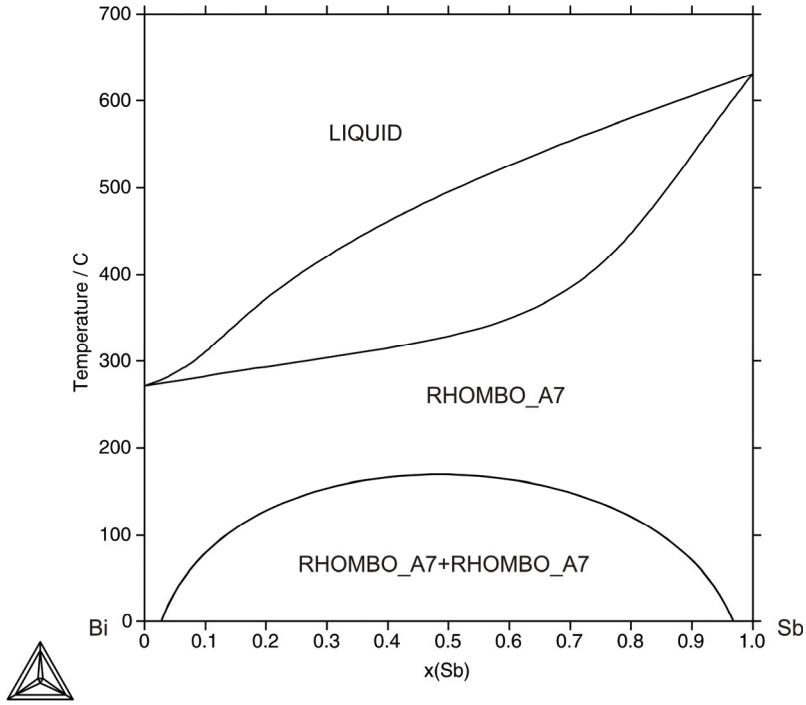

Fig. 26: Phase diagram of the Bi-Sb system

Bi-Sn System

The existing assessed data for the system by Ohtani *et al.* **[94Oht]** and Lee *et al.* **[96Lee]** were modified to reduce the solubility of Bi in BCT_A5 (Sn). The previously assessed very high solubility of Bi in BCT_A5 (Sn) (approx. 10 at% of Bi) was based on old data of Nagasaki and Fujita **[52Nag]**. Since then, newer experimental results **[07Viz, 07Bra]** indicate a significantly lower solubility of Bi in BCT_A5 (Sn). The relevant change in the phase diagram required a change of both LIQUID and BCT_A5 data. The new reassessment was carried out in the scope of the COST 531 Action and published in **[07Viz]**.

References:

[52Nag] Nagasaki, S., Fujita, E.: *J. Jpn. Inst. Met.*, 1952, **16**, 317.

[58Oel] Oelsen, W., Golücke, K. F.: *Arch. Eisenhüttenw.*, 1958, **29**, 689.

[94Oht] Ohtani, H., Ishida, K.: *J. Electron. Mater.*, 1994, **23**, 747.

[96Lee] Lee, B. J., Oh, C. S., Shim, J. H.: *J. Electron. Mater.,* 1996, **25**, 983.

[07Bra] Braga, M. H., Vízdal, J., Kroupa, A., Ferreira, J., Soares, D., Malheiros, L. F.: *CALPHAD,* 2007, **31**, 468-478.

[07Viz] Vízdal, J., Braga, M. H., Kroupa, A., Richter, K. W., Soares, D., Malheiros, L. F., Ferreira, J.: *CALPHAD*, 2007, **31**, 438-448.

Table of invariant reactions

T / °C	Phases			Compositions / x_{Sn}		
271.4	LIQUID	RHOMBO_A7		0.000	0.000	
231.9	LIQUID	BCT_A5		1.000	1.000	
138.4	RHOMBO_A7	LIQUID	BCT_A5	0.031	0.611	0.936
13.0	BCT_A5	DIAMOND_A4		1.000	1.000	
9.8	RHOMBO_A7	BCT_A5	DIAMOND_A4	0.003	0.990	1.000

Phase information

Phase Name	Common Name	Strukturbericht designation	Pearson Symbol
LIQUID	Liquid		
RHOMBO_A7	(Bi)	*A*7	*hR*2
DIAMOND_A4	(αSn)	*A*4	*cF*8
BCT_A5	(βSn)	*A*5	*tI*4

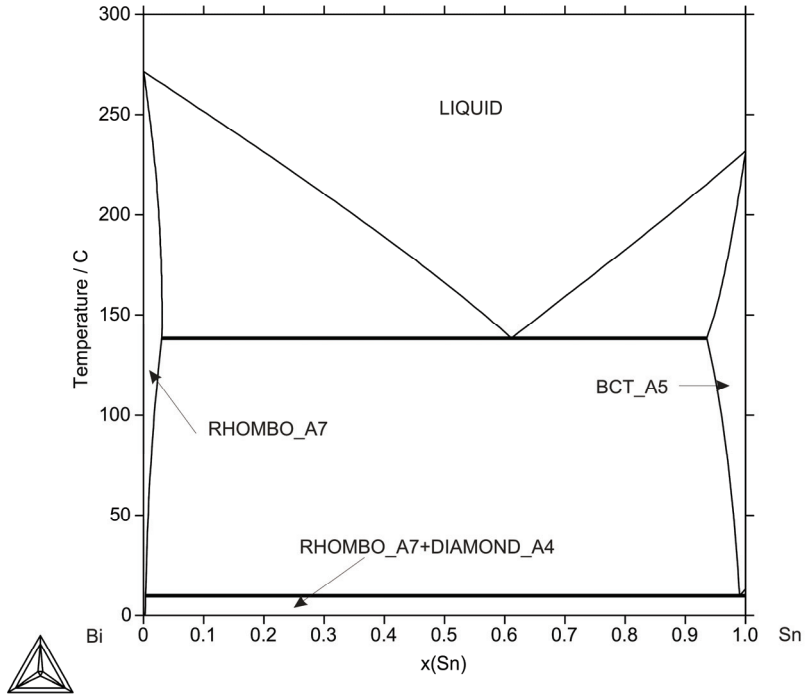

Fig. 27: Phase diagram of the Bi-Sn system

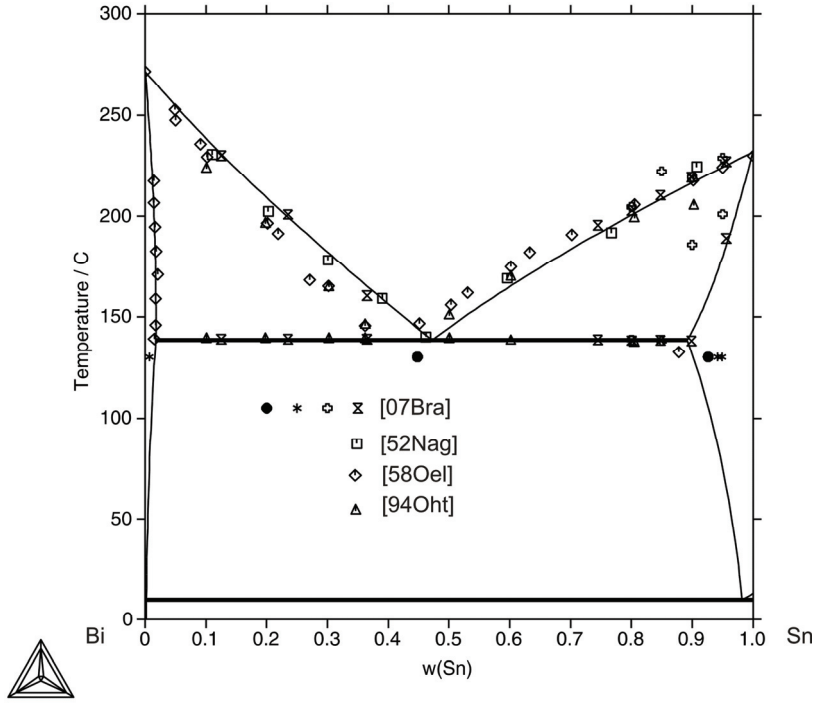

Fig. 28: Calculated phase diagram of the Bi-Sn system in comparison with experimental data (in wt. fractions)

Bi-Zn System

Several authors have assessed the Bi-Zn system – e.g. Malakhov **[00Mal]**, Oleari *et al.* **[55Ole]**, Bale *et al.* **[77Bal]**, Girard **[85Gir]** and Wang *et al.* **[93Wan]**. Kim and Sanders **[03Kim]** attempted to describe properly the segregation region in the liquid, using two *L* interaction parameters only instead of six used by Malakhov. Unfortunately, their descriptions are not mutually consistent. The data from Malakhov **[00Mal]** were used for this system, based on the conformity with experimental data. Some unary parameters are not consistent with the **[SGTE4]** database and therefore changes were introduced and new value of unary data for Bi in HCP_ZN phase from work of Moelans **[03Moe]** was accepted. The phase diagram was reassessed by Vízdal *et al.* **[07Viz]**.

References:

[55Ole] Oleari, L., Fiorani, M., Valenti, V.: *La Metallurgia Italiana*, 1955, **46**, 773.

[77Bal] Bale, C. W., Pelton, A. D., Rigaud, M.: *Z. Metallkd.*, 1977, **68**, 69-74.

[85Gir] Girard, C.: "Fonctions d'exces et diagrammes d'equilibre des phase de quatre systemes metalliques ternaires", *Ph.D. Thesis*, Universite de Provence, Marseille, 1985.

[93Wan] Wang, Z. C., Yu, S. K., Sommer, F.: *J. Chimie Phys. Physico-Chimie Biol.*, 1993, **90**, 379-385.

[00Mal] Malakhov, D. V.: *CALPHAD*, 2000, **24**, 1-14.

[03Kim] Kim, S. S., Sanders, T. H. Jr.: *Z. Metallkd.*, 2003, **94**, 390-395.

[03Moe] Moelans, N., Kumar, K. C. H., Wollants, P.: *J. Alloy. Compd.*, 2003, **360**, 98-106.

[07Viz] Vízdal, J., Braga, M. H., Kroupa, A., Richter, K. W., Soares, D., Malheiros, L. F., Ferreira, J.: *CALPHAD*, 2007, **31**, 438-448.

Table of invariant reactions

T / °C	Phases			Compositions / x_{Zn}		
579.8	LIQUID	LIQUID#1	LIQUID#2	0.870	0.870	0.870
419.5	LIQUID#2	HCP_ZN		1.000	1.000	
418.3	LIQUID#1	LIQUID#2	HCP_ZN	0.374	0.992	0.996
271.4	LIQUID#1	RHOMBO_A7		0.000	0.000	
254.5	RHOMBO_A7	LIQUID#1	HCP_ZN	0.016	0.081	0.999

Phase information

Phase Name	Common Name	Strukturbericht designation	Pearson Symbol
LIQUID	Liquid		
RHOMBO_A7	(Bi)	*A*7	*hR*2
HCP_ZN	(Zn)	*A*3 *mod*	*hP*2

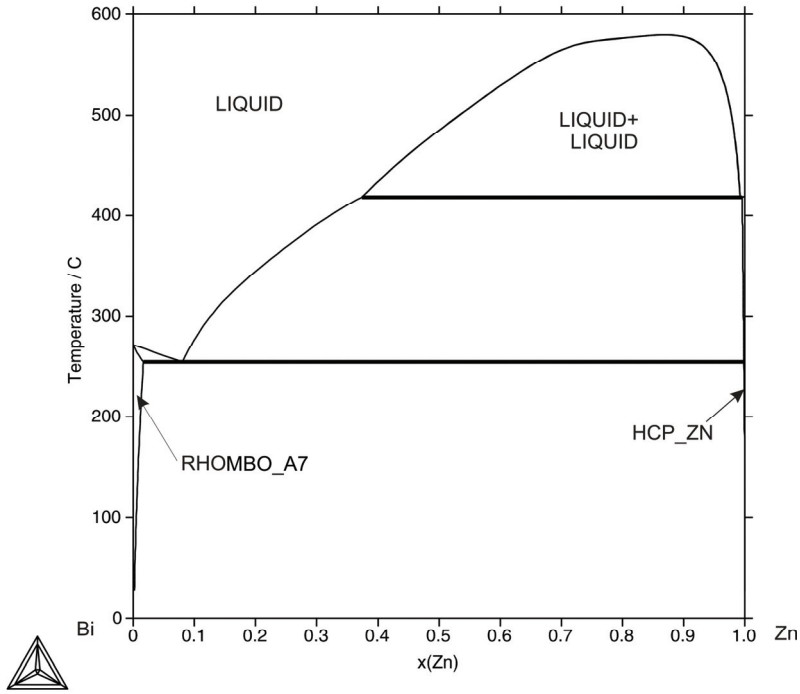

Fig. 29: Phase diagram of the Bi-Zn system

Cu-In System

The Cu-In system as presented in **[MAS]** is quite complex containing 9 intermetallic phases, all of which appear at In contents of less than 50 at%. The most complex of these is the 'η' phase, which is shown as a cascade, or bundle of polymorphs. More recent experimental work undertaken by **[93Bol]**, reduced this collection of phases to just two, which were labelled as η (CUIN_ETAP), the low temperature variant, and η' (CUIN_ETA) being stable over a higher temperature range. The thermodynamic description of this system was taken from the ternary assessment of the Cu-In-Sn system presented by **[01Liu]** (although the Cu-In binary assessment was published later in **[02Liu]**. For some reason, the order of the two phase names were switched in **[01Liu]** with respect to **[02Liu];** the high temperature phase in the former work being labelled η, whereas in the latter work (and also in **[93Bol]**) it was labelled η'. In the modelling, the higher temperature variant is described by a 3 sublattice model giving the phase a homogeneity range, unlike the lower temperature phase which is treated as a line compound. For the purposes of simplification, the δ-phase (CUIN_DELTA) is also treated as a line compound here, despite it having a measured homogeneity range of about 1.5 at% **[MAS]**.

References:

[93Bol] Bolcavage, A., Chen, S.W., Kao, C.R., Chang, Y.A.: *J. Phase Equilib.*, 1993, **14**, 14-21.

[01Liu] Liu, X.J., Liu, H.S., Ohnuma, I., Kainuma, R., Ishida, K., Itabashi, S., Kameda, K., Yamaguchi, K.: *J. Electron. Mater*., 2001, **30**, 1093-1103.

[02Liu] Liu, H.S., Liu, X.J., Cui, Y., Wang, C.P., Ohnuma, I., Kainuma, R., Jin, J.P., Ishida, K.: *J. Phase Equilib.*, 2002, **23**, 409-415.

Table of invariant reactions

T / °C	Phases			Compositions / x_{In}		
961.8	LIQUID	FCC_A1		0.000	0.000	
711.2	FCC_A1	BCC_A2	LIQUID	0.091	0.187	0.209
688.7	LIQUID	CUIN_GAMMA		0.293	0.293	
684.3	BCC_A2	LIQUID	CUIN_GAMMA	0.230	0.259	0.281
668.7	CUIN_GAMMA	CUIN_ETA	LIQUID	0.318	0.337	0.382
632.4	CUIN_GAMMA	CUIN_DELTA		0.300	0.300	
615.2	BCC_A2	CUIN_GAMMA	CUIN_DELTA	0.213	0.280	0.300
612.7	CUIN_DELTA	CUIN_GAMMA	CUIN_ETA	0.300	0.320	0.338
567.6	FCC_A1	BCC_A2	CUIN_DELTA	0.088	0.193	0.300
390.2	CUIN_DELTA	CUIN_ETAP	CUIN_ETA	0.300	0.360	0.361
306.6	CUIN_ETA	CUIN_THETA	LIQUID	0.377	0.450	0.964
294.9	CUIN_ETAP	CUIN_ETA	CUIN_THETA	0.360	0.377	0.450
156.6	LIQUID	TETRAG_A6		1.000	1.000	
153.8	CUIN_THETA	LIQUID	TETRAG_A6	0.450	0.994	1.000

Phase information

Phase Name	Common Name	Strukturbericht designation	Pearson Symbol
LIQUID	Liquid		
FCC_A1	(Cu)	*A*1	*cF*4
BCC_A2	β	*A*2	*cI*2
CUIN_GAMMA	γ	···	*cP*52
CUIN_DELTA	δ	···	*aP*40
CUIN_ETA [(a)]	η'	$B8_1$	*hP*4
CUIN_ETAP [(a)]	η	$B8_2$	*hP*6
CUIN_THETA	$Cu_{11}In_9$	···	*mC*20
TETRAG_A6	(In)	*A*6	*tI*2

[(a)] These phase names are as given in **[01Liu]**, which is the first publication of the thermodynamic parameters. The 'Common Names' are taken from the paper presenting the experimental study of this part of the system **[93Bol]**.

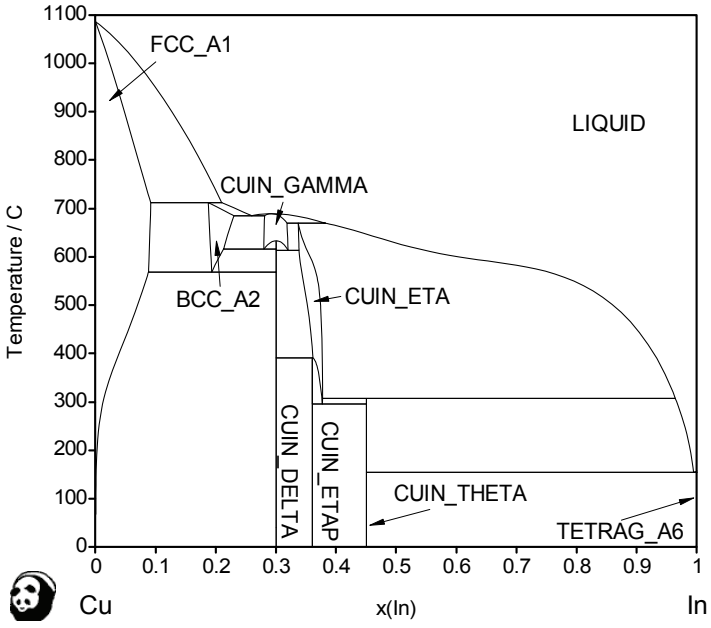

Fig. 30: Phase diagram of the Cu-In system

Cu-Ni System

The data for this system from the assessment of an Mey, published in the COST507 database **[92Mey]**, were accepted for the COST 531 database. The theoretical dataset was tested for the consistency and no disagreement was found. A miscibility gap exists in the FCC_A1 phase in this system.

References:

[92Mey] an Mey, S.: *CALPHAD*, 1992, **16**, 255-260.

Table of invariant reactions

T / °C	Phases			Compositions / x_{Ni}		
1455.1	LIQUID	FCC_A1#2		1.000	1.000	
1084.6	LIQUID	FCC_A1#1		0.000	0.000	
371.0	FCC_A1	FCC_A1#1	FCC_A1#2	0.605	0.605	0.605

Phase information

Phase Name	Common Name	Strukturbericht designation	Pearson Symbol
LIQUID	Liquid		
FCC_A1	(Cu, Ni)	*A*1	*cF*4

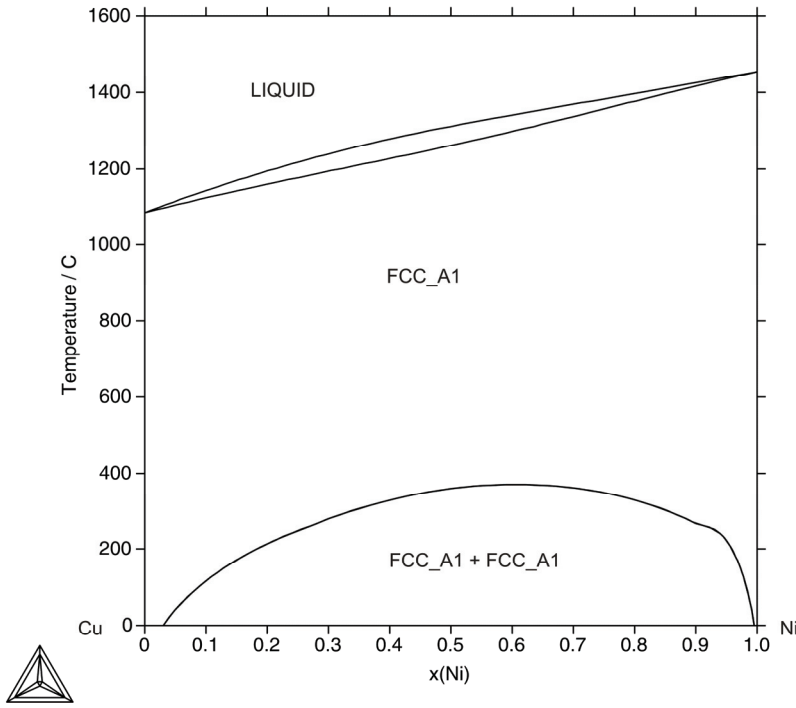

Fig. 31: Phase diagram of the Cu-Ni system

Cu-Pb System

The most prominent feature of the Cu-Pb phase diagram is the monotectic reaction leading to phase separation in the liquid phase. There is negligible mutual solid solubility between Cu and Pb. The dataset used here is taken from **[86Hay]**. As Cu and Pb have the same crystal structure, they have been treated with a single Gibbs energy expression.

References:

[86Hay] Hayes, F.H., Lukas, H.-L., Effenberg, G., Petzow, G.: *Z. Metallkde.*, 1986, **77**, 749-754.

Table of invariant reactions

T / °C	Phases			Compositions / x_{Pb}		
1084.6	LIQUID#1	FCC_A1#1		0.000	0.000	
1008.3	LIQUID	LIQUID#1	LIQUID#2	0.410	0.410	0.410
956.8	FCC_A1#1	LIQUID#1	LIQUID#2	0.008	0.222	0.631
327.5	LIQUID#2	FCC_A1#2		1.000	1.000	
326.3	FCC_A1#2[(a)]	LIQUID#2	FCC_A1#1[(b)]	0.000	0.998	1.000

[(a)] The FCC_A1#2 composition is almost pure Cu.
[(b)] The FCC_A1#1 composition is almost pure Pb.

Phase information

Phase Name	Common Name	Strukturbericht designation	Pearson Symbol
LIQUID	Liquid		
FCC_A1	(Cu),(Pb)	*A*1	*cF*4

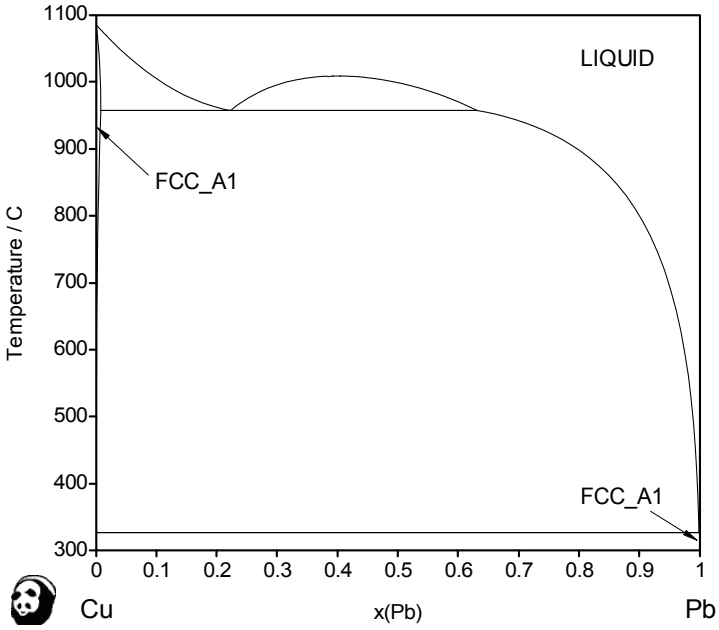

Fig. 32: Phase diagram of the Cu-Pb system

Cu-Pd System

The Cu-Pd system is a simple isomorphous system showing complete solid solubility for all compositions across the phase diagram. The thermodynamic parameters for this system were taken from **[91Sub]**, with minor modifications being made to improve the agreement between the calculated and experimentally determined phase boundaries.

References:

[91Sub] Subramanian, P.R., Laughlin, D.E.: *J. Phase Equilib.*: 1991, **12**, 231-243.

Table of invariant reactions

T / °C	Phases			Compositions / x_{Pd}		
1554.8	LIQUID	FCC_A1		1.000	1.000	
1084.6	LIQUID	FCC_A1		0.000	0.000	

Phase information

Phase Name	Common Name	Strukturbericht designation	Pearson Symbol
LIQUID	Liquid		
FCC_A1	(Cu,Pd)	*A*1	*cF*4

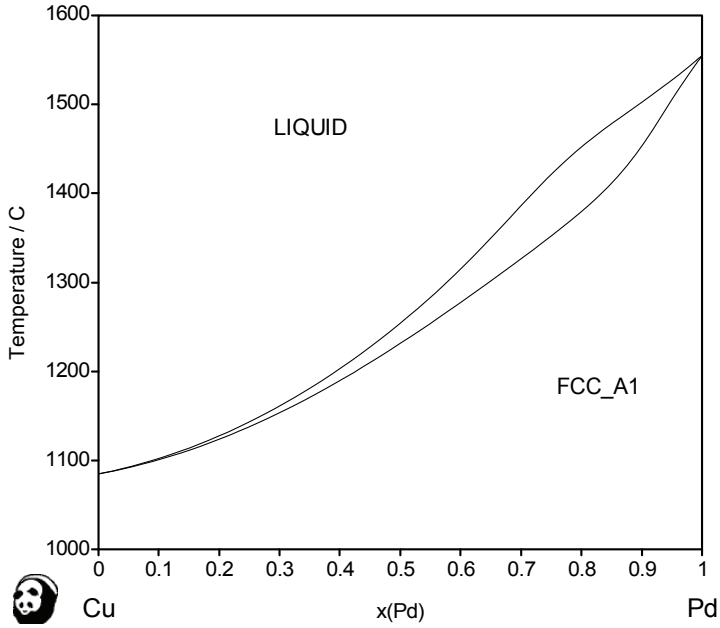

Fig. 33: Phase diagram of the Cu-Pd system

Cu-Sb System

The data for the Cu-Sb system are from the assessment of Liu *et al.* **[00Liu]**. This assessment represents a significant change from earlier assessments **[91Nit]** and **[91Tep]** in that the β phase has been treated as a disordered bcc phase (BCC_A2). Further modification to the data will probably be necessary to remodel the γ phase (CUSB_GAMMA in **[00Liu]**) using the model for the HCP_A3 phase, which corresponds to the real crystallographic structure over a range of homogeneity.

References:

[91Nit] Nitsche, R., an Mey, S., Hack, K., Spencer, P. J.: *Z. Metallkde.*, 1991, **82**, 67-72.

[91Tep] Teppo, O., Taskinen, P.: *Scand. J. Metall.*, 1991, **20**, 174-182.

[00Liu] Liu, X. J., Wang, C. P., Ohnuma, I., Kainuma, R., Ishida, K.: *J. Phase Equilib.*, 2000, **21**, 432-442.

Table of invariant reactions

T / °C	Phases			Compositions / x_{Sb}		
1084.6	LIQUID	FCC_A1		0.000	0.000	
686.5	LIQUID	BCC_A2		0.279	0.279	
647.1	FCC_A1	LIQUID	BCC_A2	0.059	0.183	0.204
630.6	LIQUID	RHOMBO_A7		1.000	1.000	
584.9	BCC_A2	CUSB_ETA	LIQUID	0.313	0.330	0.444
525.8	CUSB_ETA	LIQUID	RHOMBO_A7	0.330	0.634	1.000
488.2	FCC_A1	CUSB_GAMMA	BCC_A2	0.045	0.150	0.217
464.7	CUSB_GAMMA	CUSB_DELTA	BCC_A2	0.150	0.200	0.224
[a]434.4	BCC_A2	CUSB_EPSILON	CUSB_ETA	0.249	0.250	0.330
[a]434.2	CUSB_DELTA	BCC_A2	CUSB_EPSILON	0.200	0.247	0.250
400.4	FCC_A1	CUSB_GAMMA	CUSB_DELTA	0.024	0.150	0.200
389.0	CUSB_DELTA	CUSB_ZETA	CUSB_EPSILON	0.200	0.230	0.250
359.2	CUSB_ZETA	CUSB_EPSILON	CUSB_ETA	0.230	0.250	0.330
260.1	CUSB_DELTA	CUSB_ZETA	CUSB_ETA	0.200	0.230	0.330

[a] These invariant reactions are not distinguishable in Fig. 34 because the temperatures are very close

Phase information

Phase Name	Common Name	Strukturbericht designation	Pearson Symbol
LIQUID	Liquid		
FCC_A1	(Cu)	$A1$	$cF4$
RHOMBO_A7	(Sb)	$A7$	$hR2$
BCC_A2[(a)]	β	$D0_3$	$oF16$
CUSB_GAMMA	γ	$A3$	$hP2$
CUSB_DELTA	δ	…	$hP*$
CUSB_EPSILON	ε	$D0_a$	$oP8$
CUSB_ZETA	ζ	…	$hP26$
CUSB_ETA	η	$C38$	$tP6$

[(a)]Phase information (Common Name, Struktur. Designation and Pearson Symbol) are given for the real β phase

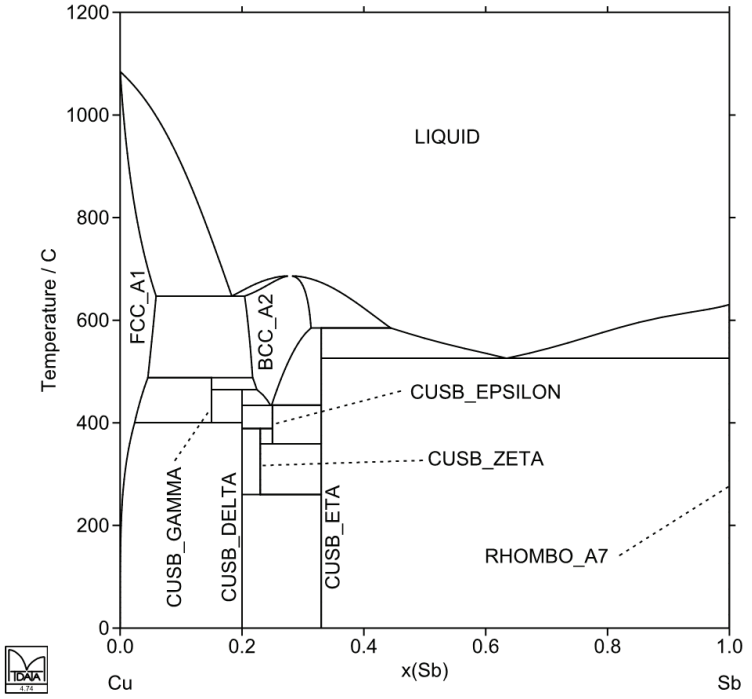

Fig. 34: Phase diagram of the Cu-Sb system

Cu-Sn System

The data for the Cu-Sn system from the assessment of Liu *et al.* **[01Liu]** were accepted for the database. This assessment is an extension of earlier work of Shim *et al.* **[96Shi]**. Also, the binary FCC_A1 solution data were modified by Lee **[04Lee]** to be consistent with the new data for FCC_A1 (Sn) adopted in the SGTE unary database v4.4 **[SGTE4]**.
Several further modifications were necessary to assure consistency with other systems in the COST 531 database. According to Liu *et. al.* **[01Liu]**, there is a complex ordering reaction around 700 °C and 0.2 Sn, which is not yet completely understood, described as BCC_A2 $\rightarrow$ $B2$ $\rightarrow$ $D0_3$ or BCC_A2 $\rightarrow$ $D0_3$. Because of remaining uncertainties about the real nature of the reactions, and to be able to model the ternary Cu-Ni-Sn system where there is mutual solubility between this bcc/γ (BCC_A2/$D0_3$) phase and Ni_3Sn phase originating in the Ni-Sn system, the high-temperature Cu-rich phase was modelled as simple disordered BCC_A2 phase. Also the high temperature modification of the Cu_6Sn_5 phase had to be remodelled as CuIn-η phase because of complete solubility between these two phases found experimentally in the Cu-In-Sn system.
The liquid phase data have also been modified within the scope of COST 531 Action to take into account the latest enthalpy of mixing data from Vienna **[08Fla].**

References:

[96Shi] Shim, J. H., Oh, C. S., Lee, B. J., Lee, D. N.: *Z. Metallkde*, 1996, **87**, 205-212.

[01Liu] Liu, X. J., Liu, H. S., Ohnuma, I., Kainuma, R., Ishida, K., Itabashi, S., Kameda, K., Yamaguchi, K.: *J. Electron. Mater.,* 2001, **30**, 1093-1103.

[04Lee] Lee, B. J.: Unpublished work, 2004.

[08Fla] Flandorfer, H., Luef, Ch., Saeed ,U.: *J. Non-Cryst. Solids,* 2008, in print.

Table of invariant reactions

T / °C	Phases			Compositions / x_{Sn}		
1084.6	LIQUID	FCC_A1		0.000	0.000	
816.3	FCC_A1	BCC_A2	LIQUID	0.069	0.133	0.151
666.5	BCC_A2	CU3SN		0.250	0.250	
647.4	CU3SN	BCC_A2	LIQUID	0.250	0.283	0.412
635.0	BCC_A2	CU10SN3	CU3SN	0.211	0.231	0.250
568.5	BCC_A2	CU41SN11	CU10SN3	0.179	0.212	0.231
540.0	CU41SN11	CU10SN3	CU3SN	0.212	0.231	0.250
523.8	FCC_A1	BCC_A2	CU41SN11	0.086	0.161	0.212
418.1	CU3SN	CUIN_ETA	LIQUID	0.250	0.455	0.868
348.1	FCC_A1	CU41SN11	CU3SN	0.054	0.212	0.250
231.9	LIQUID	BCT_A5		1.000	1.000	
227.2	CUIN_ETA	LIQUID	BCT_A5	0.455	0.985	1.000
[a]187.5	CUIN_ETA	CU6SN5_P	BCT_A5	0.455	0.455	1.000
[a]187.1	CU3SN	CUIN_ETA	CU6SN5_P	0.250	0.455	0.455
13.1	CU6SN5_P	BCT_A5	DIAMOND_A4	0.455	1.000	1.000
13.0	BCT_A5	DIAMOND_A4		1.000	1.000	

[a] These invariant reactions are not distinguishable in Fig. 35 because the temperatures are very close

Phase information

Phase Name	Common Name	Strukturbericht designation	Pearson Symbol
LIQUID	Liquid		
FCC_A1	(Cu)	$A1$	$cF4$
BCC_A2	β γ	$A2$ $D0_3$	$cI2$ $cF16$
BCT_A5	(βSn)	$A5$	$tI4$
DIAMOND_A4	(αSn)	$A4$	$CF8$
CU10SN3	ζ	···	$hP26$
CU41SN11	δ	···	$cF416$
CU3SN	ε	···	$oC80$
CU6SN5_P	η'	···	$mC44$
CUIN_ETA	η	$B8_1$	$hP4$

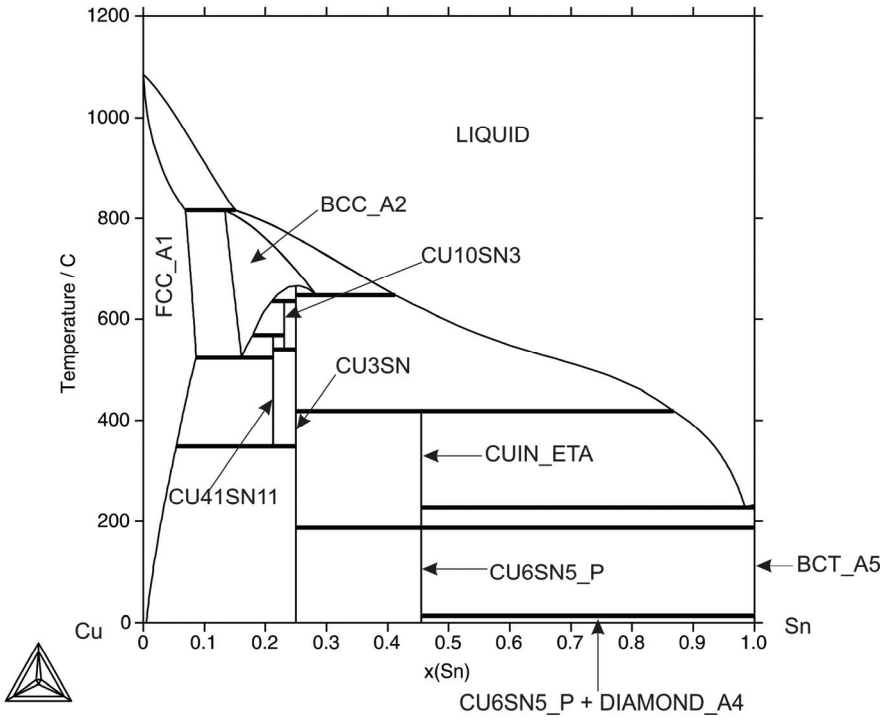

Fig. 35: Phase diagram of the Cu-Sn system

Cu-Zn System

The critically assessed data for this system are from the assessment of Kowalski and Spencer **[93Kow]** which reproduces well all the experimental data for the system. The dataset includes data for both the ordered B2_BCC phase and the associated disordered BCC_A2 phase. The δ ($CuZn_3$) phase was modelled as BCC_A2 in agreement with the result of **[49Sch]**.
The ordering temperature BCC_A2 —> B2_BCC is concentration dependent and lies between 454 – 467°C.

References:

[49Sch] Schubert, K., Wall, E.:*Z. Metallkde.,*1949, **40**, 383-385.

[93Kow] Kowalski, M., Spencer, P. J.: *J. Phase Equilib.*, 1993, **14**, 432-438.

Table of invariant reactions

T / °C	Phases			Compositions / x_{Zn}		
1084.6	LIQUID	FCC_A1		0.000	0.000	
902.2	FCC_A1	B2_BCC	LIQUID	0.319	0.353	0.373
835.2	B2_BCC	CUZN_BRASS	LIQUID	0.558	0.586	0.592
699.2	CUZN_BRASS	BCC_A2	LIQUID	0.678	0.719	0.803
600.2	BCC_A2	HCP_A3	LIQUID	0.773	0.792	0.882
558.8	CUZN_BRASS	BCC_A2	HCP_A3	0.693	0.749	0.777
421.3	HCP_A3	HCP_ZN	LIQUID	0.874	0.981	0.983
419.5	LIQUID	HCP_ZN		1.000	1.000	

Phase information

Phase Name	Common Name	Strukturbericht designation	Pearson Symbol
LIQUID	Liquid		
FCC_A1	(Cu)	*A*1	*cF*4
BCC_A2	β	*A*2	*cI*2
BCC_A2	δ	*A*2	*cI*2
B2_BCC	β'	*B*2	*cP*2
CUZN_BRASS	γ	$D8_2$	*cI*52
HCP_A3	ε	*A*3	*hP*2
HCP_ZN	(Zn)	*A*3 *mod*	*hP*2

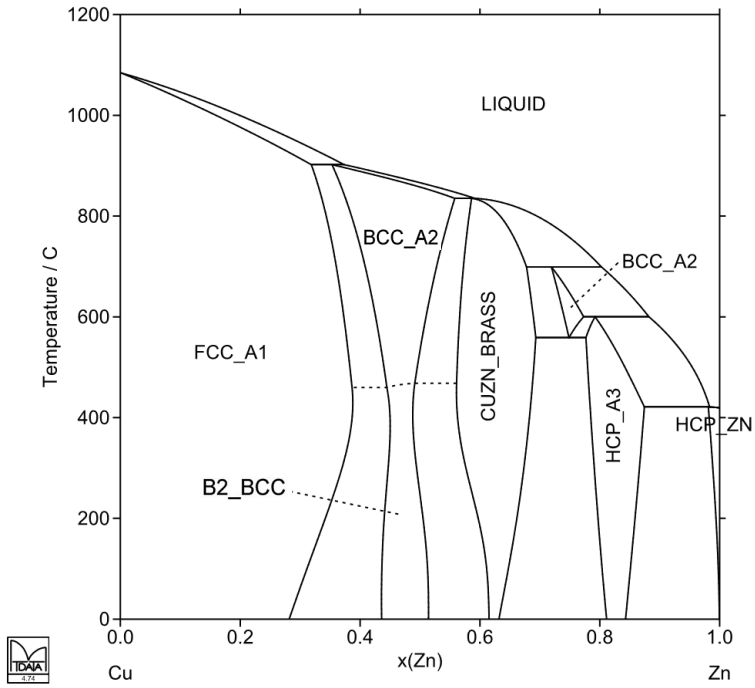

Fig. 36: Phase diagram of the Cu-Zn system

In-Ni System

This system contains a number of intermetallic phases, 5 of which are treated as stoichiometric in the modelling of the system. On the other hand, the δ (INNI_DELTA) and ζ (INNI_CHI) phases show reasonable homogeneity ranges; ~7 and 10 at%, respectively, although both of these phases are stable over only a limited temperature range. The source of the thermodynamic parameters for this system is **[02Wal]**. In the original work, the modelling included a description for the gas phase. However, the gas phase is not included in the COST 531 thermodynamic database and hence data for the In-Ni gas was removed from the dataset. This resulted in the reappearance of some of the compound phases at temperatures much higher than their true stability ranges. In the course of the compilation of the COST 531 database, modifications to the thermodynamic parameters for these compounds were made in order to ensure that the phases did not appear at higher temperatures below 3500K, the upper temperature limit of the COST 531 database.

References:

[02Wal] Waldner, P., Ipser, H.: *Z. Metallkde*., 2002, **93**, 825-832.

Table of invariant reactions

T / °C	Phases			Compositions / x_{Ni}		
1455.1	LIQUID	FCC_A1		1.000	1.000	
942.7	LIQUID	INNI_CHI		0.645	0.645	
922.1	LIQUID	INNI_DELTA		0.450	0.450	
919.3	INNI_DELTA	LIQUID	INNI_CHI	0.488	0.515	0.584
904.2	INNI_CHI	LIQUID	FCC_A1	0.686	0.750	0.924
868.7	INNI_DELTA	INNI_CHI_PRIME	INNI_CHI	0.484	0.577	0.590
867.9	LIQUID	NI2IN3	INNI_DELTA	0.246	0.400	0.407
862.8	INNI_DELTA	NIIN	INNI_CHI_PRIME	0.482	0.500	0.576
847.6	INNI_CHI	NI3IN	FCC_A1	0.684	0.750	0.933
776.4	NI2IN3	INNI_DELTA	NIIN	0.400	0.442	0.500
665.0	INNI_CHI	NI2IN	NI3IN	0.666	0.667	0.750
472.6	INNI_CHI_PRIME	INNI_CHI	NI2IN	0.591	0.647	0.667
405.5	LIQUID	NI3IN7	NI2IN3	0.037	0.300	0.400
156.6	LIQUID	TETRAG_A6		0.000	0.000	0.000
156.5	TETRAG_A6	LIQUID [(a)]	NI3IN7	0.000	0.000	0.300

[(a)] The liquid composition is almost pure In.

Phase information

Phase Name	Common Name	Strukturbericht designation	Pearson Symbol
LIQUID	Liquid		
TETRAG_A6	(In)	$A6$	$tI2$
NI3IN7	$Ni_{28}In_{72}$	$D8_{1\ to\ 3}$	$cI52$
NI2IN3	Ni_2In_3	$D5_{13}$	$hP5$
INNI_DELTA	δ(NiIn)	$B2$	$cP2$
NIIN	ε(NiIn)	$B35$	$hP6$
INNI_CHI_PRIME	ζ'($Ni_{13}In_9$)	...	$mC44$
INNI_CHI	ζ	...	...
NI2IN	Ni_2In	$B8_2$	$hP6$
NI3IN	Ni_3In	$D0_{19}$	$hP8$
FCC_A1	(Ni)	$A1$	$cF4$

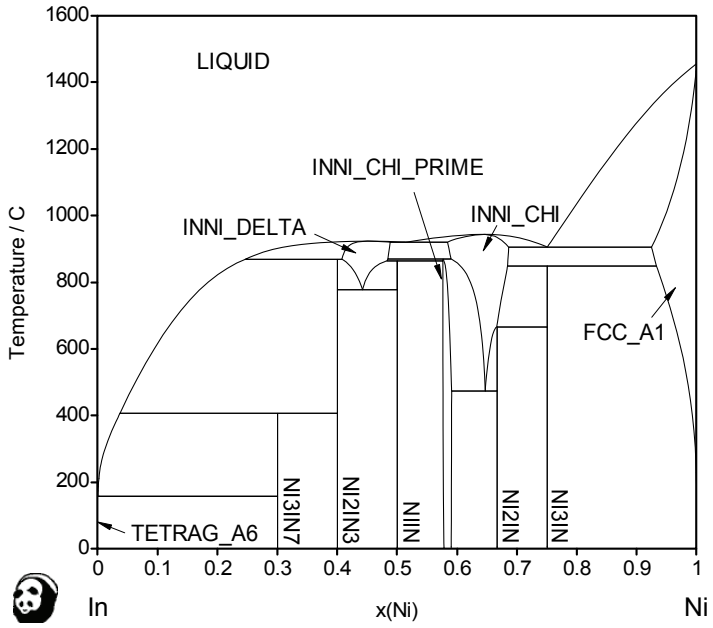

Fig. 37: Phase diagram of the In-Ni system

In-Pb System

The data for the In-Pb system are from an unpublished assessment of Bolcavage **[95Bol]** reported by Boa and Ansara **[98Boa]**. The data for the tetragonal phase were remodelled within the framework of COST 531 using revised unary data for In consistent with data used for the In-Sn system.

References:

[95Bol] Bolcavage, A., Kao, C. R., Chen, S. L., Chang, Y. A.: Proc. Conf. "Applications of Thermodynamics in the Synthesis and Processing of Materials", P. Nash and B. Sundman (eds.), The Minerals, Metals and Materials Society, 1995.

[98Boa] Boa, D., Ansara, I.: *Thermochim. Acta*, 1998, **314**, 79-86.

Table of invariant reactions

T / °C	Phases			Compositions / x_{Pb}		
327.5	LIQUID	FCC_A1		1.000	1.000	
172.5	LIQUID	TET_ALPHA1	FCC_A1	0.191	0.274	0.297
158.1	LIQUID	TETRAG_A6	TET_ALPHA1	0.090	0.103	0.113
156.6	LIQUID	TETRAG_A6		1.000	1.000	

Phase information

Phase Name	Common Name	Strukturbericht designation	Pearson Symbol
LIQUID	Liquid		
TETRAG_A6	(In)	*A*6	*tI*2
FCC_A1	(Pb)	*A*1	*cF*4
TET_ALPHA1	α	*A*6 *mod*	*tI*2

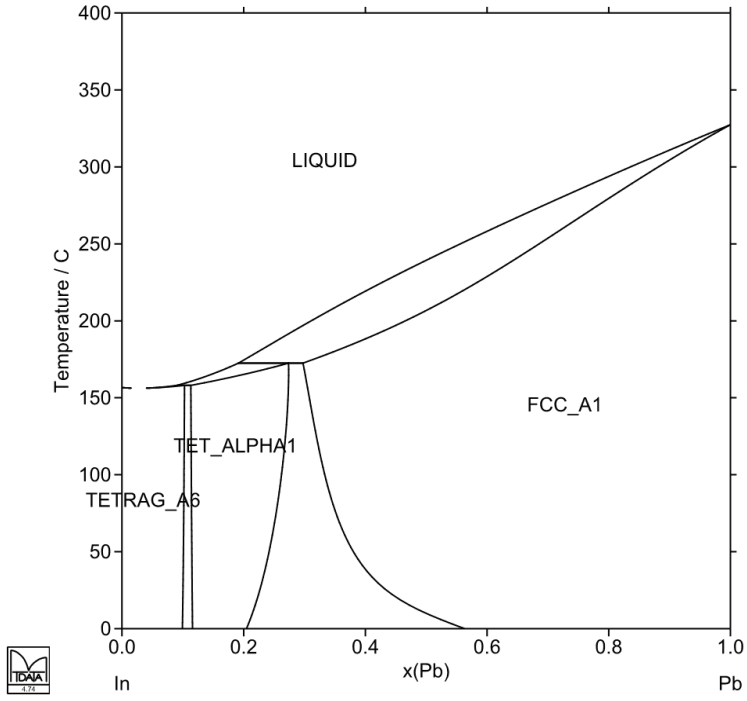

Fig. 38: Phase diagram of the In-Pb system

In-Pd System

The data from the assessment of Jiang and Liu **[02Jia]** were accepted for the COST 531 database. This system is very complex, exhibiting many intermetallic phases with high and low temperature variations. As there are insufficient experimental data, all the intermetallic phases are modelled as stoichiometric, except for InPd phase, which has an ordered BCC_B2 structure. As there is no ordering reaction in this system, the ordered phase was modelled using a two-sublattice model with the sublattice ratio 0.5:0.5. The data are not related to those for the disordered bcc phase. The crystallographic structure for many of the intermetallic phases is uncertain.

References:

[02Jia] Jiang, Ch., Liu, Z. K.: *Metall. Mater. Trans.*, 2002, **33A**, 3597-3603.

Table of invariant reactions

T / °C	Phases			Compositions / x_{Pd}		
1554.8	LIQUID	FCC_A1		1.000	1.000	
1371.3	LIQUID	INPD3_BETA		0.740	0.740	
1344.1	INPD3_BETA	LIQUID	FCC_A1	0.740	0.772	0.800
1333.2	LIQUID	INPD2_BETA		0.660	0.660	
1311.5	INPD2_BETA	LIQUID	INPD3_BETA	0.660	0.691	0.740
1288.0	LIQUID	BCC_B2		0.531	0.531	
1272.4	BCC_B2	LIQUID	INPD2_BETA	0.599	0.607	0.660
1229.2	INPD3_BETA	INPD3_ALPHA	FCC_A1	0.740	0.750	0.803
1075.7	INPD2_BETA	INPD2_ALPHA	INPD3_BETA	0.660	0.667	0.740
1029.0	INPD2_ALPHA	INPD3_BETA	INPD3_ALPHA	0.667	0.740	0.750
945.8	BCC_B2	IN3PD5	INPD2_BETA	0.594	0.625	0.660
934.4	IN3PD5	INPD2_BETA	INPD2_ALPHA	0.625	0.660	0.667
716.5	LIQUID	IN3PD2	BCC_B2	0.234	0.400	0.449
676.0	LIQUID	IN7PD3	IN3PD2	0.210	0.290	0.400
156.6	LIQUID	TETRAG_A6		0.000	0.000	
156.5	TETRAG_A6	LIQUID	IN7PD3	0.000	0.001	0.290

Phase information

Phase Name	Common Name	Strukturbericht designation	Pearson Symbol
LIQUID	Liquid		
TETRAG_A6	(In)	*A*6	*tI*2
FCC_A1	(Pd)	*A*1	*cF*4
BCC_B2	InPd	*B*2	*cP*2
IN7PD3	In_3Pd	$D8_2$	*cI*52
IN3PD2	In_3Pd_2	$D5_{13}$	*hP*5
IN3PD5	In_3Pd_5	...	*oP*16
INPD2_ ALPHA	$\alpha InPd_2$	*C*23	*oP*12
INPD3_ ALPHA	$\alpha InPd_3$	*A*6	*tI*2
INPD2_ BETA	$\beta InPd_2$	...	...
INPD3_ BETA	$\beta InPd_3$	$L6_0$	*tP*4

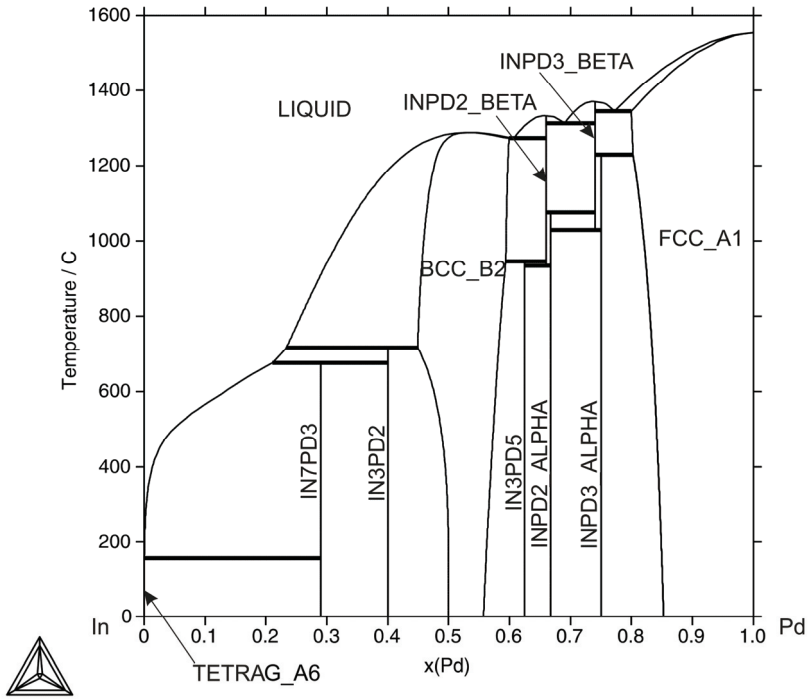

Fig. 39: Phase diagram of the In-Pd system

In-Sb System

The original data for the In-Sb system from Anderson were reported by Ansara *et al.* **[94Ans]** and referred to as a private communication. Small modification to data for the original α-InSb phase was made. The phase was remodelled and renamed ZINCBLENDE_B3 to provide compatibility with the general model for the crystallographic structure of this phase.

References:

[94Ans] Ansara, I., Chatillon, C., Lukas, H. L., Nishizawa, T., Ohtani, H., Ishida, K., Hillert, M., Sundman, B., Argent, B. B., Watson, A., Chart, T. G., Anderson, T.: *CALPHAD*, 1994, **18**, 177-222.

Table of invariant reactions

T / °C	Phases			Compositions / x_{Sb}		
630.6	LIQUID	RHOMBO_A7		1.000	1.000	
531.3	LIQUID	ZINCBLENDE_B3		0.500	0.500	
497.3	ZINCBLENDE_B3	LIQUID	RHOMBO_A7	0.500	0.692	0.995
156.6	LIQUID	TETRAG_A6		0.000	0.000	
154.7	TETRAG_A6	LIQUID	ZINCBLENDE_B3	0.000	0.004	0.500

Phase information

Phase Name	Common Name	Strukturbericht designation	Pearson Symbol
LIQUID	Liquid		
TETRAG_A6	(In)	*A*6	*tI*2
ZINCBLENDE_B3	αInSb	*B*3	*cF*8
RHOMBO_A7	(Sb)	*A*7	*hR*2

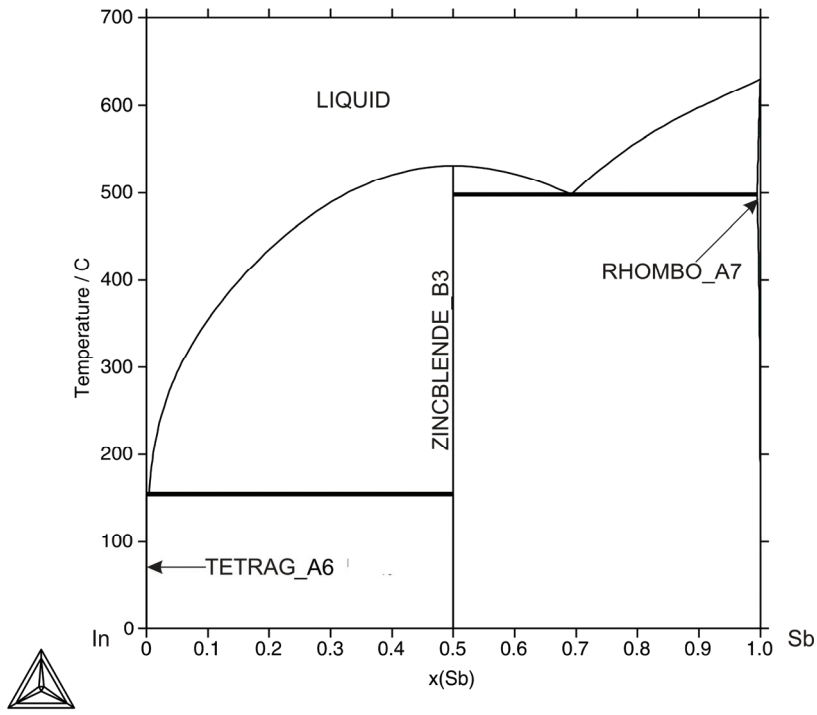

Fig. 40: Phase diagram of the In-Sb system

In-Sn System

This system has been modelled by several authors e. g. **[96Lee, 99Ans, 03Moe].** The complete assessment of this system of Lee *et al.* **[96Lee]** was later amended by **[03Moe]** who reassessed the InSn-β phase (TET_ALPHA1). Neither **[96Lee]** nor **[03Moe]** used unary data consistent with COST 531 database in their assessments and therefore the data from Ansara *et al.* **[99Ans]** were used as their dataset is consistent concerning the unary data. Small formal changes were made in the scope of the COST 531 Action. The name of the InSn-β phase was changed to TET_ALPHA1 and remodelled to maintain consistency with ternary systems since a phase with the same crystallographic structure exists in the In-Pb and Bi-In systems.
There is significant discrepancy in the experimental data in the literature concerning the composition ranges of the (INSN_GAMMA + BCT_A5) and (TETRAG_A6 + TET_ALPHA1) two phase fields. The agreement of the assessment from **[99Ans]** with currently accepted experimental phase diagram from **[MAS]** is very good.

References:

[96Lee] Lee, B.-J., Oh, C.-S., Shim, J.-H.: *J. Electron. Mater.*: 1996, **25**, 983-991.

[99Ans] Ansara, I., Fries, S. G, Lukas, H. L: Unpublished work, 1999.

[03Moe] Moelans, N., Kumar, K. C. H., Wollants, P.: *J. Alloys Compd.*, 2003, **360**, 98-106.

Table of invariant reactions

T / °C	Phases			Compositions / x_{Sn}		
231.9	LIQUID	BCT_A5		1.000	1.000	
222.2	LIQUID	INSN_GAMMA	BCT_A5	0.948	0.967	0.981
156.6	LIQUID	TETRAG_A6		0.000	0.000	
140.8	TETRAG_A6	TET_ALPHA1	LIQUID	0.124	0.132	0.145
118.2	TET_ALPHA1	LIQUID	INSN_GAMMA	0.446	0.477	0.773
13.0	BCT_A5	DIAMOND_A4		1.000	1.000	

Phase information

Phase Name	Common Name	Strukturbericht designation	Pearson Symbol
LIQUID	Liquid		
TETRAG_A6	(In)	*A*6	*tI*2
TET_ALPHA1	InSn-β	*A*6 *mod*	*tI*2
INSN_GAMMA	γ	A_f	*hP*1
DIAMOND_A4	(αSn)	*A*4	*CF*8
BCT_A5	(βSn)	*A*5	*tI*4

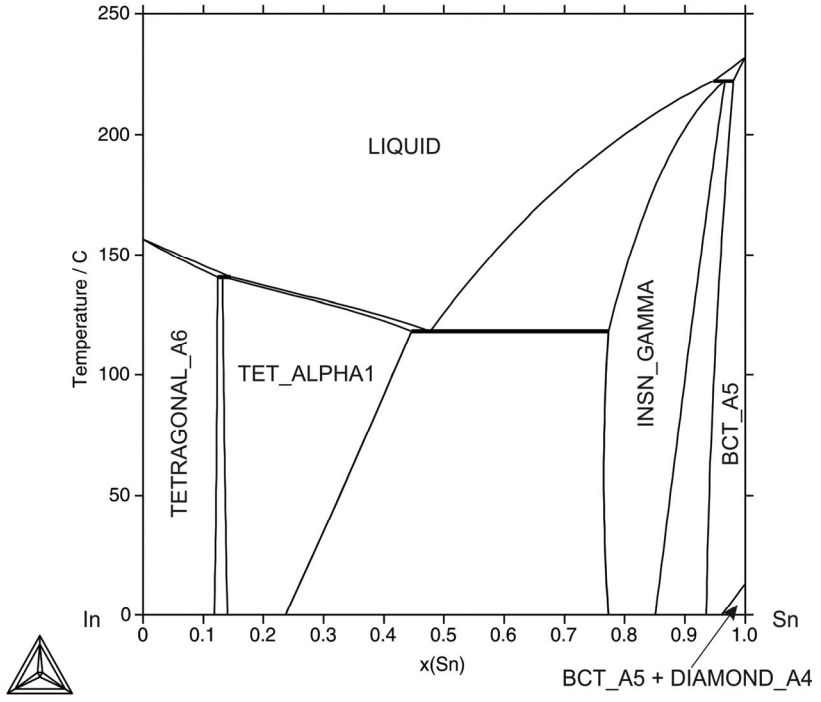

Fig. 41: Phase diagram of the In-Sn system

In-Zn System

The data from the critical assessment of Lee **[96Lee]** were used in the COST 531 database. There is significant disagreement in the eutectic concentration (in the range of 3.1-8 wt.% of Zn) between various authors e.g. **[44Rhi, 56Oel, 50Car]**. The theoretical assessment is in very good agreement with the experimental data accepted by **[MAS]**.

References:

[44Rhi] Rhines, F.N., Grobe, A.H.: *Trans. Met. Soc. AIME,* 1944, **156**, 156.

[50Car] Carapela Jr., S.C., Piretti, E.A.: *Trans. Met. Soc. AIME,* 1950, **188**, 890.

[56Oel] Oelsen,W., Zühlke, P.: *Arch. Eisenhüttenwes.,*1956, **27,** 743-752.

[96Lee] Lee, B. J.: *CALPHAD,* 1996, **20**, 471-480.

Table of invariant reactions

T / °C	Phases			Compositions / x_{Zn}		
419.5	LIQUID	HCP_ZN		1.000	1.000	
156.6	LIQUID	TETRAG_A6		0.000	0.000	
143.6	TETRAG_A6	LIQUID	HCP_ZN	0.010	0.040	0.999

Phase information

Phase Name	Common Name	Strukturbericht designation	Pearson Symbol
LIQUID	Liquid		
TETRAG_A6	(In)	*A*6	*tI*2
HCP_ZN	(Zn)	*A*3 *mod*	*hP*2

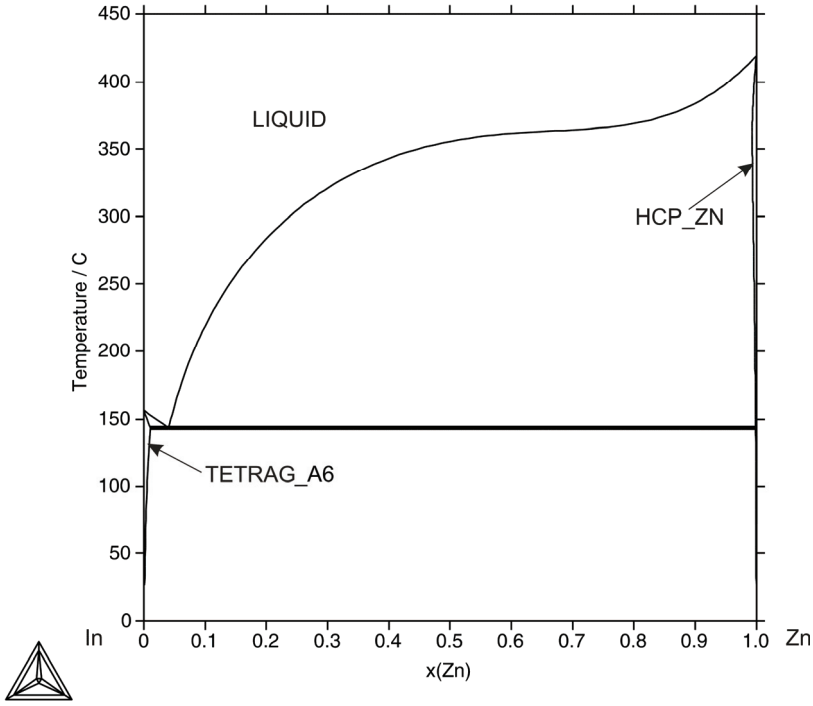

Fig. 42: Phase diagram of the In-Zn system

Ni-Pb System

The main feature of the phase diagram of this system is a monotectic reaction occurring at 1340 °C leading to a miscibility gap in the liquid phase. With little mutual solid solubility between the elements, a wide FCC_A1+FCC_A1 region is also present at lower temperatures. The eutectic point is very close to the melting point of Pb, and so the compositions of the phases involved are virtually pure Ni and pure Pb. The source of the thermodynamic model parameters for this system is **[00Wan]**.

References:

[00Wan] Wang, C.P., Liu, X.J., Ohnuma, I., Kainuma, R., Ishida, K.: *CALPHAD*, 2000, **24**, 149-167.

Table of invariant reactions

T / °C	Phases			Compositions / x_{Pb}		
1560.7	LIQUID	LIQUID#1	LIQUID#2	0.315	0.315	0.315
1455.1	LIQUID#1	FCC_A1#1		0.000	0.000	
1340.2	FCC_A1	LIQUID#1	LIQUID#2	0.011	0.136	0.601
327.5	LIQUID#2	FCC_A1#2		1.000	1.000	
326.4	FCC_A1#1	LIQUID#2[(a)]	FCC_A1#2	0.000	1.000	1.000

[(a)] The liquid composition is almost pure Pb.

Phase information

Phase Name	Common Name	Strukturbericht designation	Pearson Symbol
LIQUID	Liquid		
FCC_A1	(Ni),(Pb)	*A*1	*cF*4

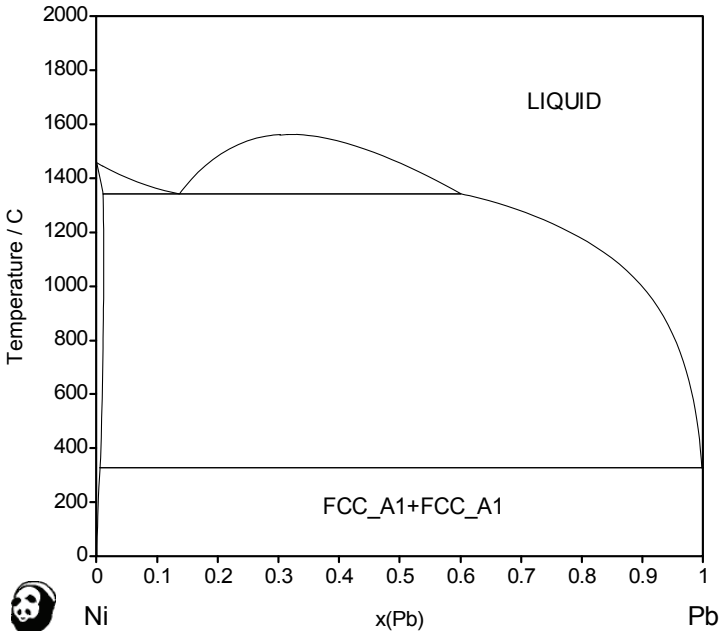

Fig. 43: Phase diagram of the Ni-Pb system

Ni-Pd System

The Ni-Pd system has a simple isomorphous phase diagram, there being complete solid solubility at all compositions. The liquidus and solidus exhibit a minimum at about 1238 °C and x_{Pd}=0.4. The thermodynamic description for this system is taken from **[99Gho]**, although calculation using these data results in the presence of a miscibility gap in the solid phase at low temperatures; a feature that is absent in the original publication. There would seem to be no experimental justification for this at this time and it would therefore warrant further study.

References:

[99Gho] Ghosh, G., Kantner, C., Olson, G.B.: *J. Phase Equilib.*, 1999, **20**, 295-308.

Table of invariant reactions

T / °C	Phases			Compositions / x_{Pd}		
1554.8	LIQUID	FCC_A1		1.000	1.000	
1455.1	LIQUID	FCC_A1		0.000	0.000	
1238.0	LIQUID	FCC_A1		0.400	0.400	
271.6	FCC_A1	FCC_A1#1	FCC_A1#2	0.110	0.110	0.110

Phase information

Phase Name	Common Name	Strukturbericht designation	Pearson Symbol
LIQUID	Liquid		
FCC_A1	(Ni,Pd)	*A*1	*cF*4

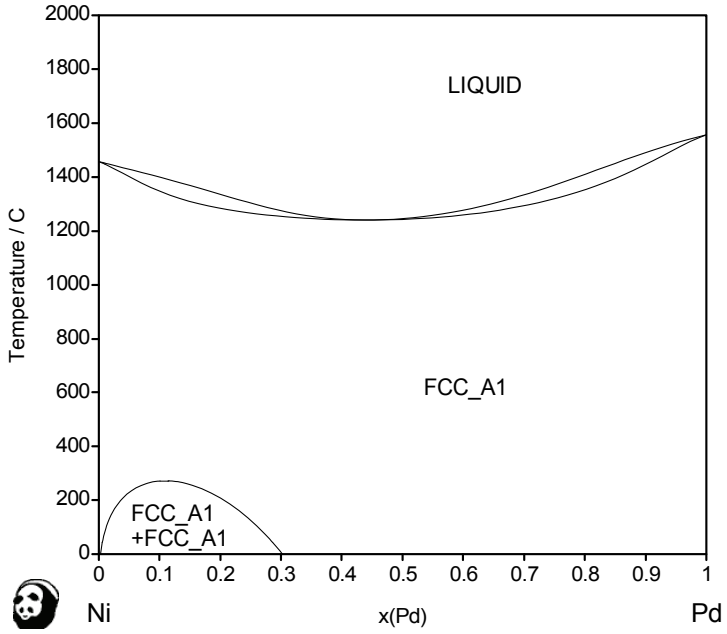

Fig. 44: Phase diagram of the Ni-Pd system

Ni-Sn System

In order to maintain consistency between the thermodynamic data for the different binary systems, the adopted data for the Ni-Sn system **[04Liu]** required modification. This was carried out within the scope of the COST 531 Action. The high temperature Ni_3Sn phase having the $D0_3$ structure has been observed in the Ni-Sn system. In the ternary Cu-Ni-Sn system, a continuous solubility region is observed between the high-temperature BCC_A2 phase originating in the Cu-Sn binary and this Ni_3Sn phase. Therefore, it was necessary to unify the models used for both phases in order to be able to model that region as a single phase. It was decided to reassess the Ni_3Sn phase as having the BCC_A2 structure to be consistent with the simplified model selected for the relevant phase in the Cu-Sn system.
It was also necessary to remodel the Ni_3Sn_2 (NI3SN2) phase to make it compatible with the Au-Ni-Sn assessment already present in the COST 531 database. A new 3-sublattice model, $(Ni,Sn)_{0.5}(Ni)_{0.25}(Ni)_{0.25}$, taking into the account the homogeneity range of NI3SN2, has been employed.

References:

[04Liu] Liu, H. S., Wang, J., Jin, Z. P.: *CALPHAD,* 2004, **28**, 363-370.

Table of invariant reactions

T / °C	Phases			Compositions / x_{Sn}		
1455.1	LIQUID	FCC_A1		0.000	0.000	
1251.9	LIQUID	NI3SN2		0.397	0.397	
1168.0	LIQUID	BCC_A2		0.259	0.259	
1165.6	BCC_A2	LIQUID	NI3SN2	0.262	0.278	0.374
1130.8	FCC_A1	LIQUID	BCC_A2	0.132	0.186	0.241
930.5	BCC_A2	NI3SN_LT		0.250	0.250	
919.2	FCC_A1	BCC_A2	NI3SN_LT	0.087	0.240	0.250
888.0	NI3SN_LT	BCC_A2	NI3SN2	0.250	0.268	0.375
794.6	NI3SN2	NI3SN4	LIQUID	0.433	0.557	0.772
231.9	LIQUID	BCT_A5		1.000	1.000	
231.4	NI3SN4	LIQUID	BCT_A5	0.575	0.998	0.100
13.1	NI3SN4	BCT_A5	DIAMOND_A4	0.577	1.000	1.000
13.0	BCT_A5	DIAMOND_A4		1.000	1.000	

Phase information

Phase Name	Common Name	Strukturbericht designation	Pearson Symbol
LIQUID	Liquid		
FCC_A1	(Ni)	*A*1	*cF*4
BCT_A5	(βSn)	*A*5	*tI*4
DIAMOND_A4	(αSn)	*A*4	*cF*8
BCC_A2[(a)]	Ni_3Sn_HT	$D0_3$	*cF*16
NI3SN_LT	Ni_3Sn_LT	$D0_{19}$	*hP*8
NI3SN2	Ni_3Sn_2_LT Ni_3Sn_2_HT	... ...	*oP*20 *hP*6
NI3SN4	Ni_3Sn_4	...	*mC*14

[(a)]Phase information (Common Name, Struktur. designation and Pearson Symbol) are given for the real Ni3Sn_HT phase

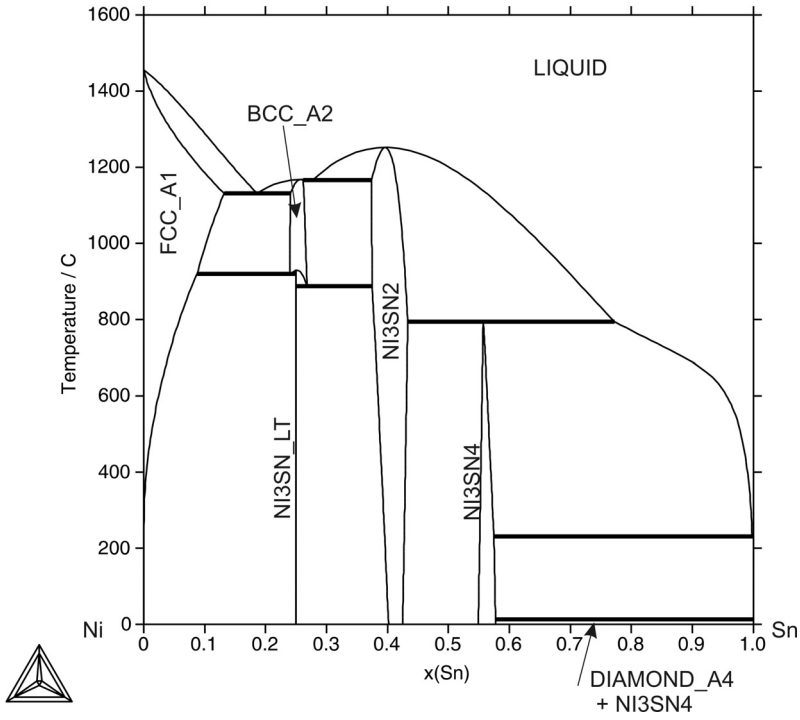

Fig. 45: Phase diagram of the Ni-Sn system

Ni-Zn System

The data for the Ni-Zn system are taken from the assessment of Miettinen **[03Mie]** which is itself a modified version of the critically assessed data of Vassilev *et al.* **[00Vas]**. The major difference between the two datasets relates to the modelling of the high temperature β phase which has a chemically ordered CsCl BCC_B2 structure. The assessment adopted for the database modelled this phase as a disordered BCC_A2 structure. The original assessment of Vassilev used a compound energy model with vacancies introduced onto the second sublattice.

References:

[00Vas] Vassilev, G. P., Gomez-Acebo, T., Tedenac, J.-C.: *J. Phase Equilib*., 2000, **21**, 287-301.

[03Mie] Miettinen, J.: *CALPHAD*, 2003, **27**, 263-274.

Table of invariant reactions

T / °C	Phases			Compositions / x_{Zn}		
1455.1	LIQUID	FCC_A1		0.000	0.000	
1040.0	FCC_A1	BCC_A2	LIQUID	0.396	0.494	0.522
878.3	LIQUID	NIZN_GAMMA		0.751	0.751	
868.7	BCC_A2	LIQUID	NIZN_GAMMA	0.551	0.704	0.740
808.7	FCC_A1	NIZN_BETA1	BCC_A2	0.354	0.466	0.474
661.7	NIZN_BETA1	BCC_A2	NIZN_GAMMA	0.519	0.536	0.740
491.1	NIZN_GAMMA	NIZN_DELTA	LIQUID	0.854	0.889	0.975
419.5	LIQUID	HCP_ZN		1.000	1.000	
413.0	NIZN_DELTA	LIQUID	HCP_ZN	0.889	0.990	1.000

Phase information

Phase Name	Common Name	Strukturbericht designation	Pearson Symbol
LIQUID	Liquid		
FCC_A1	(Ni)	*A*1	*cF*4
HCP_ZN	(Zn)	*A*3 *mod*	*hP*2
BCC_A2[(a)]	β	*B*2	*cP*2
NIZN_BETA1	β_1	...	*tP*4
NIZN_GAMMA	γ	$D8_2$	*cI*52
NIZN_DELTA	δ	...	*mC*6

[(a)]Phase information (Common Name, Struktur. Designation and Pearson Symbol) are given for the real β phase

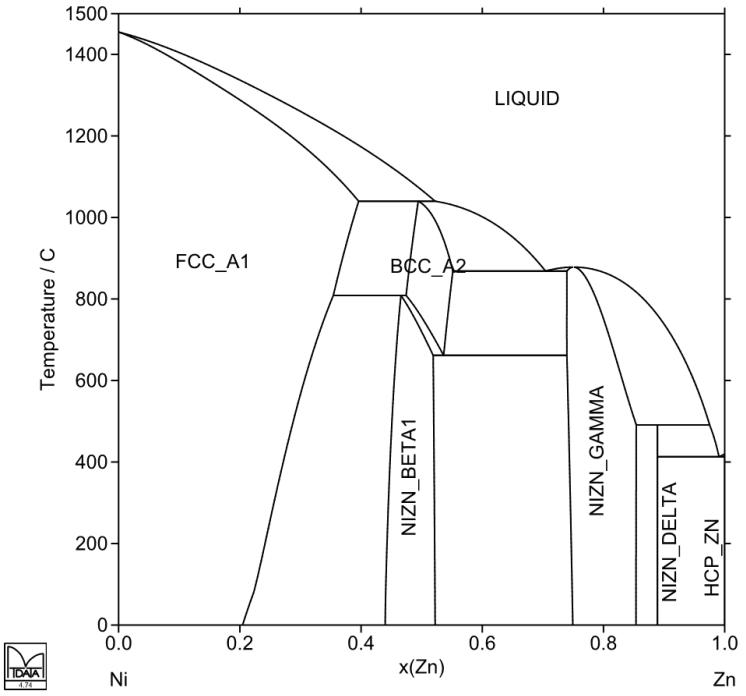

Fig. 46: Phase diagram of the Ni-Zn system

Pb-Pd System

Despite Pb and Pd having the same crystal structure, their mutual solubility is limited. Pd will dissolve up to about 20 at% Pb, whereas the solubility of Pd in Pb is negligible. The thermodynamic description for this system is taken from **[99Gho].** There are a number of intermetallic phases in the system, some of which have a number of polymorphs. According to **[MAS]**, both the Pb_9Pd_{13} and the Pb_3Pd_5 phases exist in α, β and γ forms. In the modelling, however, the description of Pb_9Pd_{13} is simplified, the phase being treated as a single stoichiometric phase PD13PB9. The PD5PB3_BETA phase at approx. x(Pd)=0.66 has not been labelled in the figure for clarity.

References:

[99Gho] Ghosh, G.: *J. Phase Equilib.*, 1999, **20**, 309-315.

Table of invariant reactions

T / °C	Phases			Compositions / x_{Pd}		
1554.8	LIQUID	FCC_A1#2		1.000	1.000	
1220.8	LIQUID	PD3PB		0.759	0.759	
1199.2	PD3PB	LIQUID	FCC_A1#2	0.772	0.797	0.833
834.4	LIQUID	PD5PB3_GAMMA	PD3PB	0.599	0.640	0.750
610.9	LIQUID	PD13PB9	PD5PB3_GAMMA	0.522	0.590	0.624
[a]520.6	PD5PB3_ GAMMA	PD5PB3_BETA	PD3PB	0.659	0.660	0.750
[a]519.8	PD13PB9	PD5PB3_GAMMA	PD5PB3_BETA	0.590	0.656	0.657
502.7	LIQUID	PDPB	PD13PB9	0.444	0.500	0.590
470.2	LIQUID	PDPB2		0.333	0.333	
452.6	PDPB2	LIQUID	PDPB	0.333	0.390	0.500
431.2	PD13PB9	PD5PB3_ALPHA	PD5PB3_BETA	0.590	0.625	0.660
416.5	PD5PB3_ ALPHA	PD5PB3_BETA	PD3PB	0.625	0.660	0.750
327.5	LIQUID	FCC_A1#1		0.000	0.000	
252.8	FCC_A1#1	LIQUID	PDPB2	0.002	0.088	0.333

[a] These invariant reactions are not distinguishable in Fig. 47 because the temperatures are very close

Phase information

Phase Name	Common Name	Strukturbericht designation	Pearson Symbol
LIQUID	Liquid		
FCC_A1	(Pb),(Pd)	$A1$	$cF4$
PDPB2	Pb_2Pd	$C16$	$tI12$
PDPB	αPbPd βPbPd	… …	$aP32$ …
PD13PB9	αPb_9Pd_{13} βPb_9Pd_{13} γPb_9Pd_{13}	… … …	$mC88$ $hP4$ …
PD5PB3_ALPHA	αPb_3Pd_5	…	$mC32$
PD5PB3_BETA	βPb_3Pd_5	$B8_1$	$hP4$
PD5PB3_GAMMA	γPb_3Pd_5	…	…
PD3PB	$PbPd_3$	$L1_2$	$cP4$

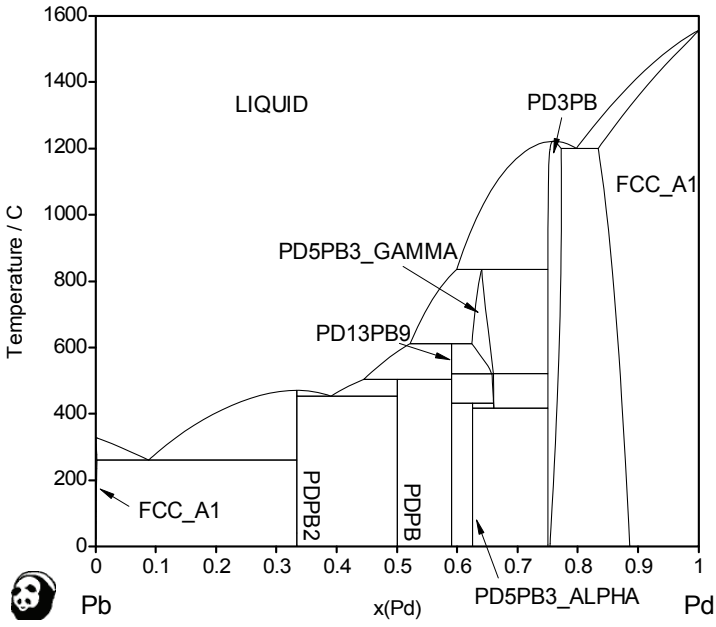

Fig. 47: Phase diagram of the Pb-Pd system

Pb-Sb System

The Pb-Sb is a simple eutectic system. There is only limited mutual solid solubility of the component elements. The thermodynamic description for this system is taken from **[95Oht]**.

References:

[95Oht] Ohtani, H., Okuda, K., Ishida, K.: *J. Phase Equilib.*, 1995, **16**, 416-429.

Table of invariant reactions

T / °C	Phases			Compositions / x_{Sb}		
630.6	LIQUID	RHOMBO_A7		1.000	1.000	
327.5	LIQUID	FCC_A1		0.000	0.000	
252.4	FCC_A1	LIQUID	RHOMBO_A7	0.060	0.177	0.987

Phase information

Phase Name	Common Name	Strukturbericht designation	Pearson Symbol
LIQUID	Liquid		
FCC_A1	(Pb)	*A*1	*cF*4
RHOMBO_A7	(Sb)	*A*7	*hR*2

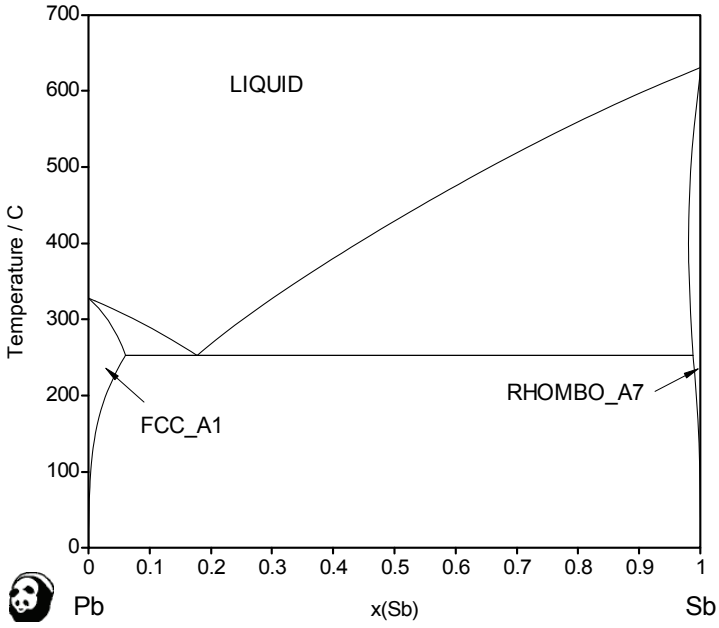

Fig. 48: Phase diagram of the Pb-Sb system

Pb-Sn System

Data for the Pb-Sn system are from the assessment of Ohtani and Ishida **[95Oht]**. The data for the FCC_A1 and LIQUID phases were modified within the framework of COST 531 to take account of new unary data for Sn in the metastable FCC_A1 structure **[SGTE4]**.

References:

[95Oht] Ohtani, H., Ishida, K.: *J. Phase Equilib.*, 1995, **16**, 416-429.

Table of invariant reactions

T / °C	Phases			Compositions / x_{Sn}		
327.5	LIQUID	FCC_A1		0.000	0.000	
231.9	LIQUID	BCT_A5		1.000	1.000	
183.0	FCC_A1	LIQUID	BCT_A5	0.269	0.740	0.980
13.0	BCT_A5	DIAMOND_A4		1.000	1.000	
12.7	FCC_A1	BCT_A5	DIAMOND_A4	0.020	0.999	1.000

Phase information

Phase Name	Common Name	Strukturbericht designation	Pearson Symbol
LIQUID	Liquid		
FCC_A1	(Pb)	*A*1	*cF*4
BCT_A5	(βSn)	*A*5	*tI*4
DIAMOND_A4	α-Sn	*A*4	*cF*8

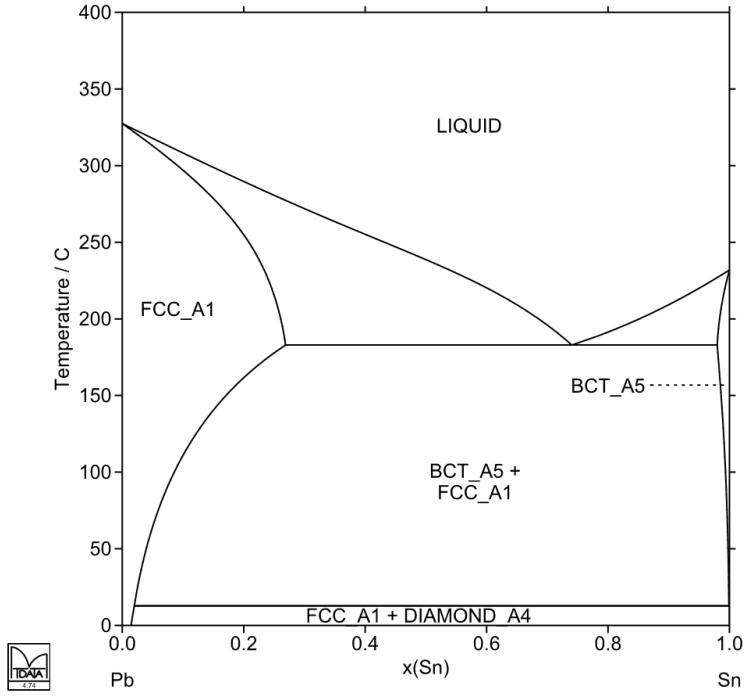

Fig. 49: Phase diagram of the Pb-Sn system

Pb-Zn System

The Pb-Zn system shows negligible mutual solid solubility of the component elements and no intermetallic phases. It is dominated by a syntectic reaction resulting from a large miscibility gap in the liquid phase. A eutectic reaction is present at a slightly lower temperature. The thermodynamic description for this system comes from **[93Sri]**.

References:

[93Sri] Srivastava, M., Sharma, R.C.: *J. Phase Equilib.*, 1993, **14**, 700-709.

Table of invariant reactions

T / °C	Phases			Compositions / x_{Zn}		
798.9	LIQUID	LIQUID#1	LIQUID#2	0.720	0.720	0.720
420.2	LIQUID#1	LIQUID#2	HCP_ZN	0.051	0.996	0.997
419.5	LIQUID#2	HCP_ZN		1.000	1.000	
327.5	LIQUID#1	FCC_A1		0.000	0.000	
317.8	FCC_A1	LIQUID#1	HCP_ZN	0.002	0.018	0.998

Phase information

Phase Name	Common Name	Strukturbericht designation	Pearson Symbol
LIQUID	Liquid		
FCC_A1	(Pb)	*A*1	*cF*4
HCP_ZN	(Zn)	*A*3 *mod*	*hP*2

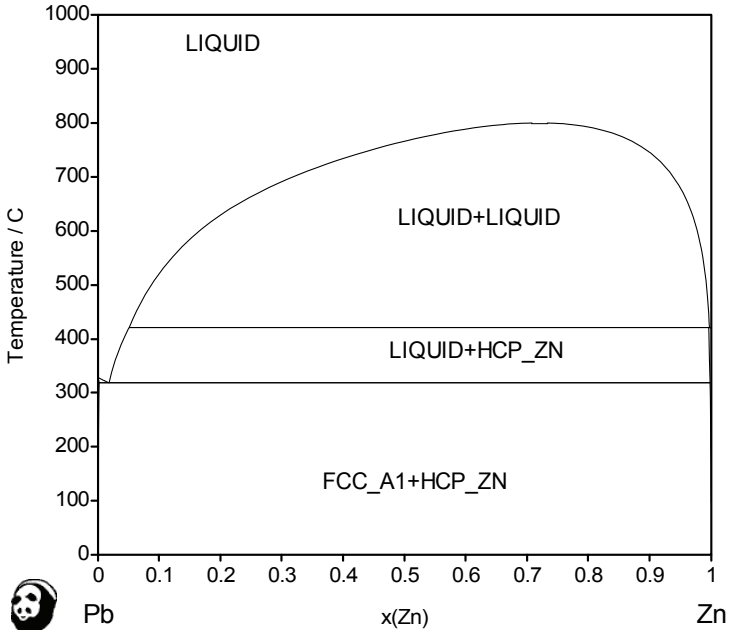

Fig. 50: Phase diagram of the Pb-Zn system

Pd-Sn System

The original assessment for the Pd-Sn system was made by Ghosh **[99Gho]** using different unary parameters from those used in the scope of the COST 531 Action **[SGTE4]**. The main difference was found in the description of the Gibbs energy of pure Sn in the metastable FCC_A1 phase. Therefore, the dataset has been modified to take account of the revised value. The phase boundary shift, resulting from using new unary data, was corrected. The rest of the diagram was accepted without change.

The phase diagram is very complicated, containing many intermetallic phases with high and low-temperature modifications. Because of the lack of experimental data most of them were modelled as stoichiometric compounds. The detail of the phase diagram with very complex phase coexistence in the region around 0.4 Pd is shown in the **Fig. 52**.

References:

[99Gho] Ghosh, G.: *Metall. Mat. Trans. A*, 1999, **30A**, 5-18.

Table of invariant reactions

T / °C	Phases			Compositions / x_{Sn}		
1584.9	LIQUID	FCC_A1		0.000	0.000	
1326.1	LIQUID	PD3SN		0.249	0.249	
1285.4	LIQUID	PD2SN_GAMMA		0.355	0.355	
1278.0	FCC_A1	LIQUID	PD3SN	0.207	0.214	0.246
1222.5	PD3SN	LIQUID	PD2SN_GAMMA	0.252	0.306	0.347
899.9	PD2SN_GAMMA	PD20SN13	LIQUID	0.377	0.405	0.495
819.9	PD3SN	PD2SN	PD2SN_GAMMA	0.250	0.333	0.343
809.6	PD20SN13	PDSN	LIQUID	0.419	0.503	0.528
659.7	PD20SN13	PD3SN2_BETA		0.400	0.400	
600.1	PDSN	PDSN2	LIQUID	0.508	0.668	0.697
[a]549.7	PD20SN13	PD3SN2_ALPHA	PD3SN2_BETA	0.398	0.400	0.400
[a]549.7	PD3SN2_BETA	PD3SN2_ALPHA	PD20SN13	0.400	0.400	0.403
512.7	PD3SN2_DELTA	PD20SN13	PDSN	0.410	0.410	0.500
477.5	PD2SN	PD2SN_GAMMA	PD20SN13	0.333	0.352	0.384
461.7	PD3SN2_ALPHA	PD20SN13	PD3SN2_DELTA	0.400	0.404	0.410
344.9	PDSN2	PDSN3	LIQUID	0.681	0.737	0.960
294.8	PDSN3	PDSN4	LIQUID	0.742	0.796	0.980
231.9	LIQUID	BCT_A5		1.000	1.000	
230.5	PDSN4	LIQUID	BCT_A5	0.799	0.996	1.000
13.1	PDSN4	BCT_A5	DIAMOND_A4	0.800	1.000	1.000
13.0	BCT_A5	DIAMOND_A4		1.000	1.000	

[a] These invariant reactions are not distinguishable in Figs. 51 and 52 because the temperatures are very close

Phase information

Phase Name	Common Name	Strukturbericht designation/type	Pearson Symbol
LIQUID	Liquid		
FCC_A1	(Pd)	$A1$	$cF4$
BCT_A5	(βSn)	$A5$	$tI4$
DIAMOND_A4	(αSn)	$A4$	$cF8$
PD3SN	Pd_3Sn	$L1_2$	$cP4$
PD2SN	Pd_2Sn	$C23$	$oP12$
PD2SN_GAMMA	γ	$B8_1$	$hP4$
PD20SN13	$Pd_{20}Sn_{13}$	···	$hP66$
PD3SN2_ALPHA	α-Pd_3Sn_2	···	···
PD3SN2_BETA	β-Pd_3Sn_2	···	···
PD3SN2_DELTA	δ	···	···
PDSN	PdSn	$B31$	$oP8$
PDSN2	$PdSn_2$	C_e	$oC24$
PDSN3	$PdSn_3$	···	$oC32$
PDSN4	$PdSn_4$	$D1_c$	$oC20$

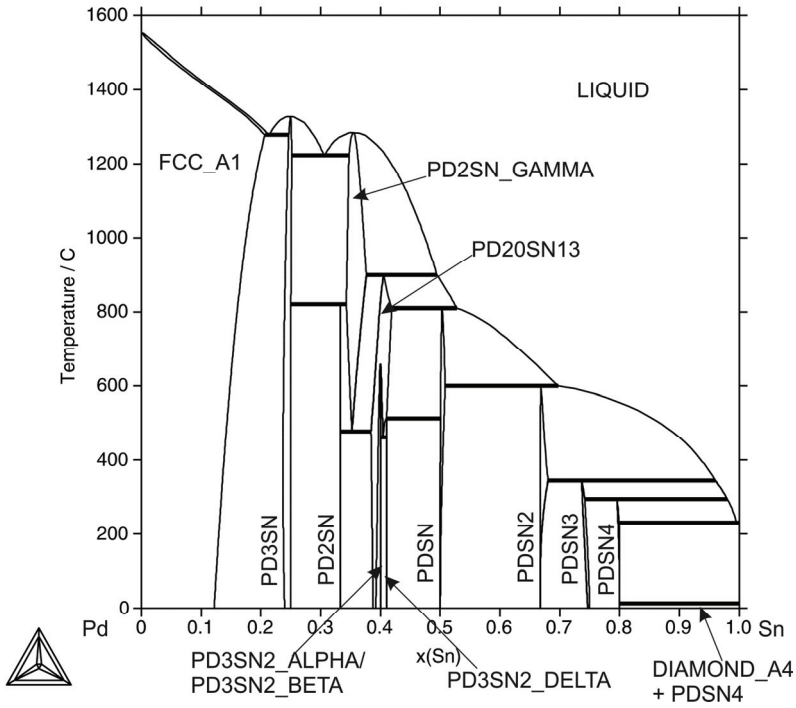

Fig. 51: Phase diagram of the Pd-Sn system

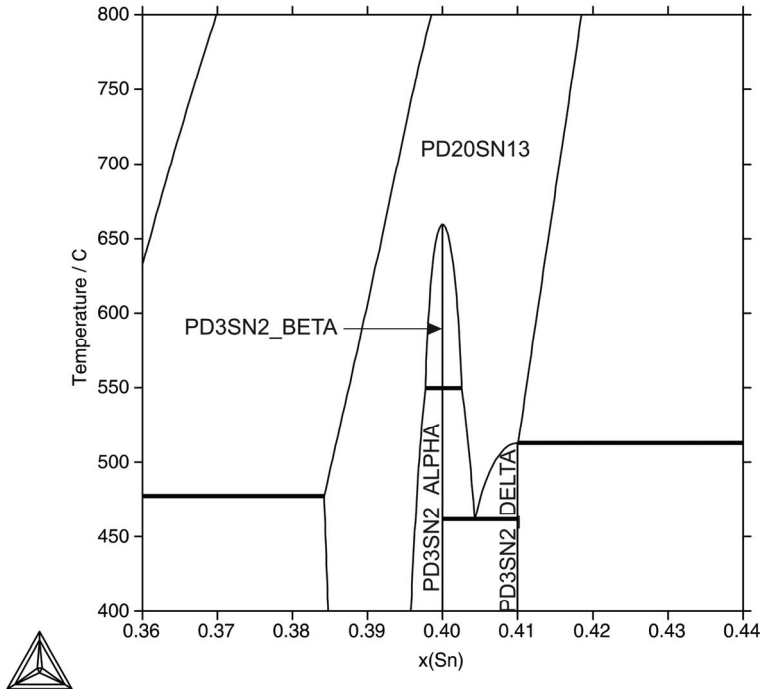

Fig. 52: Detail of phase diagram of the Pd-Sn system

Pd-Zn System

This system was assessed by **[06Viz]** within the scope of the COST 531 Action. They used the thermodynamic data from the work of Kou *et al.* **[75Kou]** and Chiang *et al.* **[77Chi]**. As there is a lack of experimental phase data for this system the authors utilised their own experimental results **[06Viz]** as well as the phase data estimated from **[MAS]** and **[58Han]**. The experimental results from **[06Viz]** led to the confirmation of the η phase, identified by **[51Now]**, and not accepted by **[MAS],** as the stable phase. They also found a different invariant reaction in the Zn-rich region in comparison with **[58Han]** and **[MAS]**. A eutectic was identified instead of a peritectic reaction.

References:

[51Now] Nowotny, H., Bauer, E., Stempfl, A.: *Monatsh. Chem.*, 1951, **82**, 1086-1093.

[58Han] Hansen, M., Anderko, K.: *Constitution of Binary Alloys*, McGraw-Hill, New York, 1958, 1130-1133.

[75Kou] Kou, S., Chang, Y. A.: *Acta Metall.*, 1975, **23**, 1185-1190.

[77Chi] Chiang, T., Ipser, H., Chang, Y. A.: *Z. Metallkd.*, 1977, **68**, 141-147.

[06Viz] Vízdal, J., Kroupa, A., Popovic, J., Zemanová, A.: *Adv. Eng. Mat.*, 2006, **8**, 164-176.

Table of invariant reactions

T / °C	Phases			Compositions / x_{Zn}		
1554.8	LIQUID	FCC_A1		0.000	0.000	
1380.0	LIQUID	PDZN_BETA		0.320	0.320	
1378.3	FCC_A1	LIQUID	PDZN_BETA	0.249	0.291	0.297
1207.7	PDZN_BETA	PDZN_1BETA		0.457	0.457	
885.2	LIQUID	PDZN_GAMMA		0.803	0.803	
857.9	PDZN_BETA	LIQUID	PDZN_GAMMA	0.657	0.737	0.765
694.7	FCC_A1	PDZN_BETA	PDZN_1BETA	0.239	0.305	0.354
691.3	FCC_A1	PD2ZN	PDZN_1BETA	0.239	0.333	0.354
564.6	PDZN_1BETA	PDZN_BETA	PDZN_GAMMA	0.618	0.655	0.772
526.5	PDZN_1BETA	PDZN2	PDZN_GAMMA	0.619	0.667	0.774
434.2	PDZN_GAMMA	PDZN_ETA	LIQUID	0.839	0.910	0.980
419.5	LIQUID	HCP_ZN		1.000	1.000	
416.6	PDZN_ETA	LIQUID	HCP_ZN	0.910	0.984	0.985
296.9	PDZN_GAMMA	PDZN_ETA	HCP_ZN	0.842	0.910	0.993

Phase information

Phase Name	Common Name	Strukturbericht designation	Pearson Symbol
LIQUID	Liquid		
FCC_A1	(Pd)	$A1$	$cF4$
HCP_ZN	(Zn)	$A3\ mod$	$hP2$
PDZN_BETA	β	$B2$	$cP2$
PDZN_1BETA	β_1	$L1_0$	$tP4$
PD2ZN	δ	$C23$	$oP12$
PDZN2	$PdZn_2$	…	$oC48$
PDZN_GAMMA	γ	$D8_2$	$cI52$
PDZN_ETA	η	…	…

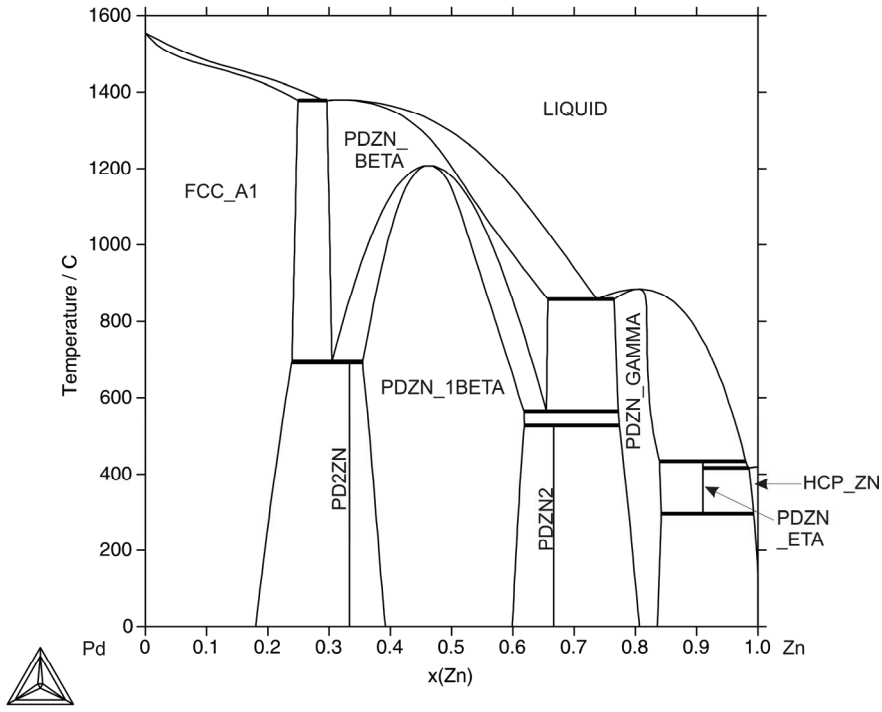

Fig. 53: Phase diagram of the Pd-Zn system

Sb-Sn System

Existing literature assessments had to be reassessed as they used different unary data for pure Sb in the hypothetical BCT_A5 structure. The dataset from Oh *et al.* **[96Oh]** was used as the base for the further work and DSC data of Vassilev *et al.* **[01Vas]**, and also data newly obtained in the scope of the COST 531 project **[04Vas]**, were taken into account. The reassessment of the system was carried out by Kroupa and Vízdal **[07Kro]**.

References:

[96Oh] Oh, C. S., Shim, J.H., Lee, B.J., Lee, D. N.: *J. Alloys Compd.*, 1996, **238**, 155-166.

[01Vas] Vassiliev, V., Feutelais, Y., Sghaier, M., Legendre, B. : *J. Alloy. Compd.,* 2001, **314**, 198-205.

[04Vas] Vassilev, G.P.: Unpublished work, 2004.

[07Kro] Kroupa, A., Vízdal, J.: *Defect and Diffusion Forum*, 2007, **263**, 99-104.

Table of invariant reactions

T / °C	Phases			Compositions / x_{Sn}		
630.6	LIQUID	RHOMBO_A7		0.000	0.000	
425.1	RHOMBO_A7	SBSN	LIQUID	0.159	0.375	0.498
325.1	SBSN	SB2SN3	LIQUID	0.508	0.600	0.786
245.8	SB2SN3	BCT_A5	LIQUID	0.600	0.892	0.910
242.4	SBSN	SB2SN3	BCT_A5	0.545	0.600	0.896
231.9	LIQUID	BCT_A5		1.000	1.000	
13.0	SBSN	BCT_A5	DIAMOND_A4	0.519	1.000	1.000
13.0	BCT_A5	DIAMOND_A4		1.000	1.000	

Phase information

Phase Name	Common Name	Strukturbericht designation	Pearson Symbol
LIQUID	Liquid		
BCT_A5	(βSn)	*A*5	*tI*4
DIAMOND_A4	(αSn)	*A*4	*CF*8
RHOMBO_A7	(βSb)	*A*7	*hR*2
SBSN	β	*B*1	*cF*8
SB2SN3	Sb_2Sn_3	…	…

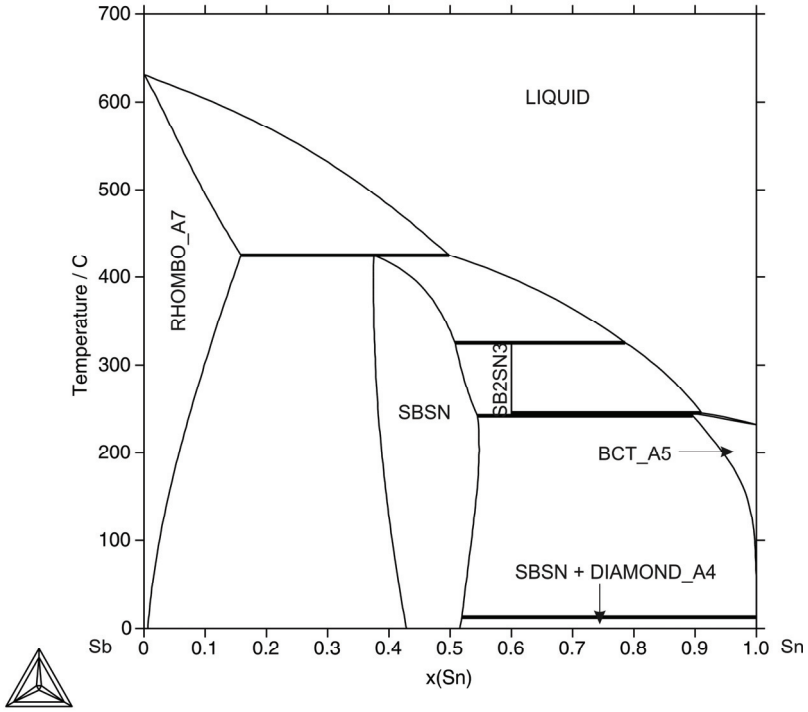

Fig. 54: Phase diagram of the Sb-Sn system

Sb-Zn System

The data for the Sb-Zn system are from the critical assessment of Liu *et al.* **[00Liu]**. The authors obtained good agreement between calculated and experimental values for a wide range of properties.

References:

[00Liu] Liu, X. J., Wang, C. P., Ohnuma, I., Kainuma, R., Ishida, K.: *J. Phase Equilib.*, 2000, **21**, 432-442.

Table of invariant reactions

T / °C	Phases			Compositions / x_{Zn}		
630.6	LIQUID	RHOMBO_A7		0.000	0.000	
563.5	LIQUID	SBZN_ZETA		0.600	0.600	
560.6	LIQUID	SBZN_DELTA	SBZN_ZETA	0.559	0.575	0.600
546.1	LIQUID	SBZN_BETA	SBZN_DELTA	0.477	0.500	0.575
527.9	SBZN_BETA	SBZN_GAMMA	SBZN_DELTA	0.500	0.550	0.575
506.4	RHOMBO_A7	LIQUID	SBZN_BETA	0.017	0.313	0.500
[a]491.8	SBZN_DELTA	SBZN_EPSILON	SBZN_ZETA	0.575	0.575	0.600
[a]491.8	SBZN_GAMMA	SBZN_DELTA	SBZN_EPSILON	0.550	0.575	0.575
[a]491.4	SBZN_BETA	SBZN_GAMMA	SBZN_EPSILON	0.500	0.550	0.575
454.8	SBZN_ZETA	SBZN_ETA	LIQUID	0.600	0.620	0.928
439.5	SBZN_EPSILON	SBZN_ZETA	SBZN_ETA	0.575	0.600	0.620
419.5	LIQUID	HCP_ZN		1.000	1.000	
[a]409.7	SBZN_ETA	LIQUID	HCP_ZN	0.620	0.978	1.000
[a]408.1	SBZN_EPSILON	SBZN_ETA	HCP_ZN	0.575	0.620	1.000
216.5	SBZN_BETA	SBZN_EPSILON	HCP_ZN	0.500	0.575	1.000

[a] These invariant reactions are not distinguishable in Fig. 55 because the temperatures are very close

Phase information

Phase Name	Common Name	Strukturbericht designation	Pearson Symbol
LIQUID	Liquid		
RHOMBO_A7	(Sb)	*A*7	*hR*2
HCP_ZN	(Zn)	*A*3 *mod*	*hP*2
SBZN_BETA	β	B_e	*oP*16
SBZN_GAMMA	γ	…	…
SBZN_DELTA	δ	…	…
SBZN_EPSILON	ε	…	…
SBZN_ZETA	ζ	…	*oI**
SBZN_ETA	η	…	*oP*30

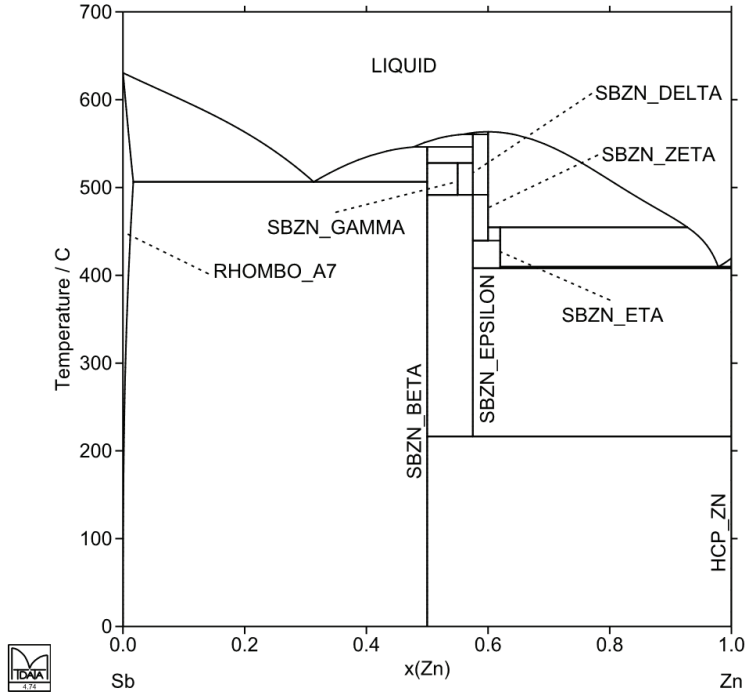

Fig. 55: Phase diagram of the Sb-Zn system

Sn-Zn System

The Sn-Zn system was assessed by several authors **[96Lee, 99Oht, 02Fri],** which differ in the unary data used and also in the temperature dependence of the solubility of Zn in pure Sn. It was difficult to evaluate the reliability of particular assessments as there is a limited number of experimental data in this region. Therefore the consistency of the unary data was taken as an important criterion and the theoretical data for the Sn-Zn system from the critical assessment of Fries **[02Fri]** published as part of the COST507 database **[98Ans]** were accepted.

References:

[96Lee] Lee, B.-J.: *CALPHAD,* 1996, **20**, 471-480.

[98Ans] Ansara, I., Dinsdale, A. T., Rand, M. H.: *Thermochemical database for light metal alloys*, EUR18499, July 1998, **2**, 288-289.

[99Oht] Ohtani, H., Miyashita, M., Ishida, K.: *J. Jpn. Inst. Met.*, 1999, **63**, 685-694.

[02Fri] Fries, S. G.: Unpublished work, 2002.

Table of invariant reactions

T / °C	Phases			Compositions / x_{Zn}		
419.5	LIQUID	HCP_ZN		1.000	1.000	
231.9	LIQUID	BCT_A5		0.000	0.000	
198.3	BCT_A5	LIQUID	HCP_ZN	0.006	0.135	0.999
13.0	BCT_A5	DIAMOND_A4		1.000	1.000	
12.7	DIAMOND_A4	BCT_A5	HCP_ZN	0.000	0.001	1.000

Phase information

Phase Name	Common Name	Strukturbericht designation	Pearson Symbol
LIQUID	Liquid		
BCT_A5	(βSn)	*A*5	*tI*4
DIAMOND_A4	(αSn)	*A*4	*CF*8
HCP_ZN	(Zn)	*A*3 *mod*	*hP*2

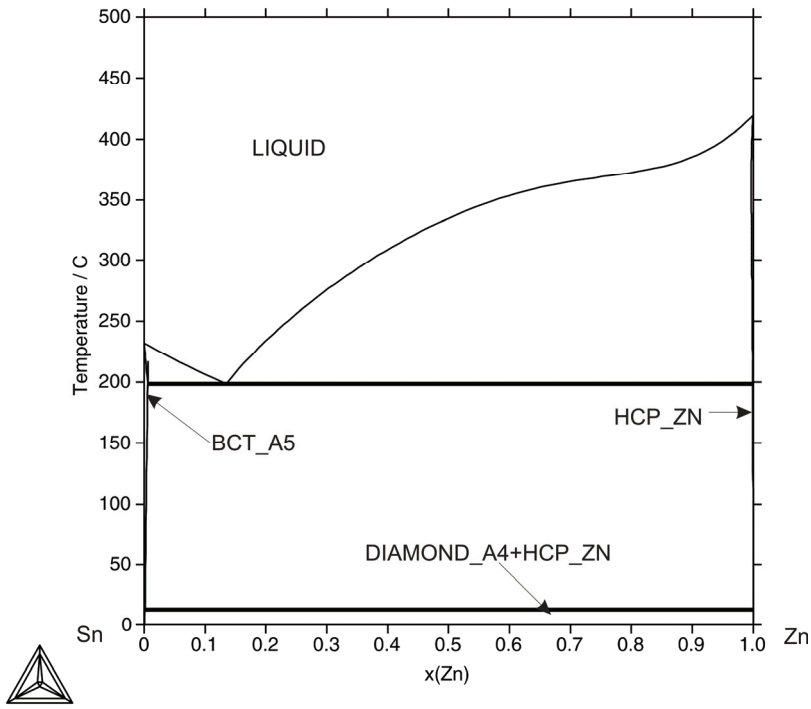

Fig. 56: Phase diagram of the Sn-Zn system

3 - Ternary systems

Ag-Au-Bi system

The data for the Ag-Au-Bi system were taken from a recent assessment by Zoro *et al.* **[07Zor1]**, **[07Zor2]** undertaken within the framework of the COST 531 Action. The assessment is based on their own experimental study of four isopleths by X-ray diffraction, differential calorimetry and electron probe microanalysis **[05Zor1]** and measurements of the enthalpies of mixing in the liquid phase **[05Zor2]**.

References:

[05Zor1] Zoro, E., Dichi, E., Servant, C., Legendre, B.: *J. Alloys Comp.,* 2005, **400**, 209-215.

[05Zor2] Zoro, E., Boa, D., Servant, C., Legendre, B.: *J. Alloys Comp.,* 2005, **398**, 106-112.

[07Zor1] Zoro, E., Servant, C., Legendre, B.: *J. Thermal Anal. Calor*., 2007, **90**, 347-353.

[07Zor2] Zoro, E., Servant, C., Legendre, B.: *CALPHAD* 2007, **31**, 89-94.

Table of invariant reactions

T / °C	Reaction type	Phases	Compositions		
			x_{Ag}	x_{Au}	x_{Bi}
251.9	U1	LIQUID	0.004	0.094	0.902
		FCC_A1	0.325	0.676	0.000
		AU2BI_C15	0.101	0.566	0.333
		RHOMBO_A7	0.000	0.000	1.000

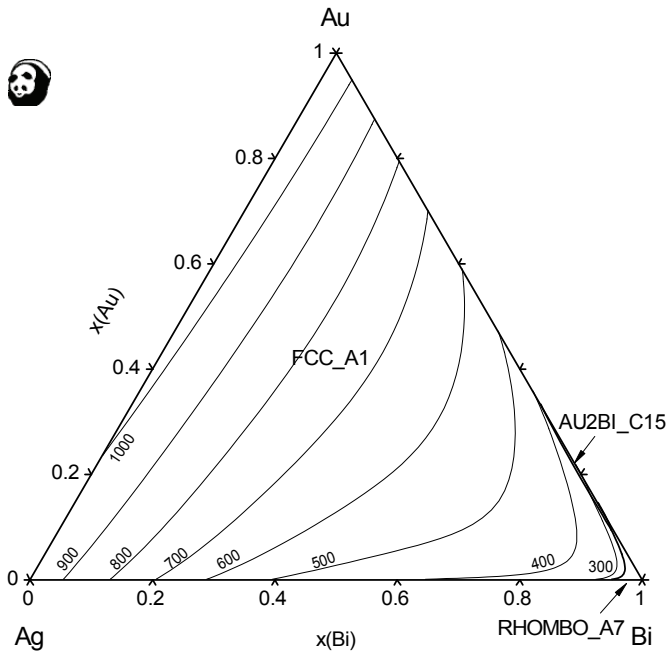

Fig. 57: Liquidus projection of the Ag-Au-Bi system

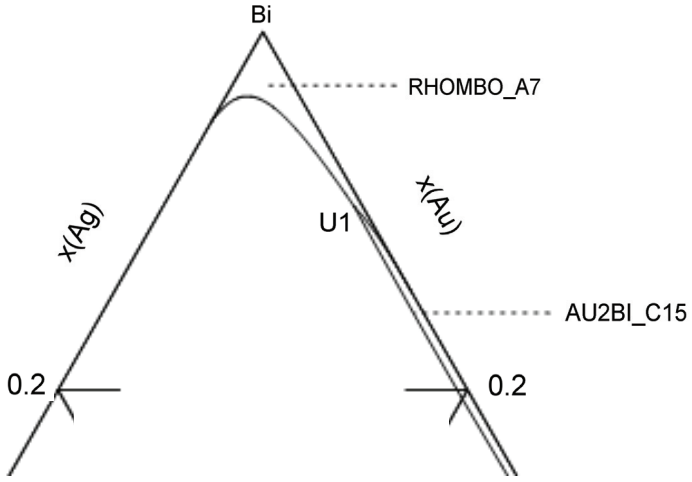

Fig. 58: Liquidus projection for the Bi rich corner of the Ag-Au-Bi system

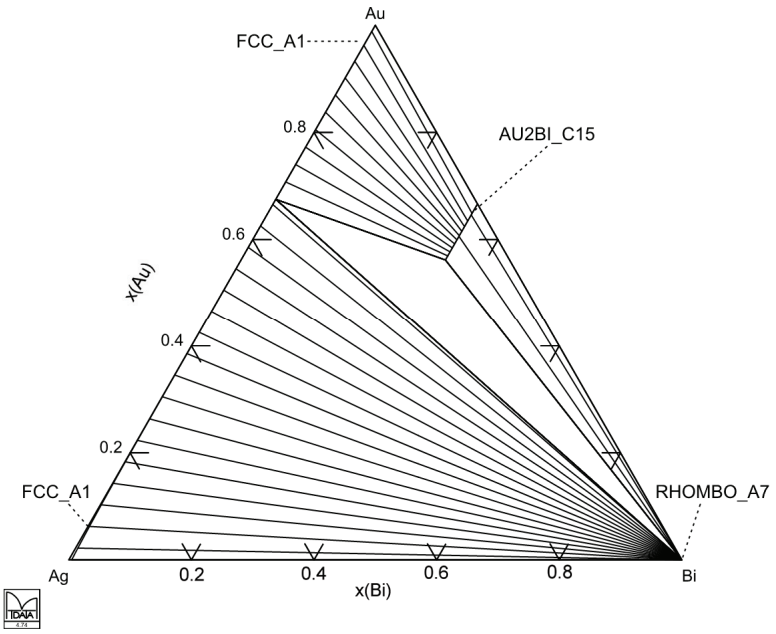

Fig. 59: Isothermal section at 230 °C

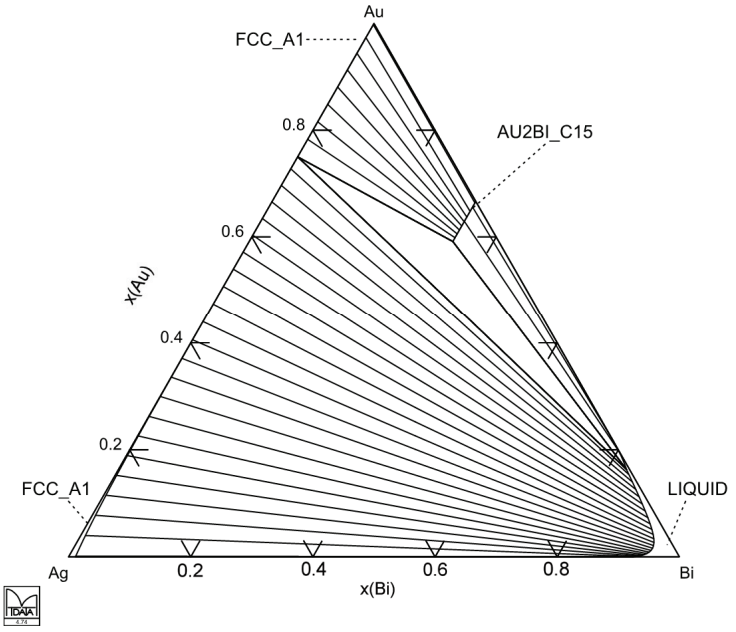

Fig. 60: Isothermal section at 300 °C

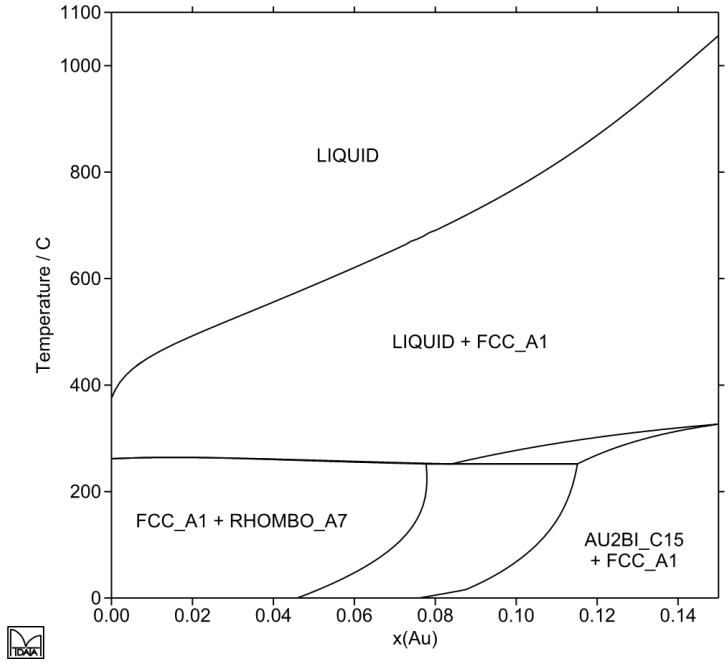

Fig. 61: Bi-rich part of the isopleth of the Ag-Au-Bi system for 20 at% Ag

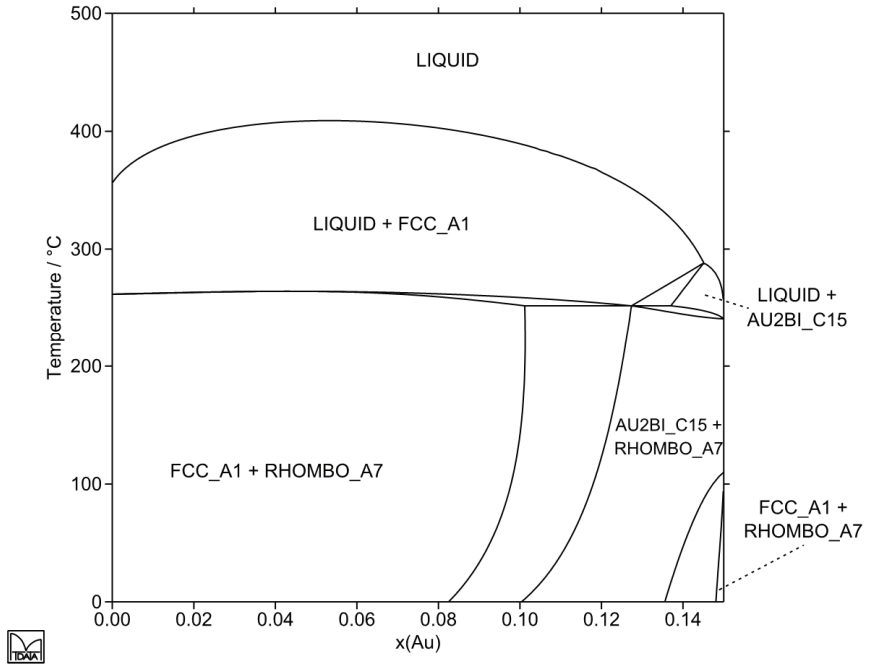

Fig. 62: Isopleth of the Ag-Au-Bi system for 85 at% Bi

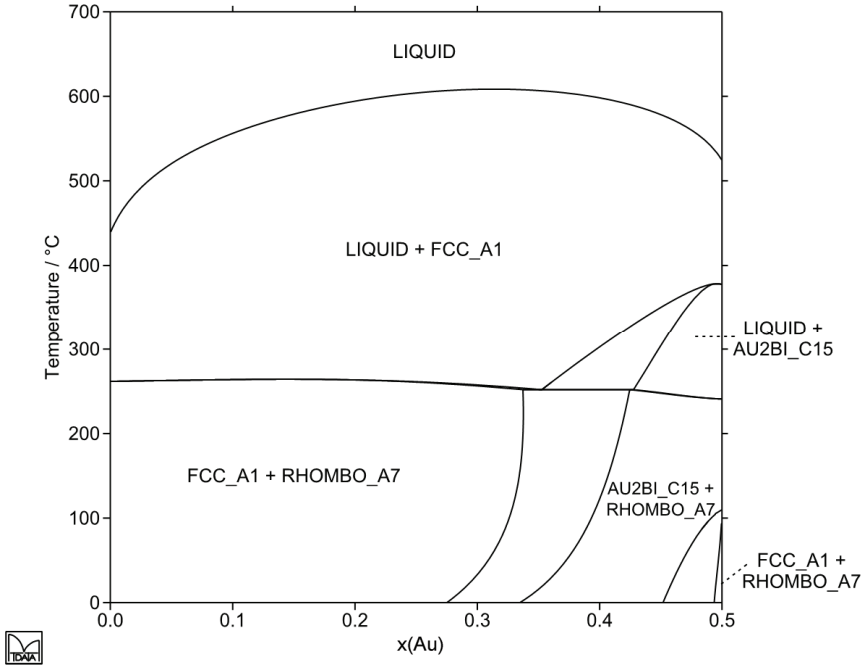

Fig. 63: Isopleth of the Ag-Au-Bi system for 50 at% Bi

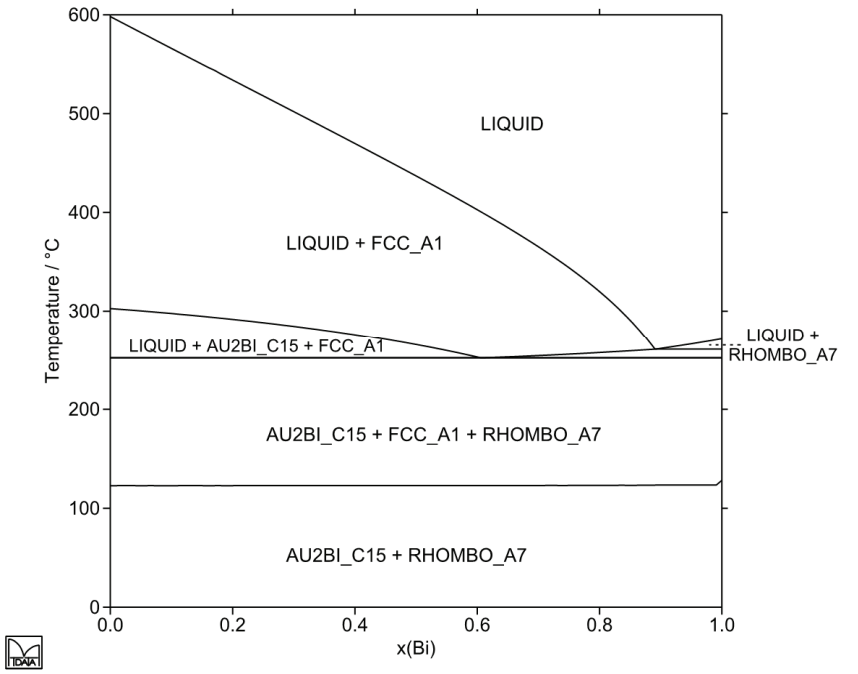

Fig. 64: Isopleth of the Ag-Au-Bi system with the ratio Ag:Au of 1:4

Ag-Au-Sb system

The data for the Ag-Au-Sb system were taken from a recent assessment by Zoro *et al.* **[07Zor1]**, **[07Zor2]** undertaken within the framework of the COST 531 Action. The assessment is based on their own experimental study of phase equilibria across seven isopleths and measurements of the enthalpies of mixing in the liquid phase.

References:

[07Zor1] Zoro, E., Servant, C., Legendre, B.: *J. Phase Equilib. Diffus.*, 2007, **28**, 250-257

[07Zor2] Zoro, E., Servant, C., Legendre, B.: *J. Thermal Anal. Calor.*, 2007, **90**, 347-353.

Table of invariant reactions

T / °C	Reaction type	Phases	Compositions		
			x_{Ag}	x_{Au}	x_{Sb}
415.0	U1	LIQUID	0.460	0.154	0.385
		AGSB_ORTHO	0.653	0.095	0.252
		HCP_A3	0.683	0.142	0.175
		RHOMBO_A7	0.000	0.000	1.000
390.0	E1	LIQUID	0.249	0.387	0.363
		AUSB2	0.005	0.328	0.667
		FCC_A1	0.430	0.567	0.003
		HCP_A3	0.488	0.407	0.106
388.6	E2	LIQUID	0.355	0.250	0.394
		AUSB2	0.022	0.312	0.667
		HCP_A3	0.601	0.241	0.158
		RHOMBO_A7	0.000	0.000	1.000

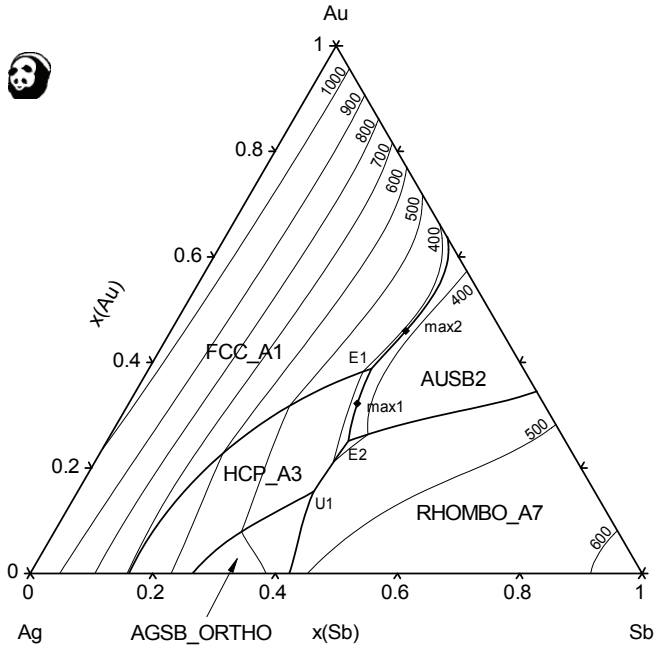

Fig. 65: Liquidus projection of the Ag-Au-Sb system

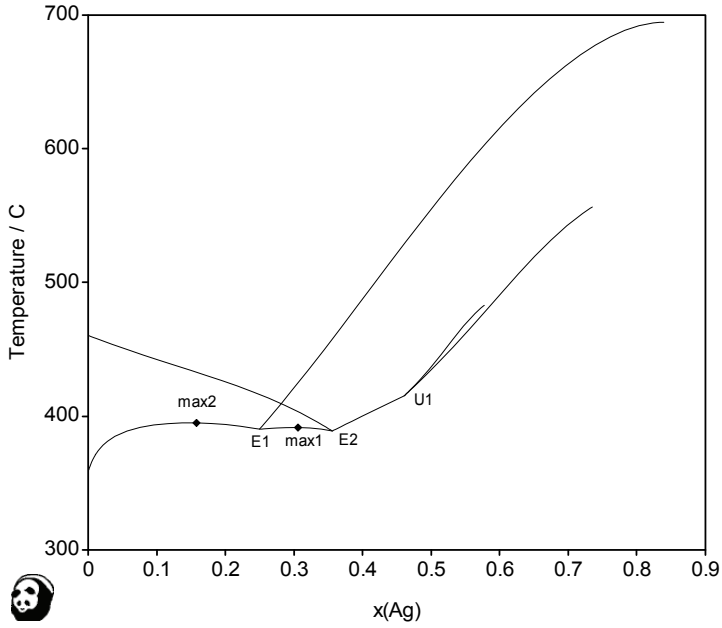

Fig. 66: Liquidus lines in the Ag-Au-Sb system projected onto the T-x(Ag) plane

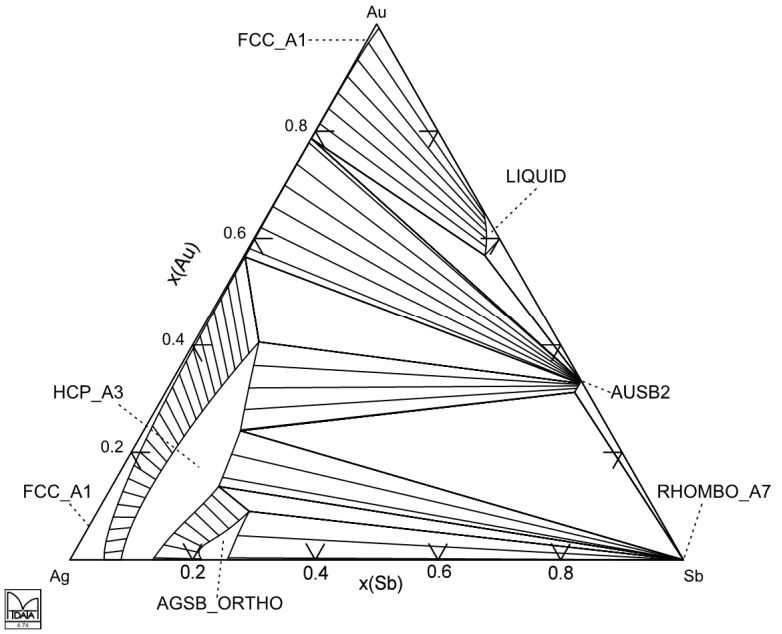

Fig. 67: Isothermal section at 385 °C

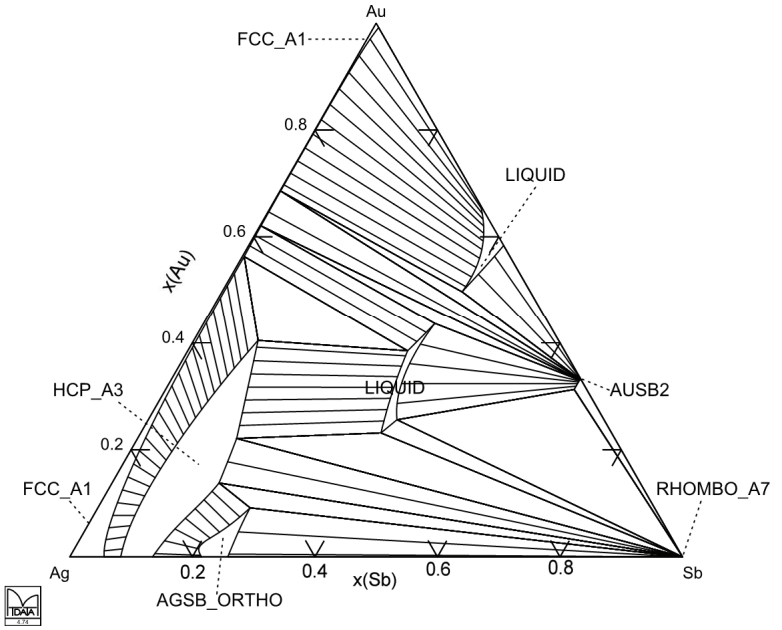

Fig. 68: Isothermal section at 394 °C

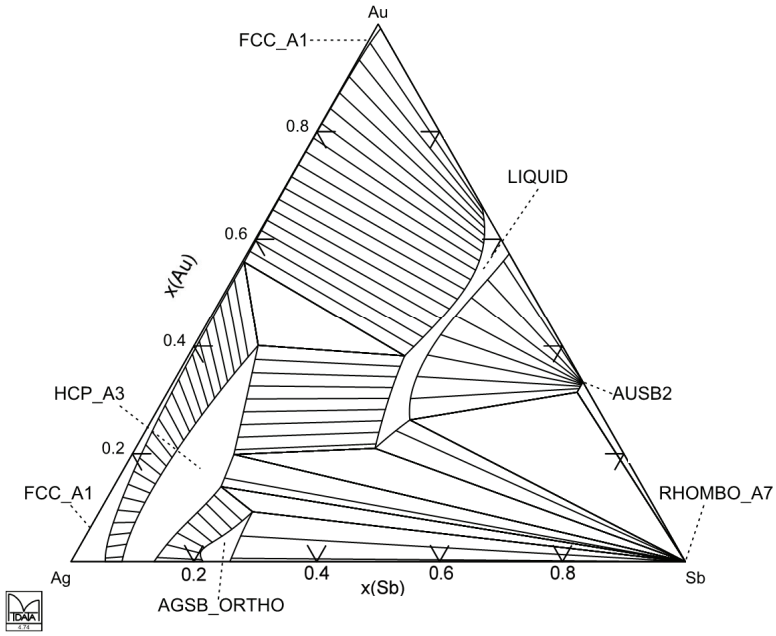

Fig. 69: Isothermal section at 400 °C

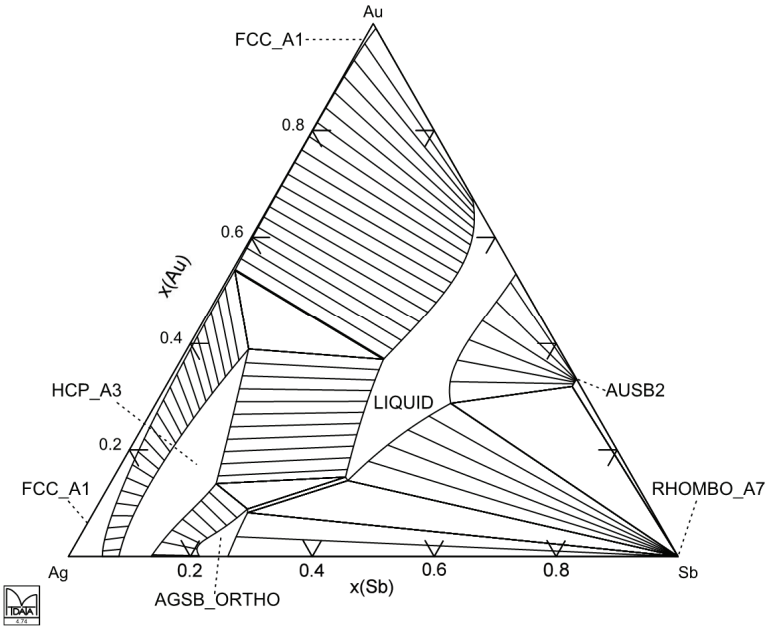

Fig. 70: Isothermal section at 420 °C

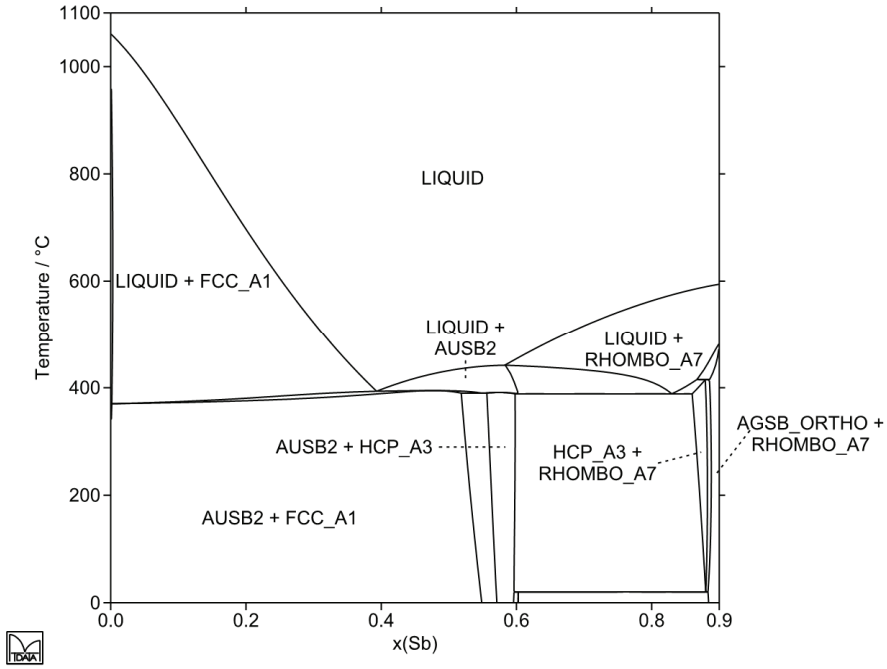

Fig. 71: Isopleth of the Ag-Au-Sb system for 10 at % Ag

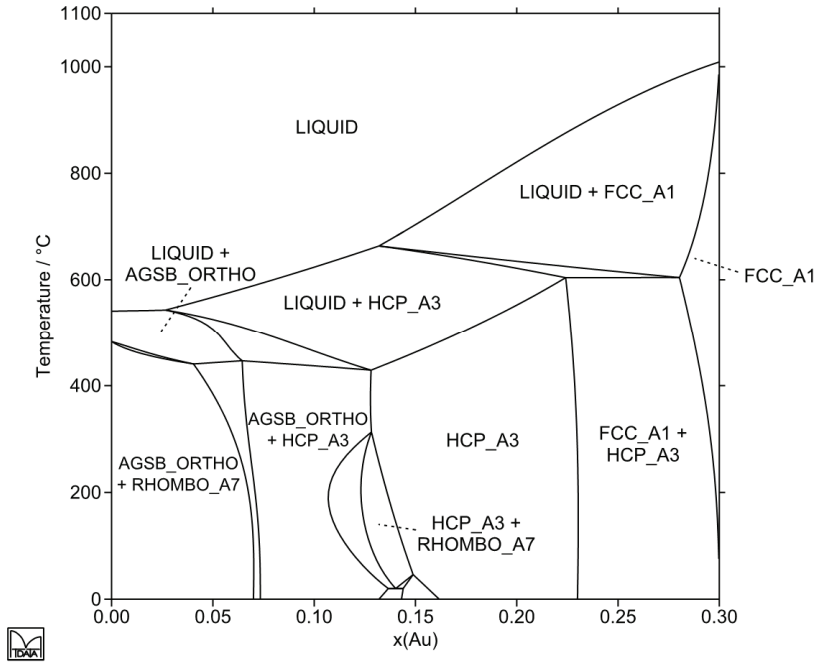

Fig. 72: Isopleth of the Ag-Au-Sb system for 70 at % Ag

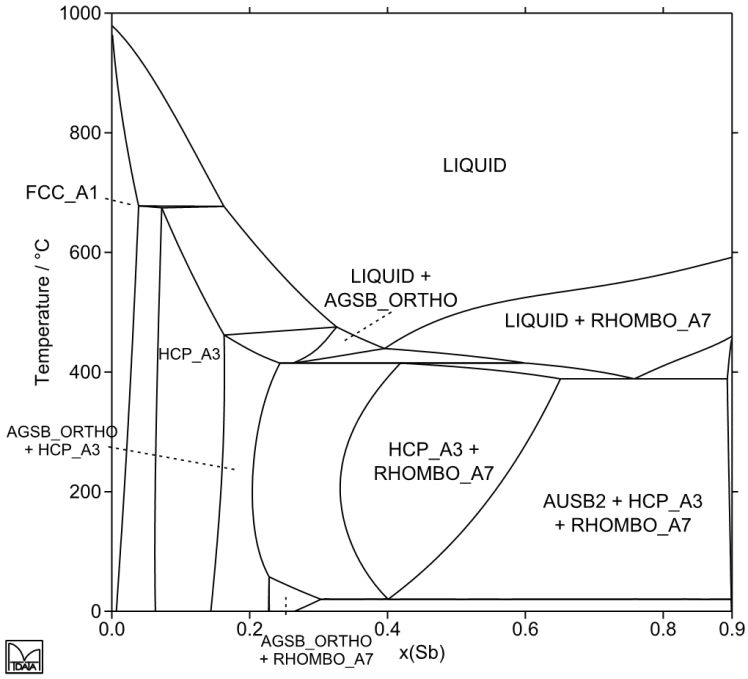

Fig. 73: Isopleth of the Ag-Au-Sb system for 10 at % Au

Ag-Bi-Sn System

The data for this system were a revision of an assessment of Garzel *et al*. **[06Gar]** based on the new experimental electromotive force (emf) data **[06Gar, 07Li]** obtained in the scope of COST 531 Action. The revision was necessary because of the change to the data for the Ag-Sn and Bi-Sn systems and is in very good agreement with all available data. These replaced the previous assessment of Ohtani *et al.* **[04Oht]**.

References:

[04Oht] Ohtani, H.: *Materials Transactions*, 2004, **42**, 722-731.

[06Gar] Garzel, G., Zabdyr, L. A.: *J. Phase Equil.*, 2006, **24**, 140-144.

[07Li] Li, Z., Knott, S., Mikula, A.: *J. Electron. Mat.*, 2007, **36**, 40-44.

Table of invariant reactions

T / °C	Reaction type	Phases	Compositions		
			x_{Ag}	x_{Bi}	x_{Sn}
263.2	D1	LIQUID	0.038	0.958	0.004
		HCP_A3	0.895	0.003	0.102
		RHOMBO_A7	0.000	1.000	0.000
		FCC_A1	0.913	0.002	0.085
262.0	U1	LIQUID	0.030	0.952	0.018
		HCP_A3	0.859	0.002	0.139
		RHOMBO_A7	0.000	0.998	0.002
		AGSB_ORTHO	0.750	0.091	0.158
136.9	E1	LIQUID	0.009	0.376	0.615
		RHOMBO_A7	0.000	0.970	0.030
		AGSB_ORTHO	0.750	0.002	0.248
		BCT_A5	0.000	0.063	0.936

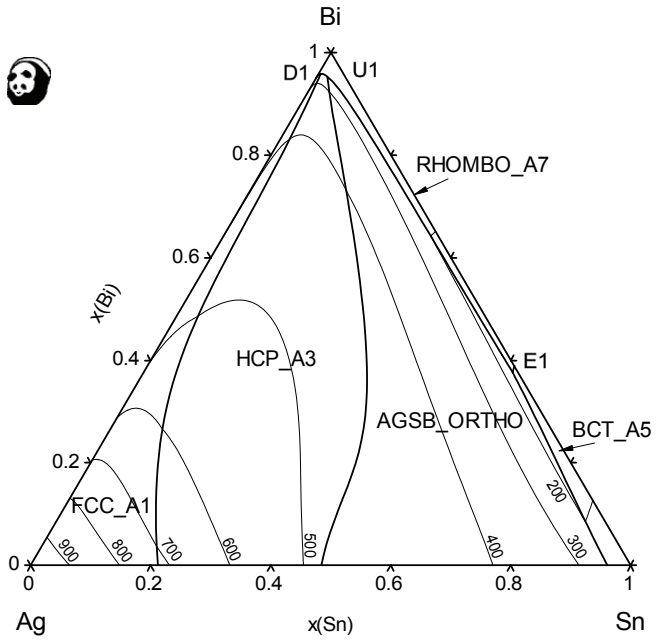

Fig. 74: Liquidus projection of the Ag-Bi-Sn system

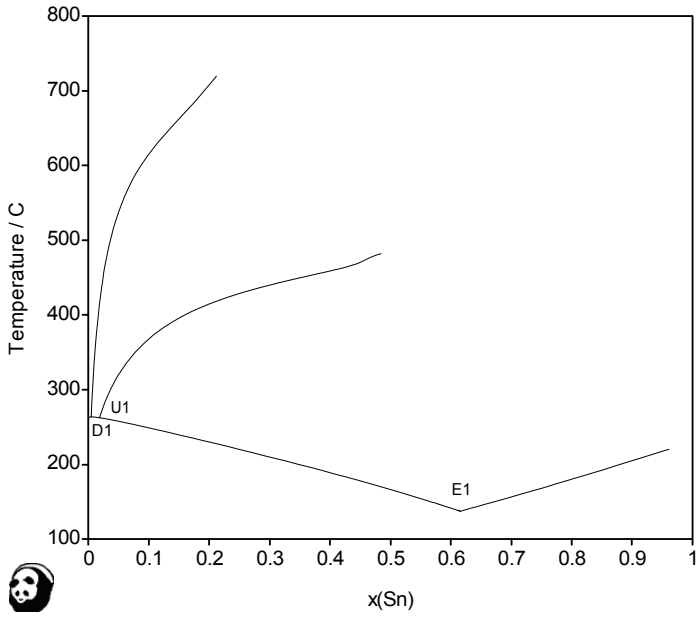

Fig. 75: Liquidus lines in the Ag-Bi-Sn system projected onto the T- x(Sn) plane

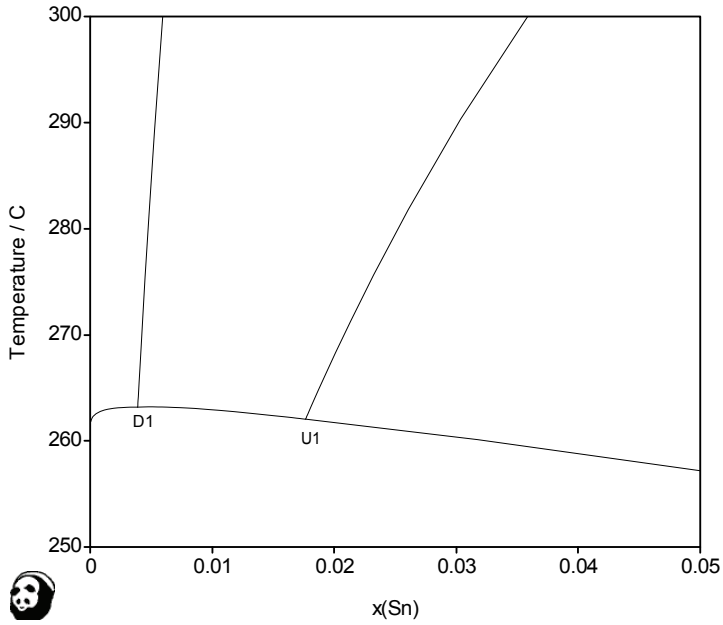

Fig. 76: Liquidus lines in the Bi-rich corner in the Ag-Bi-Sn system projected onto the T- x(Sn) plane

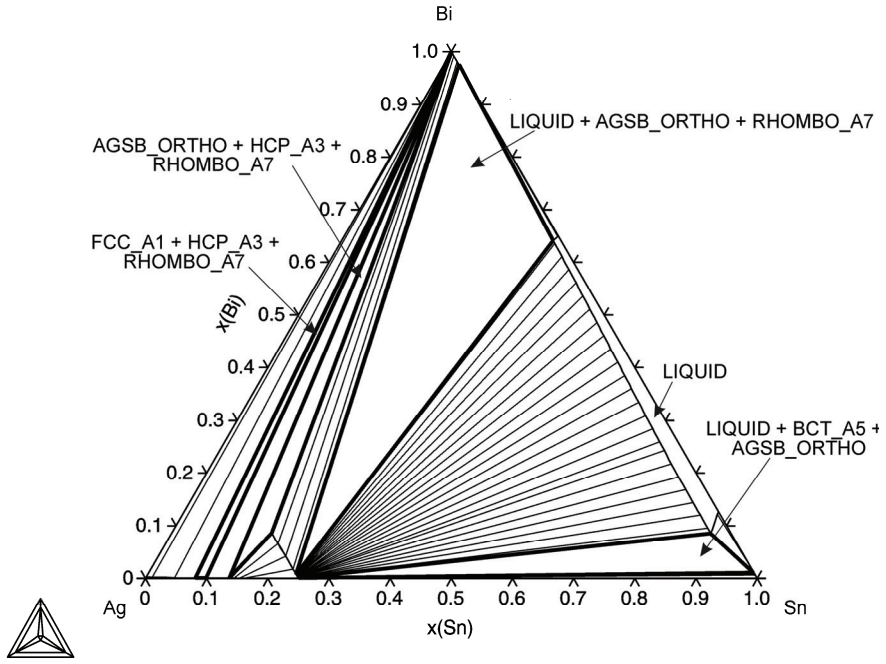

Fig. 77: Isothermal section at 200 °C

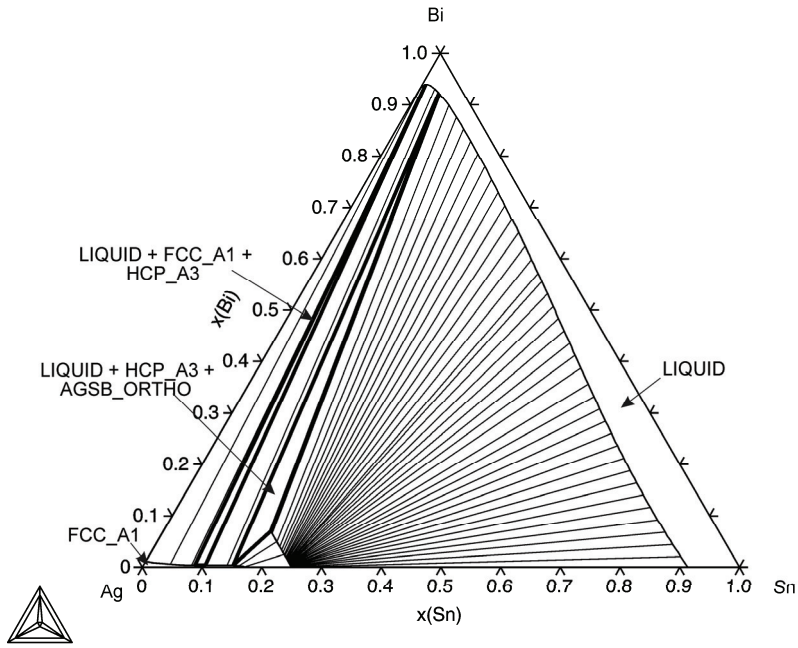

Fig. 78: Isothermal section at 300 °C

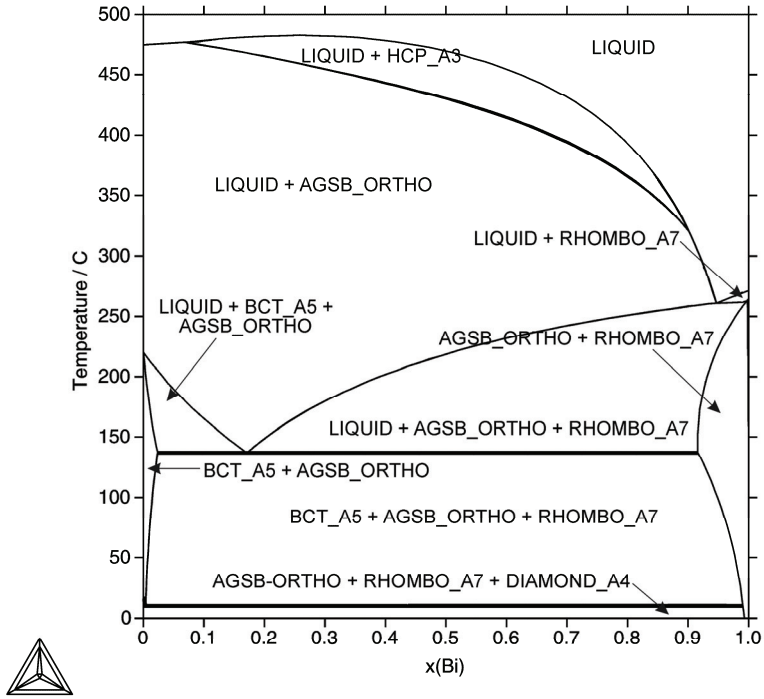

Fig. 79: Isopleth of the Ag-Bi-Sn system with the ratio Ag:Sn of 1:1

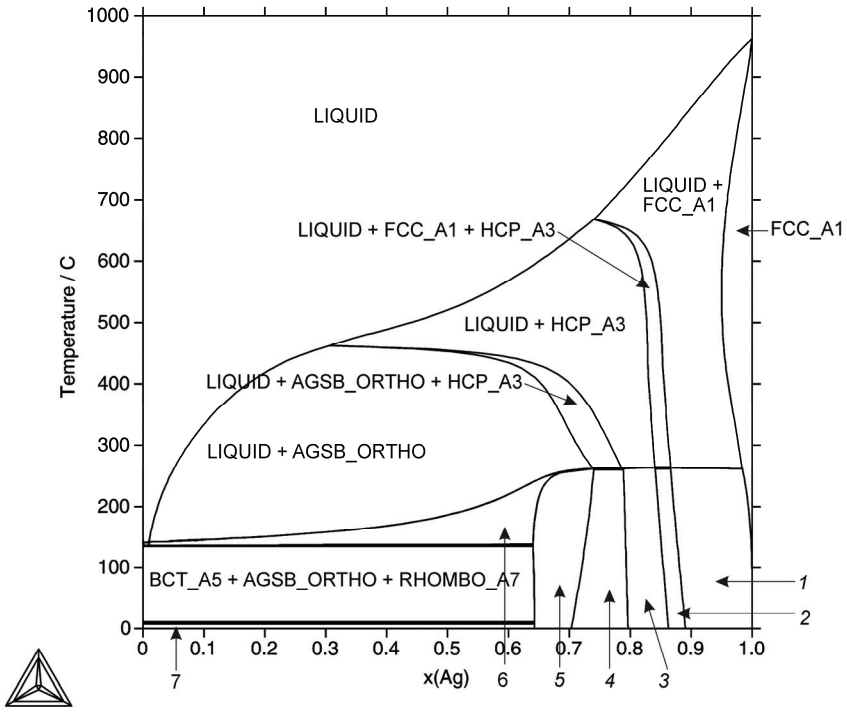

Fig. 80: Isopleth of the Ag-Bi-Sn system with the ratio Bi:Sn of 2:3

Legend:

1 – FCC_A1 + RHOMBO_A7
2 – FCC_A1 + HCP_A3 + RHOMBO_A7
3 – HCP_A3 + RHOMBO_A7
4 – AGSB_ORTHO + HCP_A3 + RHOMBO_A7
5 – AGSB_ORTHO + RHOMBO_A7
6 – LIQUID + AGSB_ORTHO + RHOMBO_A7
7 – AGSB_ORTHO + RHOMBO_A7 + DIAMOND_A4

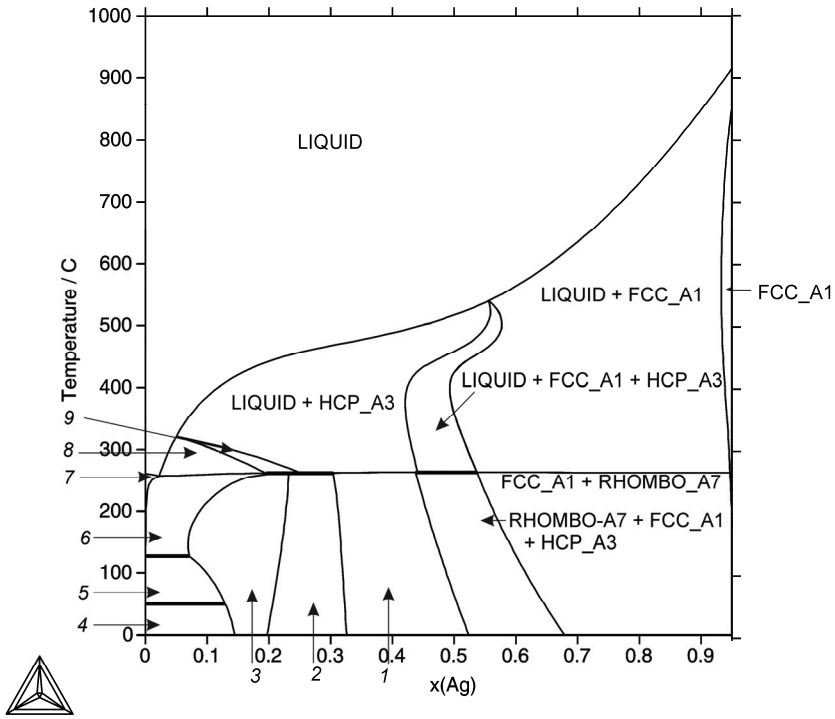

Fig. 81: Isopleth of the Ag-Bi-Sn system for 5 at% Sn

Legend:

1 – HCP_A3 + RHOMBO_A7
2 – AGSB_ORTHO + HCP_A3 + RHOMBO_A7
3 – AGSB_ORTHO + RHOMBO_A7
4 – AGSB_ORTHO + RHOMBO_A7 +DIAMOND_A4
5 – BCT_A5 + AGSB_ORTHO + RHOMBO_A7
6 – LIQUID + AGSB_ORTHO + RHOMBO_A7
7 – LIQUID + RHOMBO_A7
8 – LIQUID + AGSB_ORTHO
9 – LIQUID + AGSB_ORTHO + HCP_A3

Ag-Cu-In System

This system had not been assessed prior to COST 531. The only experimental information on this system was presented by **[88Woy]** which gave an isothermal section for 505 °C. An interesting feature of this section is what would seem at first sight to be a ternary compound lying along at approximately 30 at% In. At closer inspection, this 'ternary' compound is in fact the CUIN_GAMMA phase which exists as a complete series of solid solutions from CUIN_GAMMA, which is a high-temperature phase in the Cu-In binary system, to Ag_2In, which is a low temperature phase in the Ag-In binary system. Because of the differing temperature stabilities of the binary variants of the phase, it is not seen as a complete series of solid solutions at any one temperature.

As part of the experimental work of COST 531, a programme of study was initiated by the IMMS-PAS at Krakow, Poland to determine the thermodynamic properties of the liquid phase (enthalpies of mixing (in conjunction with the University of Leeds, UK) and the activity of In in the liquid **[08Wie]**) and the liquidus surface along three sections of the ternary system **[06Wie]**.

The modelling of this system is quite challenging. The enthalpies of mixing in the Ag-Cu system are positive whereas those for the Ag-In system are negative, and extrapolation of the binary systems into the ternary predicts a miscibility gap in the liquid phase that is not seen experimentally. The experimental data generated as part of COST 531 have been used in an attempt to model the ternary system. As a first step in this modelling it was necessary to remodel the Ag_2In phase to make it compatible with the CUIN_GAMMA phase in the Cu-In system (see binary systems section, Ag-In). The diagrams below represent the current state of the modelling of this system but it should be stressed that it is still under refinement. Although the experimental thermodynamic properties are reproduced reasonably well there is still disagreement between the experimental and calculated liquidus surface. The predicted invariant reactions involving the liquid phase are given in the table below. E1 is not a eutectic reaction in the traditional sense, although it does represent a decomposition reaction. In this case, the LIQUID phase is a product of the decomposition rather than the decomposing phase. **Fig. 82** shows the predicted liquidus surface, calculated using the current model for the system. The liquidus exhibits 3 maxima. Reactions E2 and U3 are very close together and a very small monovariant resulting from the phase separation of the CUIN_GAMMA phase is also present. These features are more likely an artefact of the calculations and it is envisaged that in the final version of the model, the phase separation will not be present resulting in the loss of one of the invariant reactions. There are a number of invariant reactions occuring in the In-corner of the diagram, which are seen more clearly in a magnified portion of the liquidus (**Fig. 83**). The projection of the liquidus

lines onto the T-x(Ag) plane is given in **Fig. 84** clearly showing the position of the lowest temperature eutectic in relation to the other reactions.
Figs. 85 to **88** show a comparison between the measured and calculated thermodynamic properties. The isothermal section for 500 °C is given in **Fig. 89**, calculated vertical sections at Cu:In ratios of 1:1 and 1:3 are given in **Figs. 90** and **91**, respectively; It can be seen how the CUIN_GAMMA phase lies across the section but without being stable in either of the Cu-In and Ag-In binaries at this temperature. Even though the modelling still requires work, the fit between the calculated and experimental data is good.

References:

[88Woy] Woychik, C.G., Massalski, T.B.: *Met. Trans.*, 1988, **19A**, 13-21.

[06Wie] Wierzbicka, A., Czeppe, T, Zabdyr, L.A.: *Arch. Met. Mater.*, 2006, **51**, 377-387.

[08Wie] Wierzbicka, A., Watson, A., Zabdyr, L.A.: to be submitted to *J. Alloys Compd*, 2008.

Table of invariant reactions

T / °C	Reaction type	Phases	Compositions		
			x_{Ag}	x_{Cu}	x_{In}
664.2	E1	BCC_A2	0.583	0.214	0.203
		LIQUID	0.291	0.483	0.226
		CUIN_GAMMA	0.421	0.277	0.303
		FCC_A1	0.670	0.174	0.156
657.7	U1	LIQUID	0.268	0.515	0.217
		FCC_A1	0.665	0.180	0.155
		FCC_A1	0.030	0.914	0.056
		CUIN_GAMMA	0.417	0.281	0.302
634.3	U2	LIQUID	0.610	0.031	0.359
		BCC_A2	0.706	0.025	0.269
		CUIN_GAMMA	0.615	0.073	0.312
		HCP_A3	0.723	0.013	0.264

615.5	U3	LIQUID	0.104	0.641	0.255
		CUIN_GAMMA	0.109	0.568	0.323
		BCC_A2	0.020	0.786	0.194
		CUIN_GAMMA	0.184	0.486	0.330
615.4	E2	LIQUID	0.106	0.641	0.253
		FCC_A1	0.013	0.894	0.093
		BCC_A2	0.020	0.787	0.193
		CUIN_GAMMA	0.204	0.467	0.329
296.6	U4	CUIN_GAMMA	0.088	0.566	0.346
		CUIN_ETA	0.000	0.623	0.377
		LIQUID	0.058	0.071	0.871
		CUIN_ETAP	0.000	0.640	0.360
294.9	U5	LIQUID	0.049	0.064	0.886
		CUIN_ETA	0.000	0.623	0.377
		CUIN_ETAP	0.000	0.640	0.360
		CUIN_THETA	0.000	0.550	0.450
292.3	U6	LIQUID	0.056	0.068	0.876
		CUIN_ETAP	0.000	0.640	0.360
		CUIN_THETA	0.000	0.550	0.450
		CUIN_GAMMA	0.090	0.564	0.346
145.8	U7	LIQUID	0.018	0.007	0.975
		CUIN_THETA	0.000	0.550	0.450
		CUIN_GAMMA	0.236	0.418	0.346
		TETRAG_A6	0.000	0.000	1.000
143.0	E3	LIQUID	0.025	0.005	0.969
		CUIN_GAMMA	0.439	0.225	0.336
		TETRAG_A6	0.000	0.000	1.000
		AGIN2	0.330	0.000	0.670

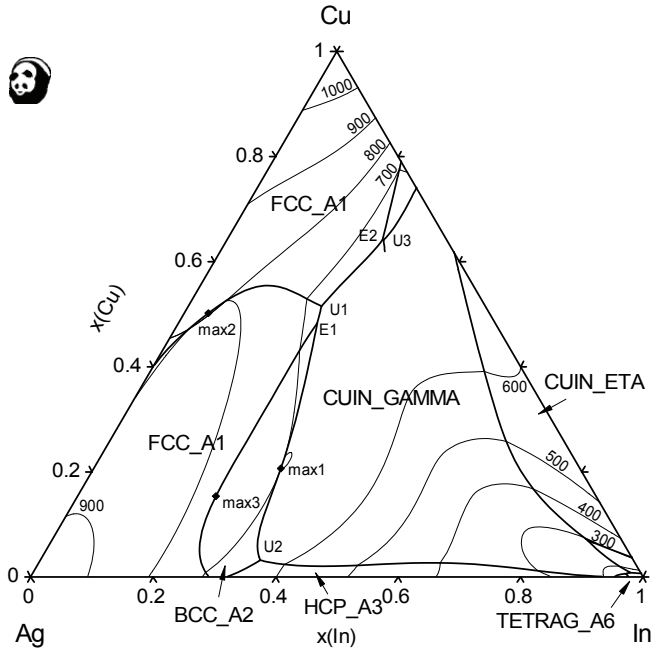

Fig. 82: Liquidus projection of the Ag-Cu-In system

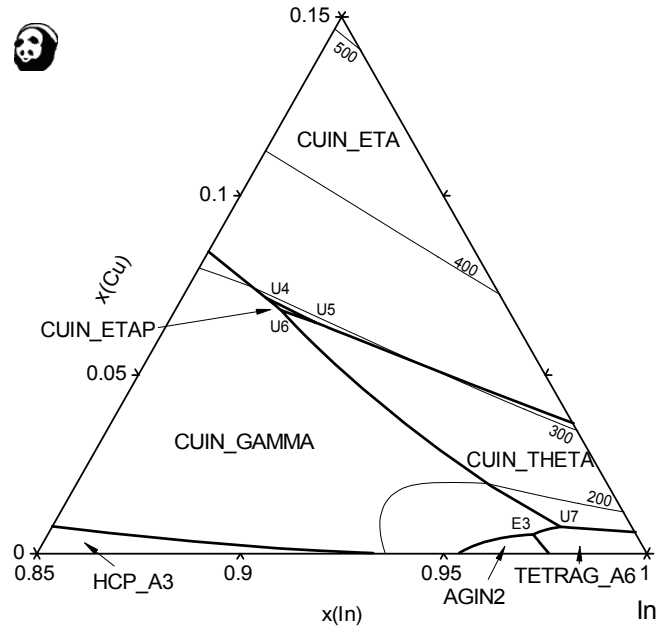

Fig. 83: Liquidus surface in the In-corner of the Ag-Cu-In system

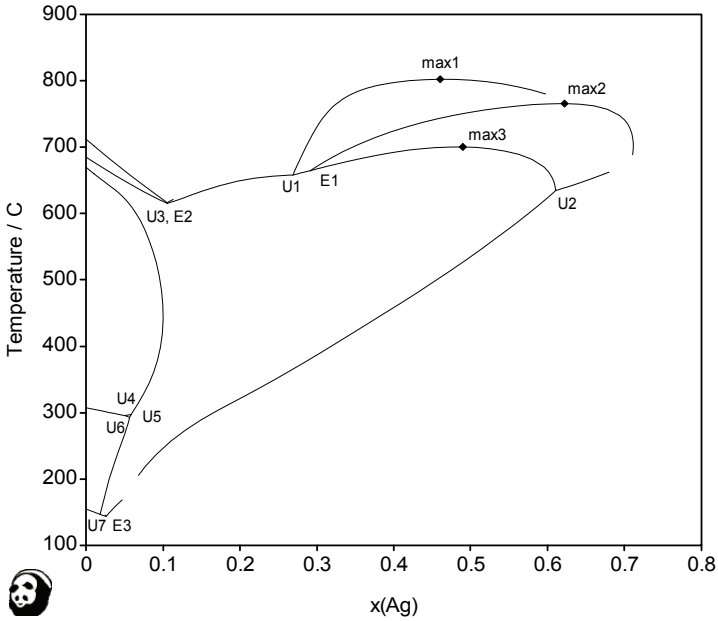

Fig. 84: Liquidus lines in the Ag-Cu-In system projected onto the T- x(Ag) plane

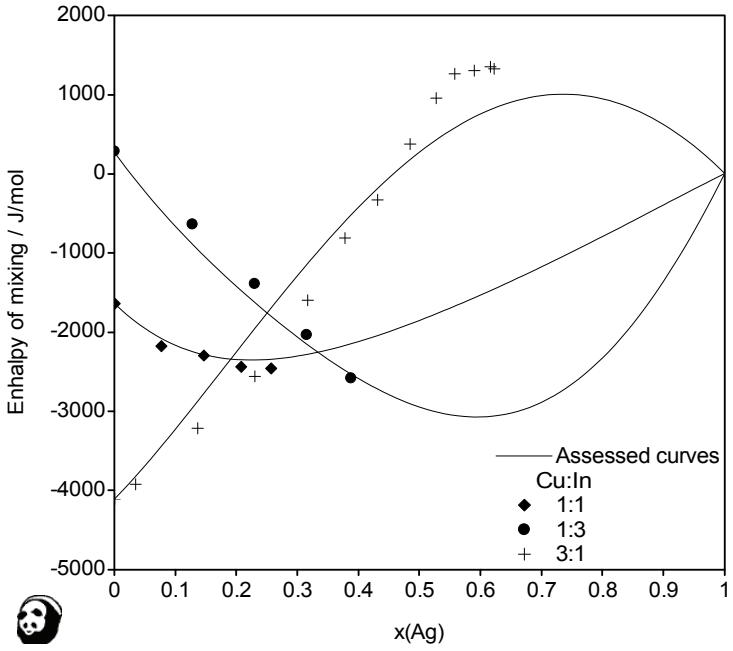

Fig. 85: Calculated enthalpies of mixing for liquid alloys at 900 °C, compared with experimental data **[08Wie]** (Ref: LIQUID)

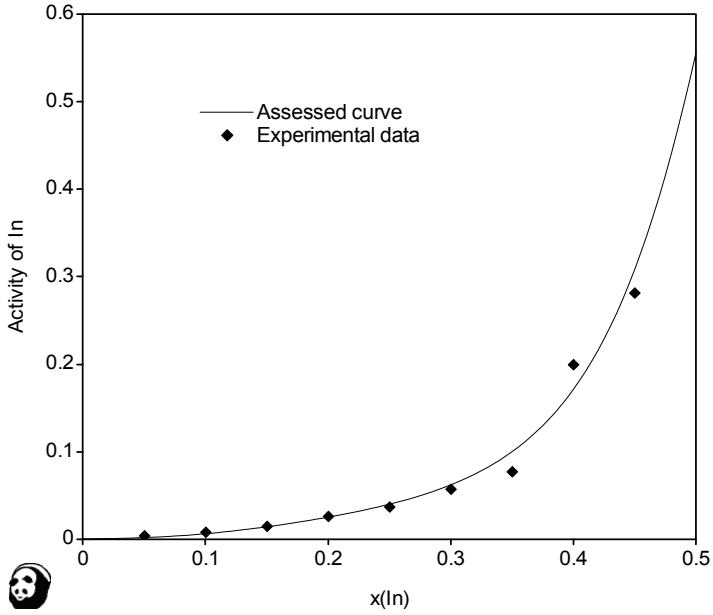

Fig. 86: Calculated In activity of liquid alloys at 900 °C at Cu:In = 1:1, compared with experimental data **[08Wie]** (Ref: LIQUID)

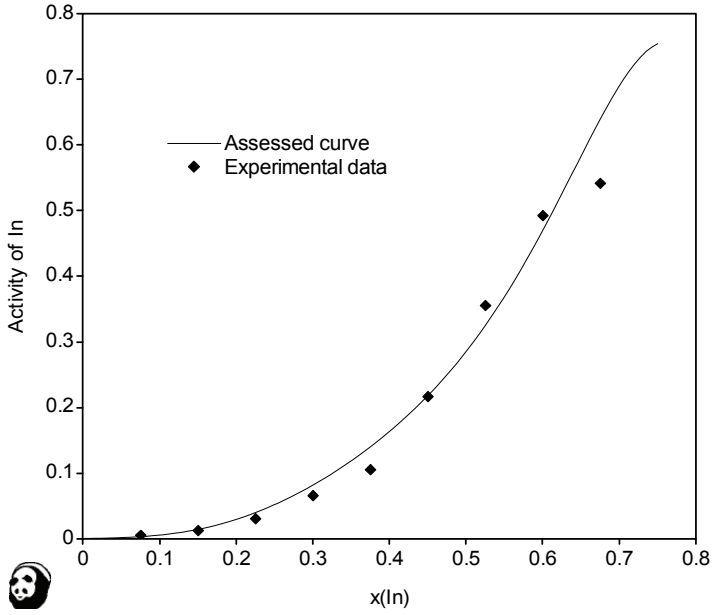

Fig. 87: Calculated In activity of liquid alloys at 900 °C at Cu:In = 1:3, compared with experimental data **[08Wie]** (Ref: LIQUID)

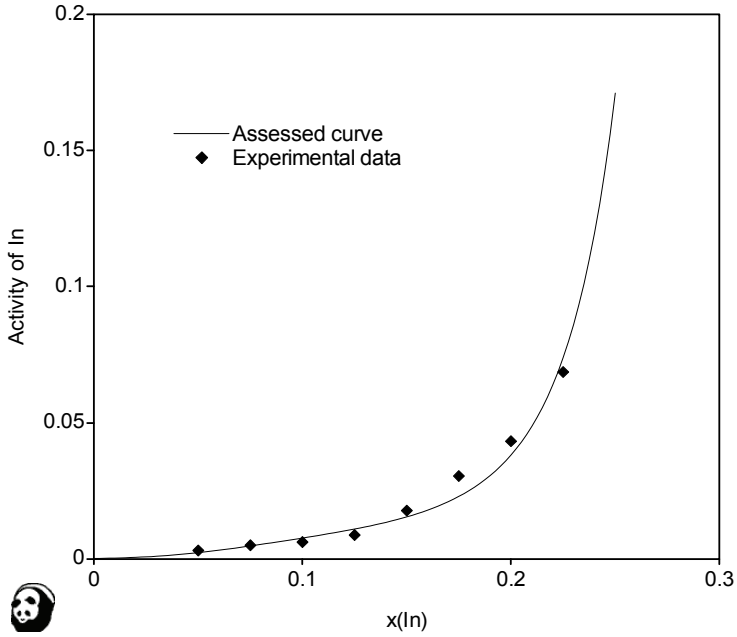

Fig. 88: Calculated In activity of liquid alloys at 900 °C at Cu:In = 3:1, compared with experimental data **[08Wie]** (Ref: LIQUID)

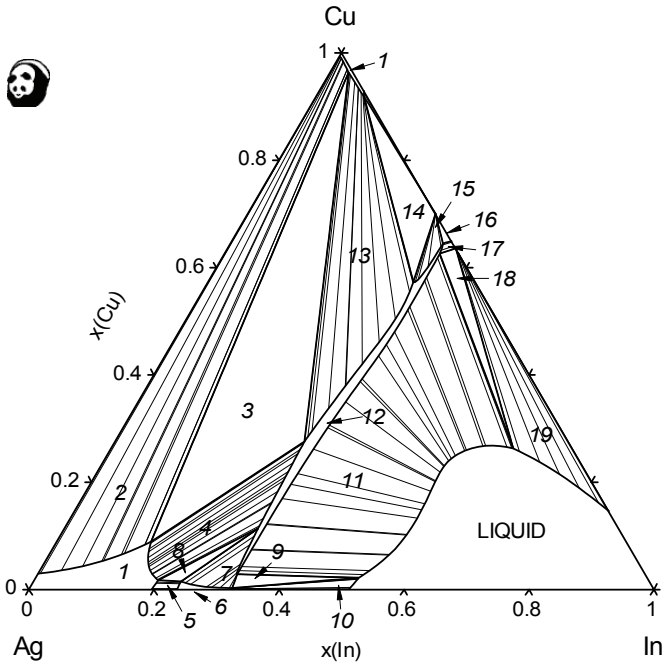

Fig. 89: Isothermal section at 500 °C

Legend:
1 - FCC_A1
2 - FCC_A1+FCC_A1
3 - FCC_A1+FCC_A1+CUIN_GAMMA
4 - FCC_A1+CUIN_GAMMA
5 - FCC_A1+HCP_A3
6 - HCP_A3
7 - HCP_A3+CUIN_GAMMA
8 - HCP_A3+CUIN_GAMMA+FCC_A1
9 - HCP_A3+LIQUID+CUIN_GAMMA
10 - LIQUID+HCP_A3
11 - LIQUID+CUIN_GAMMA
12 - CUIN_GAMMA
13 - CUIN_GAMMA+FCC_A1
14 - CUIN_GAMMA+CUIN_DELTA+FCC_A1
15 - CUIN_GAMMA+CUIN_DELTA
16 - CUIN_GAMMA+CUIN_DELTA+CUIN_ETA
17 - CUIN_ETA+CUIN_GAMMA
18 - LIQUID+CUIN_ETA+CUIN_GAMMA
19 - LIQUID+CUIN_ETA

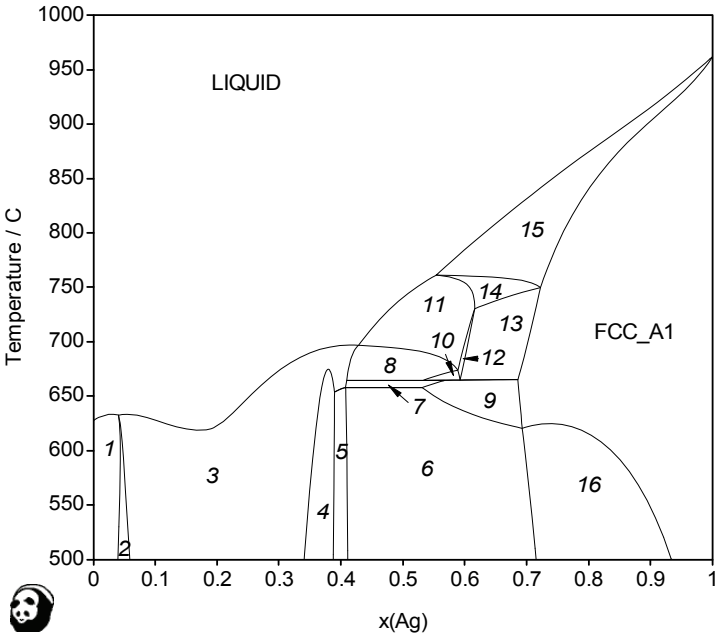

Fig. 90: Isopleth of the Ag-Cu-In system with the ratio Cu:In of 1:1

Legend:
1 - LIQUID+CUIN_ETA
2 - LIQUID+CUIN_ETA+CUIN_GAMMA
3 - LIQUID+CUIN_GAMMA
4 - CUIN_GAMMA
5 - CUIN_GAMMA+FCC_A1
6 - CUIN_GAMMA+FCC_A1+FCC_A1
7 - LIQUID+FCC_A1+CUIN_GAMMA
9 - CUIN_GAMMA+FCC_A1
10 - BCC_A2+CUIN_GAMMA
11 - LIQUID+BCC_A2
12 - BCC_A2
13 - BCC_A2+FCC_A1
14 - BCC_A2+FCC_A1+LIQUID
15 - FCC_A1+LIQUID
16 - FCC_A1+FCC_A1

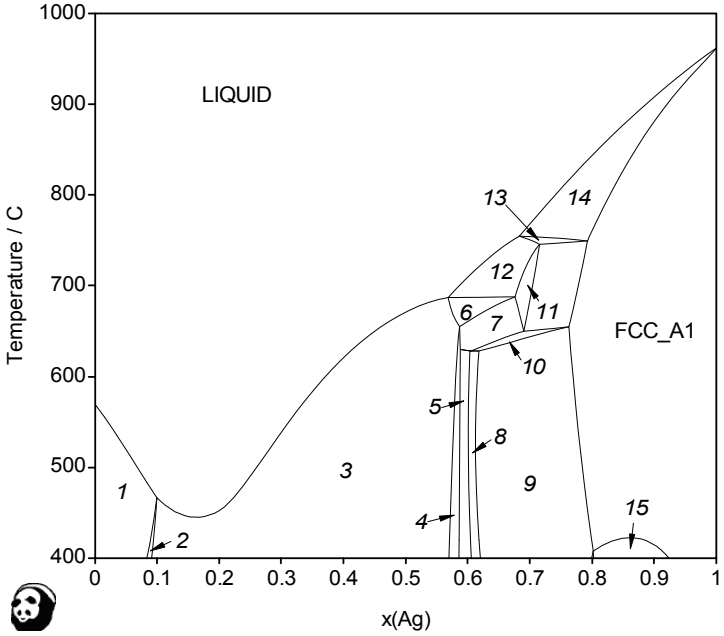

Fig. 91: Isopleth of the Ag-Cu-In system with the ratio Cu:In of 1:3

Legend:
1 - LIQUID+CUIN_ETA
2 - LIQUID+CUIN_ETA+CUIN_GAMMA
3 - LIQUID+CUIN_GAMMA
4 - CUIN_GAMMA
5 - CUIN_GAMMA+HCP_A3
6 - BCC_A2+LIQUID+CUIN_GAMMA
7 - BCC_A2+CUIN_GAMMA
8 - CUIN_GAMMA+FCC_A1+HCP_A3
9 - FCC_A1+CUIN_GAMMA
10 - BCC_A2+CUIN_GAMMA+FCC_A1
11 - BCC_A2
12 - LIQUID+BCC_A2
13 - BCC_A2+FCC_A1+LIQUID
14 - LIQUID+FCC_A1
15 - FCC_A1+FCC_A1